

1N-18-CR
141658
P.123

NASW-4435

THE FINAL REPORT ON THE DESIGN OF A COMMON LUNAR LANDER

Presented by:

The Austin ynthesis Corporation

"We're more than just your Common Lunar Lander Corporation"

Dan Driggers
Sean Hearrell
Kevin Key
Brian Le
Glen Love
Rob McMullen
Scott Messec
Jim Ruhnke

N93-18165

Unclas

G3/18 0141658

In association with:

Dr. George W. Botbyl
Department of Aerospace Engineering
The University of Texas at Austin

In support of:

NASA / USRA
Advanced Space Design Program

December 1991

(NASA-CR-192026) THE DESIGN OF A
COMMON LUNAR LANDER Final Report
(Texas Univ.) 123 p

THE FINAL REPORT ON THE DESIGN OF A COMMON LUNAR LANDER

Presented by:

The Austin ynthesis Corporation

"We're more than just your Common Lunar Lander Corporation"

Dan Driggers
Sean Hearrell
Kevin Key
Brian Le
Glen Love
Rob McMullen
Scott Messec
Jim Ruhnke

In association with:

**Dr. George W. Botbyl
Department of Aerospace Engineering
The University of Texas at Austin**

In support of:

**NASA / USRA
Advanced Space Design Program**

December 1991

Executive Overview

The Austin Cynthesis Corporation (hereafter referred to as "the Corporation") was formed to respond to a Request for Proposal for the design of a Common Lunar Lander (CLL) capable of carrying a lightweight (less than 500 kg), unspecified payload to the moon. The Corporation believes that such a system could make a large contribution towards the continued progress of the civil space program. The system could be utilized in further scientific study of the Moon by carrying payloads of scientific instruments custom-packaged for specific explorer missions. Additionally, it could help establish and/or support a manned lunar base, through the transfer of small amounts of building materials, communications equipment, a lunar rover vehicle, or other supplies. Due to its unique design philosophy, the potential missions the CLL could perform will truly be limited primarily by the payload designer.

The RFP received by the Corporation required the contractor to evaluate all mission phases: Earth launch, lunar transfer, lunar capture, and descent to the lunar surface. Additionally, the contractor was required to conceptually design a variety of potential payloads which the lander might be required to carry. To fulfill these requirements, the Corporation has divided the problem into three main parts: launch vehicle selection, lander design, and conceptual payload selection. Initial mass estimates led to the selection of a class of launch vehicles which included the Delta, Atlas, and Titan. As the design progressed, mass estimates eliminated the Delta as a possible launch vehicle, and the currently available Atlas/Centaur as well. However, planned upgrades to the Atlas/Centaur vehicle to be ready by 1993 should comfortably meet our needs.

The lander design itself has been broken into several subsystems: structure, power, thermal control, avionics, communications, and propulsion. The structures group has created a three-legged space frame design which provides for a two-meter diameter platform to which payloads will be affixed. This platform is hexagonal with diametric crossbeams. Small members may be connected between the main platform crossbeams to provide payload attachment points. At this time, the structure has been analyzed for

particular static loads only; the short time available for the completion of the design precluded any attempt to perform dynamic modeling. Dynamic analysis is an important aspect of the structure design, however, and should be included in future phases of the design effort.

Because of the short mission duration of the lander itself (its mission will end when it has reached the lunar surface), the power group has determined fuel cells to be the optimum power source. Other than offering a limited amount of startup power, the lander itself will not be responsible for powering the payloads. For payload power requirements, the possibility of carrying a "common" power supply module as additional payload has been investigated. While there is no panacea available for supplying power to payloads using a standardized module, it would probably be practical to develop a "family" of power supplies from which a "best fit" for a particular mission could be chosen.

Thermal control of the lander will be accomplished using primarily passive systems to reduce weight and complexity. Spacecraft orientation, reflective paints, insulation, heat exchangers, and phase-change devices will be used to maintain the lander subsystems inside their operational temperature ranges. Additionally, the structure of the lander itself can be used as a heat sink for the payloads, if required.

The avionics subsystem has a difficult task, as the configuration of the lander will, in general, change significantly with payload mounting configurations particular to each mission. The avionics must either be configured before flight with specific information about the configuration of the lander, or else must be adaptable for a range of lander configurations. The pace of development of fully autonomous avionics systems indicates that an acceptable system would be available before the lander is scheduled to become operational.

The communications system is based on previous NASA explorer spacecraft. It is also shared between the lander and its payloads, as duplication of antennas, transmitters, and receivers is deemed unnecessary. It is expected that communications requirements for the payloads will be minimal during

lunar transit, so that the lander will dominate communications use, and that the lander itself will not require communications at all after landing.

Finally, the propulsion system for the lander will use fine (25 N) and coarse (450 N) reaction control jets for attitude control, a solid rocket motor for lunar capture, and one storable bi-propellant engine for de-orbit, lunar descent, and landing. The fine control jets will be used for precision attitude maneuvers during free flight, while the coarse jets will be used to compensate for moments generated by the thrust vector from a main engine not passing through the center of mass of the spacecraft.

While the RFP has tasked the Corporation with the conceptual design of multiple payloads for the lander, the primary task is the design of the lander itself and most resources have been spent there. While several ideas for payloads have been advanced, time allowed for only a handful to be examined in any detail. These ideas include a common power system to satisfy various payload power requirements, a lunar experiment package, a materials utilization and testing platform, a surface rover, and a ground communications relay station. Other sample payloads which were proposed but not studied in this project included ground-based communications relay stations, families of transport containers (with options for power, pressurization, etc), modular building components, and a ballistic payload distribution system (to scatter small, shock-resistant items in an area around the lander).

This Final Design Report Document includes information on the requirements for the design project; the ideas proposed as solutions to the design problem; the work which has been completed in support of the design effort; justifications, validations, and verifications of decisions made during the project; and suggestions for future work to be done in support of the project. A project schedule, including current status of the items included on the schedule, as well as cost and management summaries is also included.

Acknowledgements

Throughout the course of this project, we received help from many sources. While it is impossible to thank everyone who helped us, we would especially like to express our gratitude to the following people for their contributions to our project:

Wallace Fowler, George Botbyl, Tony Economopolous, Elfego Piñon, John Lundberg, Danny Quiroz, Chris Varner, Mark Snaufer, Russel Carpenter, Steve Bailey, Kenneth Baker, George Gafka, and Darrell Monroe.

Table of Contents

Executive Overview.....	i
Table of Contents	v
List of Illustrations.....	vii
List of Tables.....	ix
List of Acronyms.....	x
1.0 General Design Requirements.....	1
2.0 Mission Scenario.....	1
2.1 Trajectory Analysis.....	3
2.1.1 Patched-Conic Approximation Method.....	3
2.1.2 Non-Coplanar Trajectories.....	5
2.1.3 Lunar Descent.....	6
2.2 Launch Vehicle.....	7
3.0 Common Lunar Lander Design.....	10
3.1 Structure.....	10
3.2 Power Subsystem.....	18
3.3 Thermal Control Subsystem.....	21
3.4 Avionics Subsystem.....	28
3.4.1 Constraints on the Avionics Subsystem.....	29
3.4.2 Operation of the Avionics Subsystem.....	30
3.5 Communications Subsystem.....	32
3.6 Propulsion Subsystem.....	33
4.0 Conceptual Payload Design.....	45
4.1 Common Payload Power Supply.....	45
4.2 Sample Return Mission.....	46
4.3 Experimental Packages.....	47
5.0 Corporate Structure and Cost Status.....	49
5.1 Management Overview.....	49
5.2 Critical Design Path and Scheduling.....	50
5.3 Cost Information.....	53
5.3.1 Personnel Cost.....	53
5.3.2 Material and Hardware Cost.....	54
5.3.3 Total Costs.....	55
6.0 Bibliography.....	56
7.0 Appendix A	
Background and History of Other Lunar and Martian Landers.....	60
7.1 Surveyor.....	60
7.2 Apollo.....	63
7.3 Viking.....	64
7.4 References.....	66
8.0 Appendix B	
TK! Solver Models and Output Used for Trajectory Analysis.....	67
8.1 TK! Solver Patched Conic Model Variables.....	67

8.2	Equations used in the TK! Solver Patched-Conic Approximation Model.....	69
8.3	Trajectory Analysis Diagrams	71
8.4	Input and Output from LANDER Sample Run.....	73
9.0	Appendix C	
	Static Structural Modeling.....	78
9.1	Sample NASTRAN model.....	78
9.2	Sample Output	80
10.0	Appendix D	
	Structural Design Evolution	84
10.1	Early Conceptual Designs.....	84
	10.1.1 Conceptual Lander Configuration 1	85
	10.1.2 Conceptual Lander Configuration 2	85
	10.1.3 Conceptual Lander Configuration 3	87
	10.1.4 Conceptual Lander Configuration 4	87
10.2	Evolution of Final Design.....	88
	10.2.1 Engine and Fuel Tank Placement.....	88
	10.2.2 CLL Footprint Considerations.....	90
	10.2.3 Final Configuration.....	92
11.0	Appendix E	
	Center of Gravity Analysis.....	94
12.0	Appendix F	
	Propulsion Sizing Information	99

List of Illustrations

Figure 2.1.1.	The Minimum ΔV Trajectory.....	5
Figure 2.1.2.	The Non-coplanar Lunar Transfer Orbit.....	6
Figure 2.2.1.	Atlas IIAS Medium Payload Fairing.....	9
Figure 3.1.1.	Space Frame Design.....	13
Figure 3.1.2.	Semi-Monocoque Design.....	14
Figure 3.3.1.	Energy Balance of Lunar Lander.....	23
Figure 3.3.2.	Lunar Surface Temperature	24
Figure 3.6.1.	STAR 30E Schematic.....	36
Figure 3.6.2.	CLL Third Stage Propulsion System Schematic.....	41
Figure 3.8.1.	Final Common Lunar Lander Design (Fully Configured).....	43
Figure 4.2.1.	Soil Sample Auger.....	47
Figure 5.1.1.	Corporate Structure.....	50
Figure 5.2.1.	Critical Design Path	51
Figure 5.2.2.	Schedule of Project Milestones.....	52
Figure 5.3.1.1.	Actual Hours and Projected Hours Through Completion.....	53
Figure A1.	Surveyor in Stored Configuration.....	62
Figure A2.	Surveyor in Operational Configuration.....	62
Figure A3.	The Apollo Lunar Module	64
Figure A4.	The Viking Lander	65
Figure B1.	Geocentric Transfer Orbit.....	71
Figure B2.	Patch Conditions.....	72
Figure B3.	Selenocentric Orbit	73
Figure D1.	Conceptual Lander Configuration 1	85
Figure D2.	Conceptual Lander Configuration 2	86
Figure D3.	Conceptual Lander Configuration 3	87
Figure D4.	Conceptual Lander Configuration 4	87
Figure D5.	Three Outboard Vernier Engines with Spherical Fuel Tank..	89
Figure D6.	One Central Descent Engine and Cylindrical Fuel Tanks.....	90
Figure D7.	Top View of CLL Showing 4-Meter Footprint.....	91
Figure D8.	Legs in Folded Configuration.....	92
Figure D9.	Final Common Lunar Lander Design (Fully Configured).....	93

Figure D10.	CLL Clearance Inside Atlas Medium Payload Fairing	93
Figure E1.	Spacecraft Coordinate System	94
Figure E2.	Allowable Center of Gravity Range for the CLL	95
Figure F1.	Bipropellant Propulsion System Sizing.....	99
Figure F2.	CLL Propulsion Subsystem Evolution.....	100
Figure F3.	Flight-Proven Cryogenic Engines.....	104
Figure F4.	Storable Bipropellant Engines.....	105
Figure F5.	Solid Motors.....	106

List of Tables

Table 2.1.1.	TK! Solver Patched Conic Results and ΔV s.....	4
Table 3.2.1.	Power Subsystem Decision Matrix.....	19
Table 3.2.2.	Subsystem Power Requirements.....	20
Table 3.2.3.	Space Shuttle Fuel Cell Data.....	21
Table 3.3.1	Component Temperature Limits.....	22
Table 3.3.2.	Thermal Coating Properties	25
Table 3.3.3.	Thermal Control Techniques and Applications.....	27
Table 3.3.4.	Thermal Control Subsystem Mass Summary	28
Table 3.6.1.	CLL Propulsion Subsystem Requirements.....	34
Table 3.6.2.	Selection of Engine Type.....	35
Table 3.6.3.	LPO Insertion Motor Specifications.....	36
Table 3.6.4.	Descent and Landing Engine Specifications.....	37
Table 3.6.5.	Coarse Attitude Control Thruster Specifications.....	38
Table 3.6.6.	Fine Attitude Control Thruster Specifications.....	38
Table 3.6.7.	Propellant Summary.....	39
Table 3.6.8.	Propellant Tanks.....	40
Table 3.6.9.	CLL Propulsion Subsystem Mass Summary.....	42
Table 3.8.1.	CLL Mass Summary	44
Table 5.3.1.1.	Summary of Personnel Costs.....	54
Table 5.3.2.1.	Material and Hardware Costs.....	55
Table 5.3.3.1.	Total Costs	55
Table C1.	Gridpoint Displacements (Meters).....	80
Table C2.	Load Vector (Newtons).....	81
Table C3.	Stresses in ROD Elements (N/m ²).....	81
Table C4.	Stresses in BAR Elements (N/m ²).....	82
Table E1.	Mass Distribution / Center of Gravity Spreadsheet.....	97
Table F1.	Database of Available Propulsion Systems	107

List of Acronyms

AMU	Atomic Mass Unit
CG	Center of Gravity
CLL	Common Lunar Lander
ΔV	(Delta-V) Velocity increment
GNC	Guidance, Navigation, and Control
HGA	High Gain Antenna
IMU	Inertial Measurement Unit
LEO	Low-Earth Orbit
LGA	Low Gain Antenna
LH2	Liquid Hydrogen
LM	Lunar Module
LOX	Liquid Oxygen
LPO	Lunar Parking Orbit
NASTRAN	NASA Structural Analysis language
RCS	Reaction Control System
RFP	Request For Proposal
RTG	Radioisotope Thermal Generator
SRM	Sample Return Module
TCS	Thermal Control Subsystem
VHF	Very High Frequency

1.0 General Design Requirements

According to the Request for Proposal received by the Corporation, the contractor was required to develop designs for a Common Lunar Lander (CLL) to deliver lightweight payloads (less than 500 kg) to the surface of the Moon. The design task additionally required the contractor to address four main phases of the lander's mission: Earth launch, lunar transfer, lunar capture, and landing. While the lander and its mission comprise the main focus of the design effort, the RFP also tasked the contractor with the conceptual design of several payload packages to be carried by the lander.

The Austin Cynthesis Corporation has assumed more project specifications in addition to those stated explicitly by the RFP. The RFP specified a single-mission lander; therefore, to be cost-effective, the lander must be relatively inexpensive. Almost as a corollary, the lander must be simple. Since its primary function is to transfer generic payloads, all facets of the lander design were undertaken with this in mind. As a result, as few payload support systems have been designed into the lander as possible, lest it succumb to the pitfall of trying to be "all things to all people." Additionally, the Corporation set a development timeline of three to five years, with 1995 as the target launch date, which constrained the design to using available technology and near-future upgrades (which also helped achieve the low-cost objective). Finally, the Corporation decided to make the lander as autonomous as possible. If all systems function correctly, the lander should be able to land successfully on the surface of the Moon at a predetermined site with no commands from Earth. However, there will be command channels available to allow for Earth control in case of malfunctions.

2.0 Mission Scenario

A typical mission for the CLL will begin with a launch from Cape Kennedy atop an Atlas/Centaur launch vehicle. After the Atlas booster is expended, the spin-stabilized Centaur upper stage will fire to place the CLL into a

circular low-Earth orbit, and shortly after that will fire again to start the lander on its trans-lunar trajectory. At this point, the Centaur will be jettisoned.

Next, the legs on the CLL will extend, allowing the RCS jets to become operative. Three-axis stabilization of the spacecraft begins at this point. The lander will then perform any necessary maneuvers to obtain locks on all necessary celestial references (for instance, the Earth, the Sun, and a star such as Polaris or Canopus). After these maneuvers are completed, at least one low-gain antenna will be aligned with Earth and communications will be established.

Very little will happen during the trans-lunar coast phase. Attitude control will be maintained using signals from Sun, Earth (or Moon), and star sensors/trackers, backed up by an inertial measurement unit, to drive the fine RCS jets. Position will be determined using information from the sensors, in conjunction with an on-board ephemeris. Velocity information will be determined using information from the sensors combined with mathematical models. Position and velocity determinations will be backed up by using information from the ground-based communications/tracking stations of the Deep Space Network. A midcourse correction will probably be required during the transit phase, and can be accomplished using the coarse reaction control jets.

When the CLL reaches the proper lunar altitude, the solid rocket capture motor will fire to place the lander in a circular parking orbit around the Moon. From here, the lander can loiter until conditions allow it to land where desired (this circular parking orbit may be at any inclination, including a polar orbit, to allow for global access to the Moon). At the proper time, the main liquid descent engine will fire a short deorbit burn to begin the descent to the surface. A short time later, it will begin to fire continuously to follow a descent trajectory to the surface. During this descent phase, a radar altimeter will be active, and some type of terrain evaluation procedure will be active to evaluate possible landing sites in the target area. An inertial measurement unit (IMU) will provide information on descent rate and lateral velocity, and attitude control will be performed using a gyro-based reference from the IMU.

The CLL will hover for a predetermined time to complete its evaluation of possible landing sites. This hover time can be used to allow Earth-based controllers make the final decision, if desired.

During this design project, we have concentrated on the most efficient mission to the Moon, that which requires the least amount of fuel. Trajectories which should be considered in future work are those which involve polar orbits around the Moon, necessary for global lunar surface access.

2.1 Trajectory Analysis

The trajectory of the CLL will be established using four propulsive burns. It is assumed that the launch vehicle will place the CLL in a circular orbit around the Earth. The first burn will occur when the Centaur upper stage rocket injects the CLL into a lunar intercept trajectory. The second burn will occur at lunar capture and place the CLL in a Selenocentric (Moon-centered) circular orbit. The third burn will take the CLL out of circular orbit to begin its descent, and the fourth burn will decelerate the CLL prior to landing.

2.1.1 Patched-Conic Approximation Method

A patched-conic method was used to determine the minimum velocity change (ΔV) required to place the CLL into a circular lunar orbit. The following assumptions are required:

- 1) The Earth and the Moon are considered to be spherical and uniform in shape.
- 2) The Moon's orbit about the Earth is circular.
- 3) The gravities of the Earth and Moon can be turned off and turned on; this is the sphere of influence concept.
- 4) There are no perturbing forces; this is a two-body problem with the CLL in the same plane as the Moon.

The initial condition used in the optimization is a 166 km altitude at injection into low-Earth orbit (LEO). The final condition is a circular orbit

about the Moon at an altitude of 200 km. The minimum ΔV solution to this problem is the trajectory desired.

Table 2.1.1 contains the results of the simplified model and Figure 2.1.1 shows a typical trajectory for the lander. For details on the method used for the TKI Solver model, see Appendix B.

Table 2.1.1. TKI Solver Patched Conic Results and ΔV s

	Initial Altitude	166 Km
	Initial Velocity	10.95 Km/s
	Initial Flight Path Angle	0 deg
	Initial Angle at Arrival of Moon's sphere of influence	61.06 deg
	Final Altitude	200.3 Km
	Final ΔV	.7942 Km/s
	Time of Flight	91.45 Hrs
<u>Bum</u>		
1	ΔV provided by Launch Vehicle	3.146 Km/s
2	ΔV upon arrival at the Moon	.7942 Km/s
3	ΔV for Lunar Decent	.0329 Km/s
4	ΔV at Touch Down	1.973 Km/s
	Total ΔV required during flight	5.926 Km/s
	Total ΔV required from Lander	2.780 Km/s

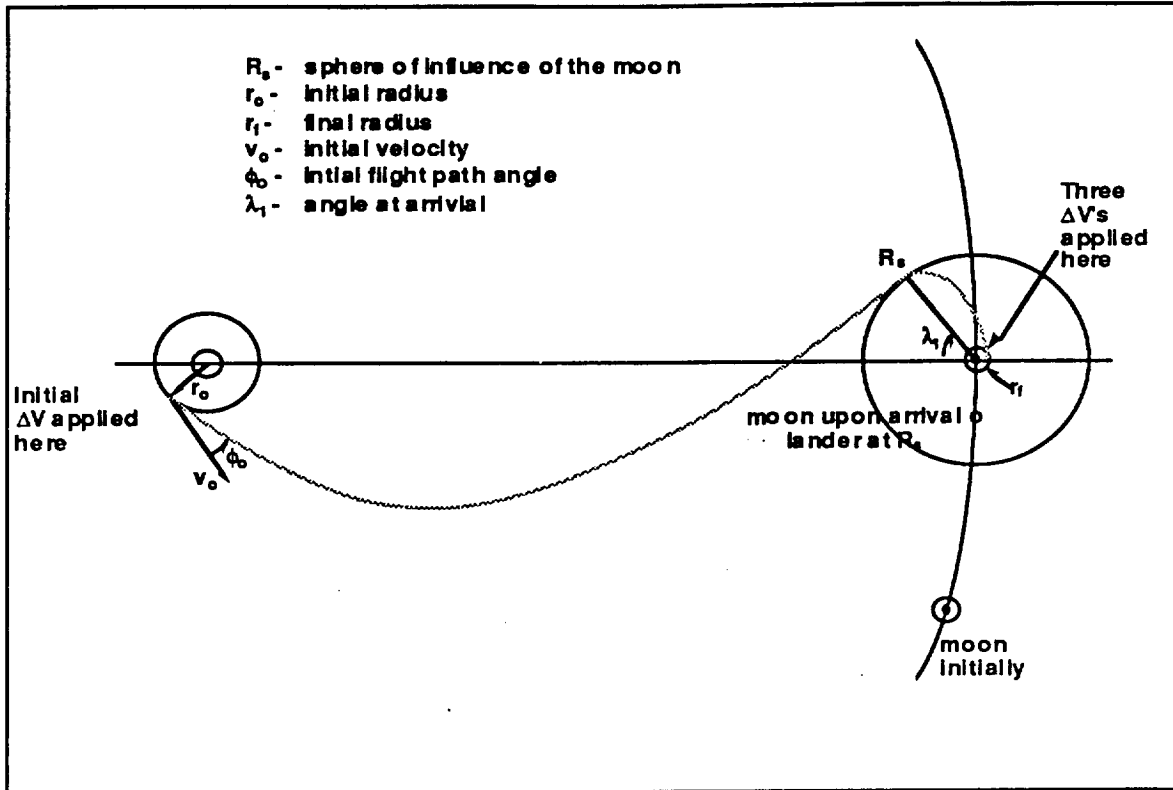


Figure 2.1.1. The Minimum ΔV Trajectory

2.1.2 Non-Coplanar Trajectories

The patched conic method above assumes that the CLL is in the same plane as the Moon. However, because the Moon's inclination is between 28.5 and 18.2 degrees (relative to the equator of the Earth) and Cape Kennedy is at 28.5 degrees North latitude (implying a minimum 28.5 degree inclination orbit), it is impossible to launch the CLL into a coplanar orbit more than once every 18.6 years. Therefore, non-coplanar trajectories must be considered.

Figure 2.1.2 shows the relationship of the relevant angles in a non-coplanar orbit. The names of the symbols used are:

- δ_0 - Launch Declination
- δ_1 - Intercept Declination
- β_0 - Launch Azimuth
- ψ_1 - Geocentric Sweep Angle

The launch declination is determined by the longitude of the launch site. The geocentric sweep angle is determined by the initial injection conditions,

r_o , v_o , and ϕ_o (position, velocity, and flight path angle) plus the angle from launch to injection. The launch azimuth must be between 40 and 115 degrees as specified by Eastern Test Range safety requirements for Cape Kennedy. The intercept is determined by the inclination of the desired final orbit around the Moon.

From the law of cosines for spherical triangles, we obtain from Figure 2.1.2:

$$\sin(\delta_1) = \sin(\delta_o) \cdot \cos(\psi_t) + \cos(\delta_o) \cdot \sin(\psi_t) \cdot \cos(\beta_o)$$

Any desired orbit can be attained by choosing the intercept declination at the sphere of influence and determining an acceptable geocentric sweep angle and launch azimuth for the given launch site.

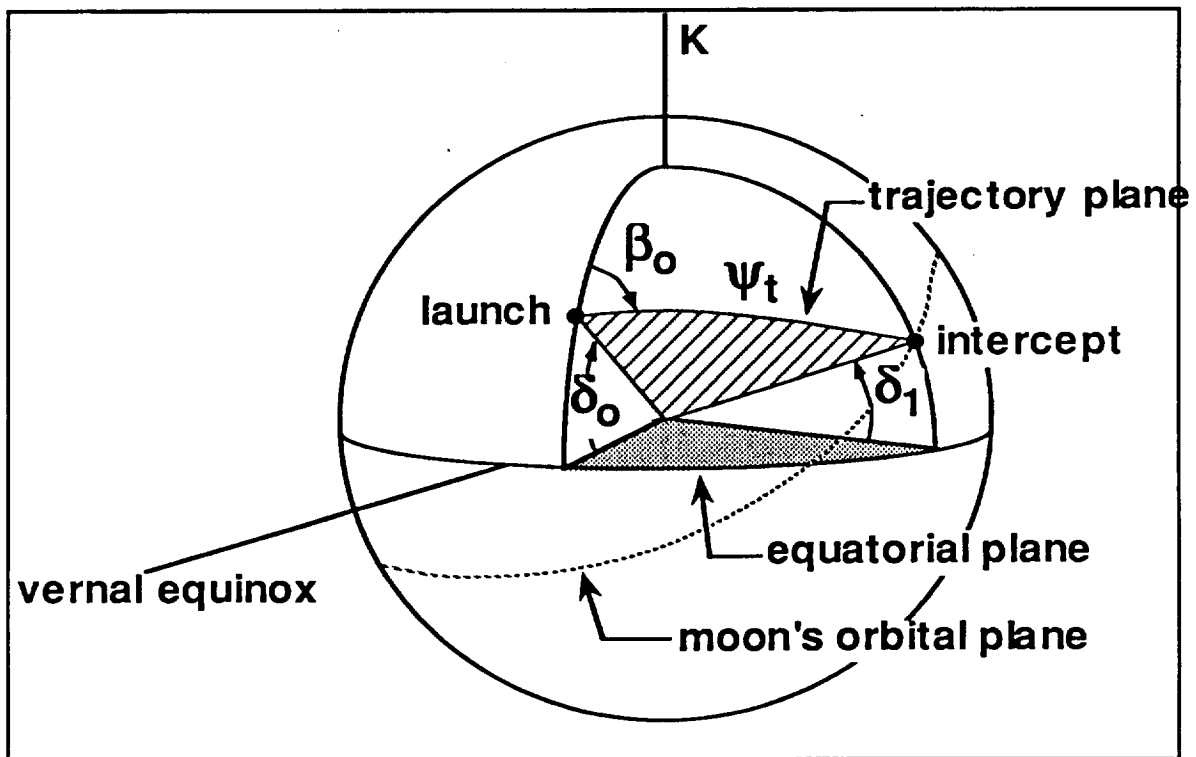


Figure 2.1.2. The Non-coplanar Lunar Transfer Orbit

2.1.3 Lunar Descent

A lunar descent program was used to determine the descent trajectory, which includes the third and fourth burns. The program, named LANDER and written by Chris Varner at Eagle Engineering, is a three degree-of-freedom

simulation which analyzes translational motion. Attitude dynamics and rotational motion are not considered in the computations of LANDER.

During the descent, the lander begins in the holding orbit and performs a deorbit burn. It then coasts to pericyynthion, where it reignites its engines and begins a gravity turn descent. When the local horizontal velocity becomes zero, the lander pitches up to a vertical orientation and begins to hover in search of a landing site. The lander hovers for a period of time specified by the user, and then lands. Appendix B includes the input and output from a sample execution of the LANDER simulation program, using a simple equatorial parking orbit with a landing on the equator. The ΔV s obtained from this program using several representative descent profiles were used to size the main descent engine and refine fuel requirements.

Trajectory Analysis Reference

1. Bate, Roger, Donald Mueller, and Jerry White, **Fundamentals of Astrodynamics**, Dover Publications, Inc., New York, 1971, Chapter 7: The Earth-Moon System.
2. Eagle Engineering Inc., **Lander Program Manual**, NASA Contract Number NAS9-17878, EEI Report 88-195, 1988.

2.2 Launch Vehicle

As part of the overall mission design, an examination of Earth launch systems was carried out. Due to the projected three to five year development time for the lander, the focus was placed on systems which are either currently available or will be available within this period of time.

Additionally, due to the many difficulties and risks involved in using foreign launch services, as well as the domestic economic benefits, emphasis was placed on finding a suitable U.S. launch service. Of the three U.S. commercial launch vehicles currently available (the Delta II, the Atlas II, and the Titan III), the Atlas II was determined to be the vehicle most capable of meeting the requirements for this mission.

Atlas launch vehicles, manufactured by General Dynamics, have a long history of successfully placing satellites into Earth orbit and launching lunar and planetary probes¹. Atlas launch vehicles have played a major role in the U.S. space program from its beginning. Atlas vehicles were used in the launch of the world's first communications satellite, the placement of the first free-world man in orbit, and the launch of the first lunar mission. The first stage of the Atlas II launch vehicle, the Atlas booster, originally served as an intercontinental ballistic missile. Over the past decade, Atlas launch vehicles, using primarily Centaur and Agena upper stages, have demonstrated a flight reliability record of 96%². The upper stage of the Atlas II launch vehicle, the LOX/LH₂ fueled Centaur, was designed and developed for the Surveyor program which placed several unmanned landers on the surface of the moon.

There are currently three versions of the Atlas II either available or in development: the Atlas II, the Atlas IIA, and the Atlas IIAS. In order to meet the 500 kg payload capability specified for the lander, the use of the Atlas IIAS version will be required. This version is scheduled to be available in 1992, well within the required time frame. The Atlas IIAS is simply an updated version of the Atlas II with modifications made to the Centaur upper stage and the addition of solid fuel boosters.

The Centaur upper stage of the Atlas IIAS uses two Pratt & Whitney RL10-4N engines which provide a combined thrust of 177.8 kN². They deliver a nominal specific impulse of 448.9 seconds and have an operating life of 4000 seconds. The nozzle arrangement consists of a fixed primary nozzle and a secondary extendable nozzle which provides an additional 6.5 seconds of specific impulse. These extendable nozzles have accumulated over 2.5 hours of running time in 69 firings. In addition to the engine upgrade, the Centaur avionics are also upgraded to provide weight, cost, and reliability improvements over the baseline Atlas II avionics.

In addition to upgrades in the Centaur upper stage, the Atlas IIAS adds two Castor II solid rocket motors manufactured by Morton Thiokol. These solid rocket motors are ignited shortly after liftoff and have a nominal burn time of 37 seconds². They produce a combined thrust of 463 kN.

There are two different payload fairings available for the Atlas IIAS: a medium payload fairing and a large payload fairing. To achieve maximum launch vehicle performance, the medium payload fairing will be used to launch the CLL. The medium payload fairing provides a usable diameter of 2.92 m and a usable length of 3.23 m in the cylindrical portion of the fairing². This cylindrical section is topped with a conical section of half angle 14.5° to minimize aerodynamic drag and weight losses. The volume enclosed by the conical section of the fairing is also usable, providing a total usable volume of 33.8 cubic meters. The fairing is a two half-shell structure of aluminum skin/stringer/frame construction. The purpose of the fairing is to provide both thermal and acoustic protection for the payload during launch and ascent. The Atlas IIAS medium payload fairing is shown in Figure 2.2.1.

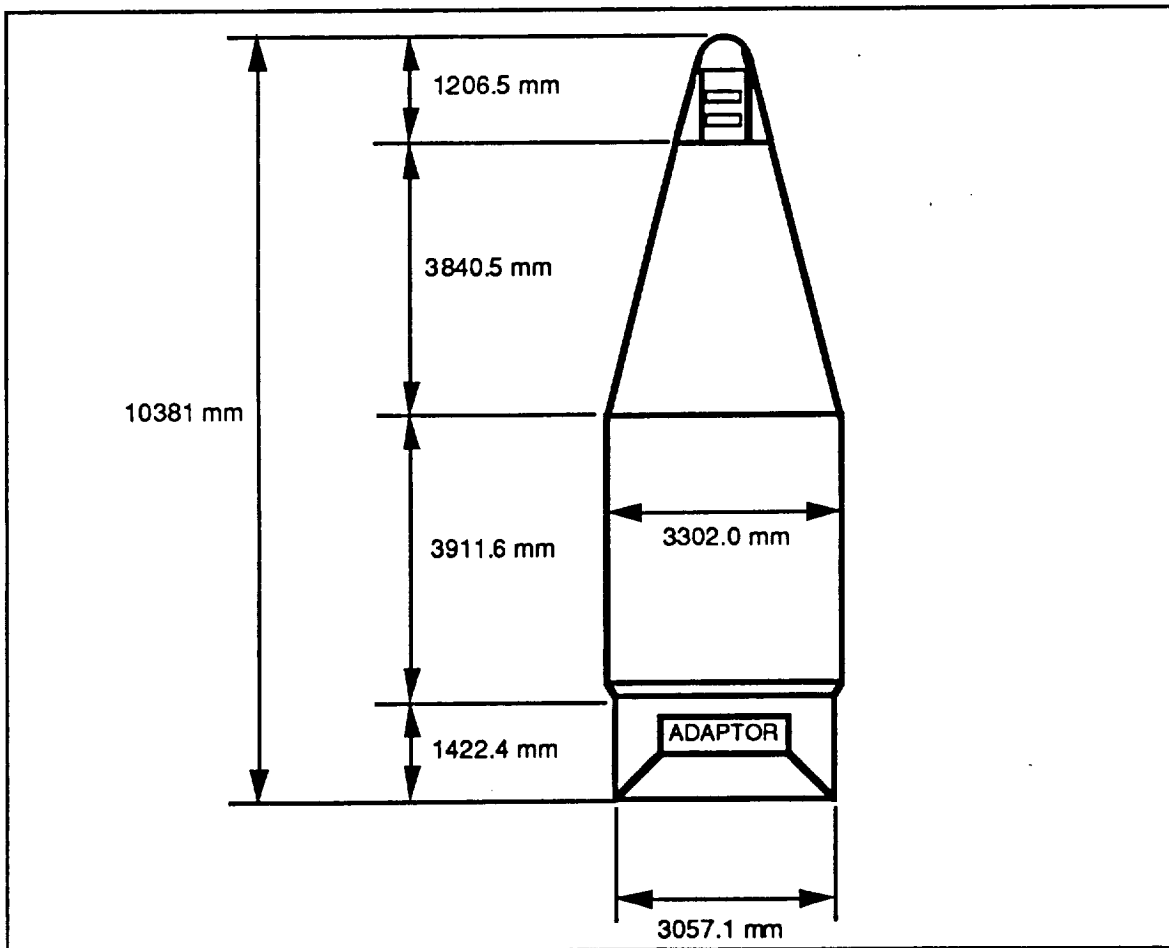


Figure 2.2.1. Atlas IIAS Medium Payload Fairing

The Atlas IIAS with the medium payload fairing has an Earth escape capability ($C_3=0$) of 2670 kg². Since the total injected mass of the lander, assuming the maximum 500 kg payload, is under 2400 kg, the Atlas IIAS has sufficient lifting capability to inject the lander into lunar transfer orbit. For payloads which meet the weight requirements for the lander but have difficulty fitting in the medium payload fairing, the large payload fairing can be used with minimal loss of performance. The large payload fairing provides a usable diameter of 3.65 m and a usable length of 3.67 m in the cylindrical portion of the fairing. The Earth escape performance of the Atlas IIAS with the large payload fairing is 2550 kg.

Launch Vehicle References

1. Curtis, Anthony, **Space Almanac**, Arcsoft Publishers, Woodsboro, MD, 1990.
2. **Atlas Mission Planners Guide**, General Dynamics Commercial Launch Services, San Diego, CA.

3.0 Common Lunar Lander Design

At the conception of the design project, the design of the CLL was divided into several separate subsystems: structure, power, thermal control, avionics, communications, and propulsion. This section discusses the ideas proposed as potential designs for each subsystem; the work which has been completed in support of the design effort; justifications, validations, and verifications of decisions made during the project; and identifies issues which should be addressed during future work.

3.1 Structure

The design of the CLL reflects the desire for modularity. The lander must fulfill a variety of missions with highly varied payloads. Because of this requirement, the lander structure itself also retains the concept of modularity.

The goal of the structural design is twofold: to carry all the loads required of it, and to provide a baseline configuration which can be easily modified for future missions.

There are three general types of structures which were considered for the CLL: monocoque, semi-monocoque, and space frame. Each has its own advantages and disadvantages. Monocoque designs are useful for resisting pressure loads and for operation in a fluid. They also provide a greater flexibility for attachment of surface mounted parts, since holes can be bored anywhere on the skin. Space frame designs are the most efficient for supporting loads, in terms of the mass required for the structure. However, the surface attachment points are limited, and necessitate the addition of substructural support elements. Semi-monocoque designs merge the benefits of both designs, but still weigh more than space frames.

Several factors enter in to the choice of an acceptable design. The critical parameter is the structure weight, since the cost and capability of the entire lander program is directly related to the weight of the lander itself. The next most critical factor is the support of all the loads necessary for the successful operation of the vehicle. The structure of the CLL must carry the stresses due to launch transients, launch acceleration, acoustic excitation, booster separations, lunar decelerations, impact landing, and static lunar operations¹. Thirdly, the lander must provide connectivity to all the subsystems, and must also connect to the launch vehicle. Additionally, the structure must function as a heat sink for thermal control, provide attachments for all the antennas and communications systems, and, of course, provide the structural platform for the mounting of payload packages.

All of the general structural design approaches considered could be made to satisfy the second, third and fourth criteria outlined above. Modifications to the strength and size of the various support members and skins could allow any of the three general types of structures to meet the criteria set out above. Therefore, the critical design factor becomes the first parameter listed in the above paragraph: the weight of the structure. The monocoque design is discarded at this point, since it will be heavier than the other two design

types. The remaining two, semi-monocoque and space frame, are considered for the structural system.

One of the design requirements of this project was to use current technology in all facets of the lander and its subsystems. For the structures system, this requires that complex materials will not be considered, and designs that require excessive preliminary testing will not be used. To minimize the required testing, it would be beneficial to use or modify designs that have already been tested. There have been several different designs that have been used for missions to the Moon, Mars, and Venus. The two major designs that are considered here are those used for the Surveyor mission to the moon, and the Viking mission to Mars (a brief overview of historical lander designs may be found in Appendix A).

The Surveyor used a space frame system, constructed from tubular aluminum, for weight efficiency and payload modularity. Its modularity was highlighted during its five successful missions to the moon. A variety of instrument packages were carried, using the same structural frame.²

The Viking lander used a semi-monocoque design for its missions to the surface of Mars. It had the task of resisting some (small) Martian atmosphere, in addition to carrying its payload. Both Viking landers were very similar, and modularity was not as much of an issue as it was for the Surveyors³.

The two designs that were considered for the structure of the CLL were based on the Surveyor and the Viking landers. Like those landers, the CLL has triangular symmetry, with three landing legs. The payload platform has a two meter nominal diameter, and it stands one meter above the lander feet. The legs are designed to provide a four meter diameter footprint, which allows stability during landing and static operations. Both designs were constrained by an axially-mounted main solid retrorotor, and an inboard liquid-fueled primary engine for final descent. The subsystems are to be attached externally, under the payload platform or attached between structural elements using minor support bars. The payloads will be bolted to the top of the payload platform, accounting for constraints in the location of the center of gravity.

The space frame (Surveyor-type) design is based on six tetrahedrons forming a flat base and connected at their apexes, forming a triangularly symmetric structure. It can also be considered as two parallel hexagons separated by .5 meters, rotated 30 degrees with respect to their perpendicular axis, and connected to their nearest nodes. The structure is shown in Figure 3.1.1. Each landing leg is attached to three vertices of the structure, one on the top hexagon, and two on the bottom hexagon. The logic behind this is to minimize the compression elements in the structure. The top element will be the main load carrying member with the bottom two providing lateral support. All the elements are tubular aluminum, connected by a series of cluster fittings. The legs are attached by pins, providing a statically determinate substructure to the main structure.

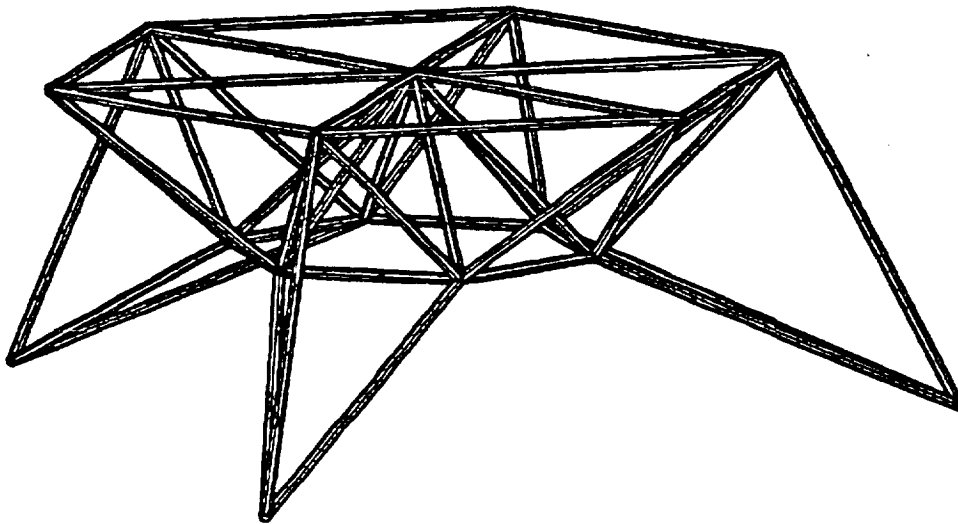


Figure 3.1.1. Space Frame Design

The semi-monocoque (Viking-type) design is based on two non-regular hexagons. The landing legs are attached at the shorter sides, as shown in Figure 3.1.2. The structure is braced by tubular aluminum, connecting adjacent nodes in a rectangular pattern. The payload platform is .5 meters above the bottom platform, reinforced by members radiating out from the center of the triangle. The legs are again designed such that most of the load is carried by a single compression member.

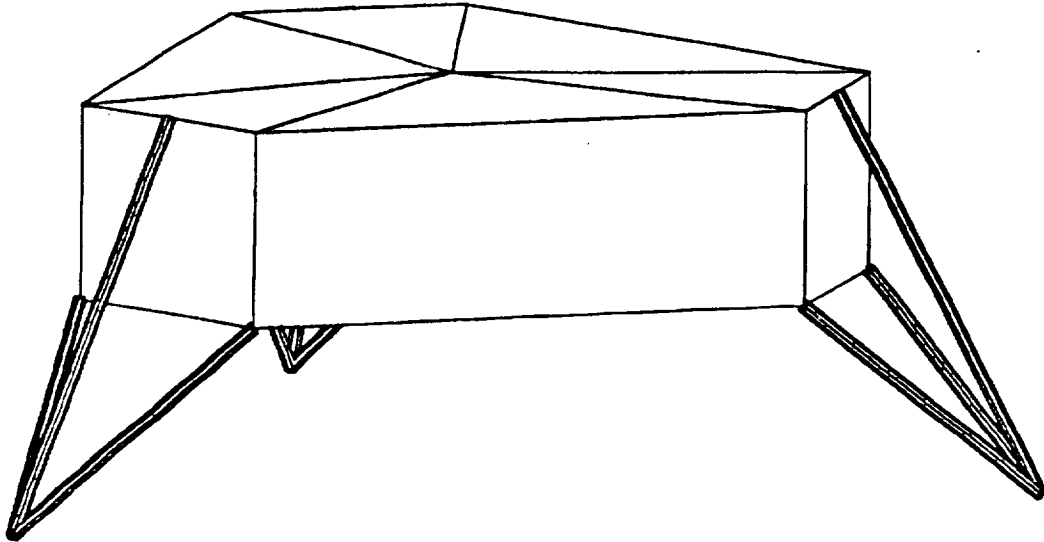


Figure 3.1.2. Semi-Monocoque Design

A consideration for both designs is the method that is used to attach the members. It would be advantageous if the structure could be bolted, rather than welded together. If the structure were bolted, it could be easily disassembled and recycled as building material. Most landers in the past have been connected by welding the joining fittings, so the bolting-only concept would require some background testing. If the feasibility study takes little time, and proves the bolting adequate, this concept will work to our advantage. However, it may violate our axiom of using only current technology and tested systems. With the high cost of carrying material to the moon, every small amount that can be recycled would be advantageous, and this may outweigh the relatively small amount of time and resources spent testing the concept.

Both designs have been statically tested using NASTRAN models, and have proven adequate for supporting the structural loads in all tested static situations. With neither design distinguishing itself as the best structurally, the weight constraint becomes the deciding factor. The semi-monocoque design is abandoned at this point. The skin that is carried along with the lander serves no useful purpose. There is no atmosphere, so no pressure loads need to be resisted, and even though holes can be bored at any place on the skin, some backing structure would be needed. This is analogous to the substructural support members of the space frame design, and is also

comparable in weight. Therefore, the difference in weight becomes the skin, and the semi-monocoque design will weigh more than the space frame.

The space frame design has been statically tested using NASTRAN models. (For details of the model, see Appendix C.) The purpose of the static tests was to locate the structural elements having the maximum stresses during lunar operations (after landing). Time constraints on the design project prohibited dynamic modeling of the structure. The dynamic testing of the current configuration would be an important facet of any future design work. However, the static factors of safety are well over 20, and warrant the continuation of the development, using the results from only static tests. Dynamic tests at a later date would be used to optimize the structural members.

The static tests entailed using axial/bending elements for most of each structure, and modeling the legs in various ways. The structure was modeled using circular cross section tubing of aluminum 7075-T6, having a diameter of 3 centimeters and a thickness of 1.5 millimeters. This tubing was selected as being representative of the kinds of aluminum tubing available for space structures. Future work on the project would address optimization of the elements for weight and safety factor.

The NASTRAN model was tested under various loading conditions. Present in all of the tests were the static loads expected during lunar operation. The payloads were modeled as distributed loads along the payload platform, totalling 600 kg in lunar gravity (500 kg plus a 16% margin of safety). The structure was also loaded in a uniform lunar gravity field, such that it deflects under its own weight. In addition, weights of component subsystems were added. The static loadings described above constituted the primary NASTRAN modeling of the structure. Other tests were performed, such as side loading on the legs due to either reaction control jets or landing with a horizontal velocity. An example of the NASTRAN models used may be found in Appendix C.

The static tests allowed the calculation of important stresses and their locations in the space frame. In the main structure, the maximum

compressive loads were located in the central support members. The maximum tension was located in the bottom hexagon, the members between the leg attachments. Members in compression will be stiffened compared to the members that have to resist only tension, due to the hazards of buckling and local crippling effects of columns in compression.

The landing legs are an important substructure due to the high dynamic impact loads, and other factors such as mounting of the reaction control jets. The NASTRAN model in Appendix C details the structural characteristics of the lander under the static lunar loadings and a static force of 100 Newtons applied on one leg, parallel to the lunar surface and perpendicular to the main strut of the landing leg. The maximum compressive stresses were located in the main load carrying member of the legs. Normally, under no side force, the two lateral support members are in tension. However, the side force causes compression to build in the leeward lateral member. The element itself remains in tension, but a large enough side force would cause compression in the beam. This places constraints on the allowable landing velocity, and the thrust of the reaction control jets. The horizontal landing impact velocity calculation will be available pending the dynamic analysis.

The landing attenuation system has other components that were not modeled in the NASTRAN system. Three examples are the hinged legs for folding, the crushable feet, and the shock absorbing system.

The legs are designed to be folded when the spacecraft is stored in the launch shroud. The two lateral support members are hinged at the midpoint of their lengths, and the main leg support member is rigid. (Hinging provides an alternate load path that would weaken the ability for the rod to take compression, since it would be easier to buckle. Hinging is much less influential on the ability to take tension, as a corresponding problem related to buckling does not exist.) Rotational springs at the hinge point are used to straighten the legs, after explosive retaining bolts are fired. The legs would be deployed after separation from the Centaur, very early in the flight, to allow the reaction control jets to operate.

The feet are made from a crushable aluminum honeycomb, and are attached at the ends of the landing legs. Crushable material is used to absorb impact energy as an added protection from dynamic loading. The foot is rigidly attached to the central leg member, and is pinned to the two lateral support members. This is to allow rotation of the joint during transition from folded leg storage to the extended, landing position.

The main leg support member also includes a fluidic damping-based shock absorbing system. It serves to cushion the dynamic impact load of moon landing, and also to level the spacecraft after touchdown. Specifications of this system depend on the results from dynamic analysis of the spacecraft. One concern here involves the placement of the reaction control system jets at the end of the legs; the shock absorber will cause deflections when the jets fire. Some mechanism will probably be required to prevent shock absorber deflection until touchdown on the lunar surface.

Other important substructural elements have to do with attaching the lander to the rocket motors, and to the launch vehicle. The truss attaching the lunar capture solid rocket motor is a space frame nominally based on truss systems used on Surveyor. It is a simple twelve member arrangement, attached to the solid rocket motor by a ring and bolts, and mounted to the lander frame by explosive bolts. Attachment structure to the upper stage is pending more detailed analysis of the structural hardpoints of the Centaur.

Time constraints forced the reduction of scale of the planned NASTRAN modeling. Dynamic testing of the structure was unavailable, due to the limitations of a single semester project. When testing resumes, it should concentrate on drop tests, acceleration tests, and vibration tests. These tests will result in the sizing of structural members. Beams that have excessive margins of safety can be scaled down, and members that are too weak can be reinforced. Re-sizing of the structure will probably also imply a reduction of the structure weight, since the current margins of safety are extremely high. However, the tests that were run indicate that the design is sound, and warrants further consideration.

Structure Subsystem References:

1. **Surveyor Project Final Report Part I: Project Description & Performance, Vol II. Technical Report 32-1265. JPL, California Institute of Technology. Pasadena, California. July 1969. p. 68.**
2. **Surveyor Project Final Report, pp. 67-75.**
3. **The Viking Mission to Mars, Martin Marietta Corporation. Denver, Colorado. 1979. pp. III-35 - III-38.**

3.2 Power Subsystem

Several criteria were used in the selection of a power system for the CLL. First, since the CLL will not be responsible for powering the payloads, the power supply is only needed for five to fourteen days, depending on the type of mission. For versatility, the CLL is required to function in darkness. Finally, the power supply needs to be reliable and as lightweight as possible. Using these criteria, the following power systems were evaluated:

- Solar photovoltaic
- Batteries
- Radioisotope thermal generators (RTGs)
- Fuel cells

From the condition that the power supply need only last a few days, RTGs were eliminated. Since the lander needed to be able to function in darkness, solar cells were discounted. The remaining options were batteries and fuel cells, both of which could be optimally sized for a short mission. Ultimately, it was determined that fuel cells would probably provide the lighter weight solution. Table 3.2.1 is a decision matrix summarizing the benefits and disadvantages of each system.

Table 3.2.1. Power Subsystem Decision Matrix

Criteria	Weight Factor*	Possible Selections**			
		RTG	Solar	Battery	Fuel Cell
Weight	10	1	5	2	4
Cost	8	1	4	3	3
Reliability	8	5	4	5	4
Size	8	4	3	4	3
Availability	6	1	5	5	4
Reusable	5	1	5	3	4
Power Avail.	4	5	5	5	5
Dark Side Use	6	5	1	5	5
	Total:	151	181	211	216

*Weight scale: 10-important, 1-not important

**Performance scale: 5-good, 1-poor

Fuel cells use a chemical reaction between two reactants to generate electricity. The reactants are gaseous hydrogen (H₂) and gaseous oxygen (O₂). The reaction of the H₂-O₂ fuel cell produces water as a by-product.

The lander has an average power requirement of about 200 W. The power requirements of the subsystems are shown in Table 3.2.2. Not listed in the table is a transient 50 W power requirement for the propulsion subsystem to ignite the STAR 30E. This is because it is required only once for approximately 1 second. The fuel cell will be able to accommodate this propulsion requirement because the other subsystems will not always be at maximum consumption.

Table 3.2.2. Subsystem Power Requirements

Subsystem	Power (W)
Avionics	68
Communication	85
Thermal control	45
TOTAL	200

The 200 W power requirement was used to calculate H₂-O₂ fuel cell mass sizing. Currently, there is little demand for low-power, short duration fuel cells, and information on sizing for such a power supply is unavailable. As a first approximation, fuel cells for the CLL were sized using data from the Space Shuttle fuel cells, which are shown in Table 3.2.3². Extrapolating from this data for a 200 W average power output, 2.2 kg of H₂-O₂ reactants would yield power for 240 hours (10 days). A similar extrapolation for the size of the fuel cell itself yields the unlikely mass of 2.6 kg; a fuel cell mass of 15 kg (including wiring, piping, and reactant vessels) is probably somewhat more reasonable, but this may still be a low estimate. Since the fuel cell uses the H₂-O₂ reactants in their gaseous state, they may be stored as a pressurized gas, so none of the problems associated with cryogenic storage will be encountered. Also, the water by-product will have to be collected and stored.

Table 3.2.3. Space Shuttle Fuel Cell Data

Net Powerplant Output, Steady-State	
Min-Max, kW	2-12
Average, kW	7
Voltage, V	27.5-32.5
Restarts Allowed	
Without Maintenance	50
With Maintenance	125
Lifetime	
Without Maintenance, hours	2000
With Maintenance, hours	5000
Mass, kg	91.6
Specific Mass, kg/kW	13.2
Flow Rate, Average Power	
H ₂ , kg/hr	0.032
O ₂ , kg/hr	0.284

Power Subsystem References

1. Othon, Bill, "Moonport: Transportation Node In Lunar Orbit", The University of Texas at Austin, 1987, p. 142.
2. "Session 7: Propulsion and Power Space Shuttle Electrical Power Generation and Reactant Supply System," (Space Shuttle Technical Conference Part II), pp. 7-16, 7-17.

3.3 Thermal Control Subsystem

The CLL, like any spacecraft, contains many components which will function properly only if they are maintained within specified temperature ranges. The objective of thermal control design is to provide the proper heat transfer between various subsystems and the lander structural elements so that

temperature-sensitive components will remain within their specified limits during all mission phases.

In designing the TCS, solar flux is probably the largest factor to be considered. The lander's attitude relative to the Sun can significantly influence the design of the thermal control subsystem, since it determines the amount of thermal radiation absorbed from the Sun (and the Moon as well, although this quantity is much smaller). Other major heat sources of concern are the communications system, fuel cells, control elements of the power system, the payload, and the exhaust from engines. Table 3.3.1 and Figure 3.3.1 illustrate and summarize some of the temperature margins and environmental conditions which drive the design of the TCS.

Table 3.3.1. Component Temperature Limits

Subsystem/Equipment	Design Operating Range (°C) Min/Max
Structure	-115 / +65
Electronics	0 / +40
Batteries	+5 / +20
Solid apogee motor	+5 / +35
Fuel tank	+7 / +35
Oxidizer tank	-18 / +38
Helium tank	-18 / +43
Earth/Sun sensor	-30 / +50
Angular rate assembly	+1 / +55
Momentum wheel	+1 / +45
Receiver	+10 / +45
Antenna	-170 / +90

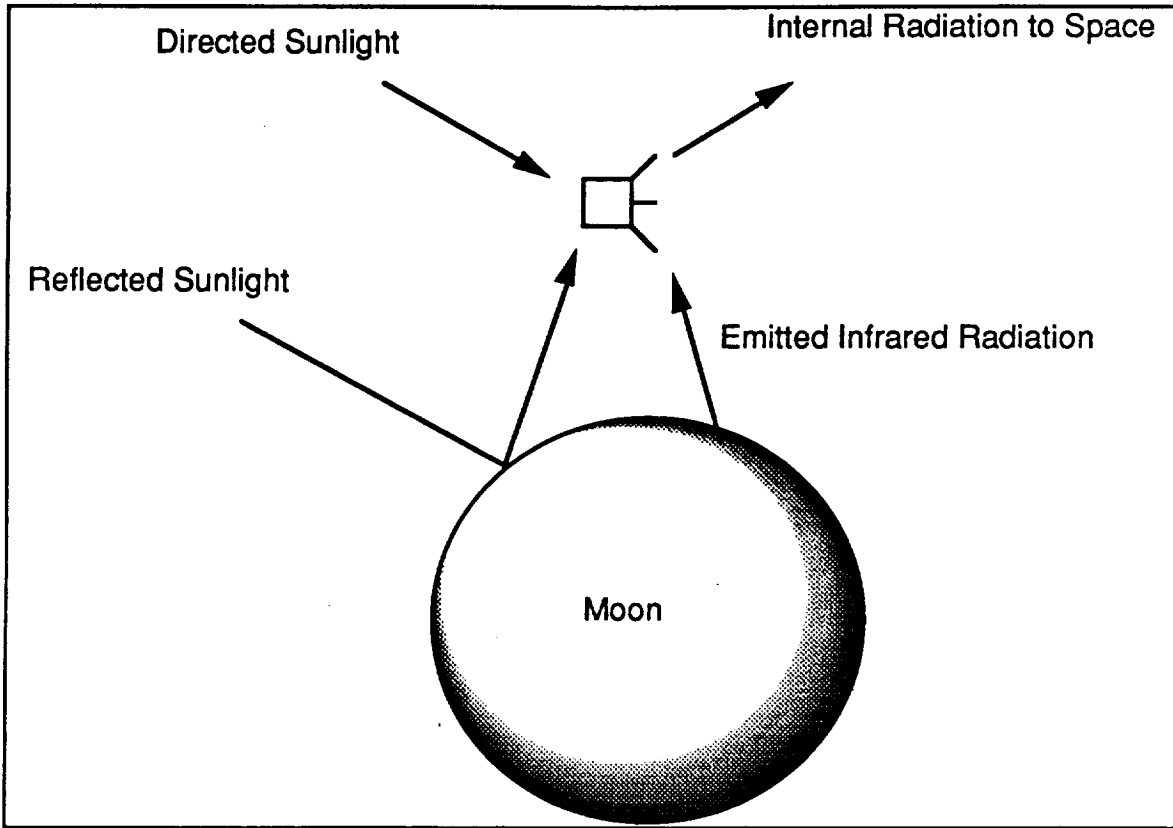


Figure 3.3.1. Energy Balance of Lunar Lander

Before the TCS can be quantitatively designed, information about the flux from the Sun and the heat rejected by various components of the CLL must be known. Since the Earth-Moon distance is considered small compared to the Earth-Sun distance, a nominal direct solar flux of 1371 W/m^2 may be assumed to satisfy the requirement for information about the Sun. The total internal heat radiated from all subsystems, however, can only be determined once the exact systems to be used are known. Therefore, at this stage in the design process, the TCS may only be discussed qualitatively.

Figure 3.3.2 shows variations in lunar surface temperature in two ways: first, the variation of maximum lunar daily temperatures with the latitude of the surface location, and second, the variation of surface temperatures (at the equator) with the position of the Sun in the sky.

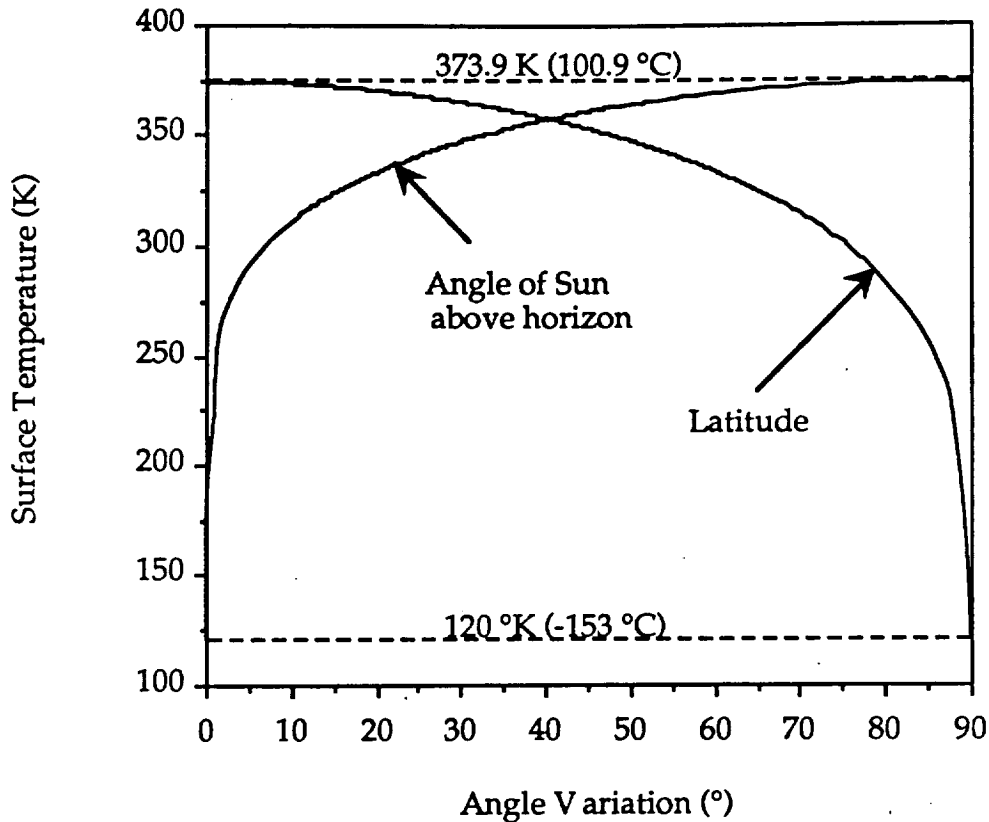


Figure 3.3.2. Lunar Surface Temperature

The maximum temperature during the day can reach up to 100°C and fall well below freezing (-153°C) during the lunar night. The subsystems that operate only during the transit portion of the missions are not designed for post-landing survival, but those that function only on the lunar surface have to survive during transit.

Three main techniques characterize the possible ways of handling the thermal control task: passive, semi-passive, and active systems. Passive systems rely on thermal coatings, multi-layer insulation, phase-change devices, and space radiators as heat sinks. Passive systems usually have no moving parts, require no power, and use thermal radiative properties of external surfaces for temperature control. Semi-passive systems use thermal-mechanical controls to close or open the heat paths, transport heat through heat pipes, and activate louvers to maintain equilibrium temperature during the lunar night. Active systems include pumped-loop heat transfer systems and heaters.

Most of the time, unmanned spacecraft employ passive thermal control techniques¹. Passive thermal control systems will be used whenever possible on the CLL to take advantage of their light weight and low complexity. Passive techniques such as thermal coatings, radiators and heat sinks, insulation, and phase change devices will probably be used in the design of the TCS.

Thermal coatings are highly effective and lightweight. Commonly used surface coatings include paints, gold foil, silver foil, aluminum foil, and silverized plastics. The two characteristic properties of thermal coatings are the emittance of the surface and the solar absorptance. Table 3.3.2 shows the properties of several typical thermal coatings².

Table 3.3.2. Thermal Coating Properties

Surface	Absorptivity (α)	Emissivity (ϵ)
Black paint	0.9	0.9
White paint	0.2	0.9
Silvered Teflon	0.08	0.66
Aluminum	0.12	0.06
Optical solar reflector	0.08	0.8
Titanium	0.6	0.6

Heat sinks are materials of large thermal capacity which are placed in thermal contact with the component whose temperature is to be controlled; a common application is to control the temperature of those items of electronic equipment which have high dissipation. Heat sinks are often combined with radiators to dissipate the heat which they conduct. The equipment and structure of the lander itself could be used as a heat sink and a radiator. For a radiator, low absorptivity (α) and high emissivity (ϵ) are desirable to minimize solar input and maximize heat rejection to space. Multi-layer thermal insulators are insulated blankets, usually made of Kapton separated by Dacron mesh, with low absorptivity and high emissivity. These insulation blankets reduce the heat flow rate of the system while preventing large heat flux. They can be used to wrap around sensors and payloads for thermal insulation and to reduce thermal requirements. The lander structure may be

coated with silver teflon because it has a high emissivity of 0.66 and a low absorptivity of 0.08. Phase change materials are solid materials that melt upon heating, thus absorbing heat; they are usually useful only when on-board equipment dissipation changes widely for short periods.

While passive techniques should satisfy most of the requirements for the thermal control system, some semi-passive and active components, such as louvers and heaters, are required to keep some components from temperature extremes. Figure 3.3.3 shows a design sample of a hybrid thermal-control system using a combination of a phase-change device, a cold plate, a radiator, and an array of louvers¹.

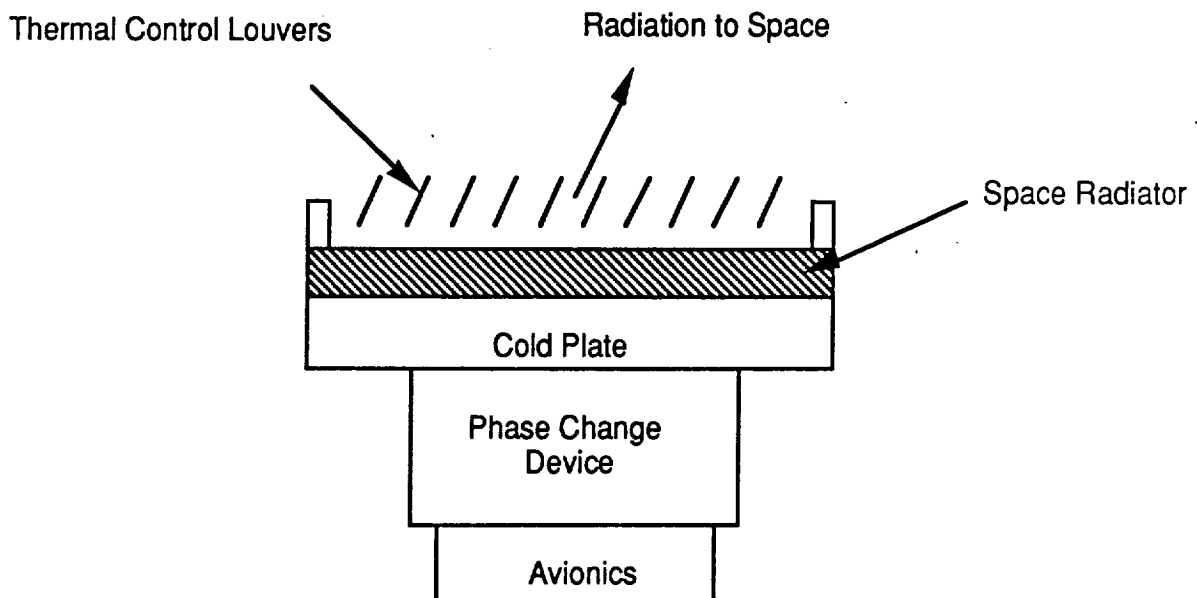


Figure 3.3.3. Hybrid Thermal Control Design Example

The cold plate is used to transfer waste heat dissipated from the bolted electrical equipment. This waste heat is then transported to the radiator which rejects heat to space. A phase-change device is added to absorb thermal energy by changing from a solid to a liquid phase. For lunar night, louvers can be used to reduce heat transfer from the lander to the low-temperature lunar surface. The louvers act like Venetian blinds and are located between a radiator surface and the environment. Opening or closing the louver blades modulates the rate of heat flow away from the lander.

A summary of thermal control techniques and applications is shown in Table 3.3.3.

Table 3.3.3. Thermal Control Techniques and Applications

Techniques	Applications
Surface coatings <ul style="list-style-type: none"> • silvered teflon • optical solar reflector • white paint • black paint 	lander structure radiator surface antenna, interior finishes interior finishes
Multilayer insulation	Earth/Sun sensor, tanks, lines, apogee motor, antenna, payloads
Heat sinks	lander structure, other radiators
Electrical heaters	tanks, valves, lines, thrusters
Phase-change devices	electrical equipment

The thermal control system typically accounts for about five percent of the total spacecraft dry weight. Similarly, the cost of thermal control applications is also about five percent of the total spacecraft cost¹. Adapting information from the Surveyor missions to the CLL, the designed weight for the thermal control subsystem is estimated to be about 43 kg compared to the 264 kg dry weight of the lander, or about twenty percent of the CLL's mass. This is a result of the large volume of fuel required for the lander; the bulk of the mass of the TCS is due to the tank heaters (see Table 3.3.4). The TCS mass of each component is determined based on information of the Surveyor, as shown in Table 3.3.4.

Table 3.3.4. Thermal Control Subsystem Mass Summary

Subsystems	Mass (kg)
Structure	0.36
Propulsion	41.9
Avionics	0.22
Payloads	0.23
Power	0.20
Total	42.9

Thermal Control System References

1. McMordie, Dr. Robert K., "Thermal [Subsystem]," **Spacecraft Mission Analysis and Design** (ed. James Wertz and Wiley Larson), Kluwer Academic Publishers, Dordrecht, The Netherlands, 1991, pp. 370-386.
2. Agraway, Brij N, **Design of Geosynchronous Spacecraft**, Prentice-Hall Inc., Englewood Cliffs, New Jersey, 1986, pp. 265-307.
3. Dubrawsky, Ido, Jeff Kline, John Neff, and Steve Hirshorn, "Thermal Control System Design," **Space Systems Design/Spacecraft Mission Design**, University of Texas at Austin, Fall, 1991, p. 5.

3.4 Avionics Subsystem

The avionics subsystem and the communications subsystem are the only primarily electric/electronic systems on the lander itself, and so constitute the main demand on the power subsystem. Work on the avionics subsystem during this phase of the design concentrated primarily on the guidance, navigation, and control (GNC) of the CLL. This subsystem includes the

mechanisms for determining attitude and position, the actuators for changing attitude and position, the software required to coordinate the two, and the hardware required to execute the software and handle the flow of data.

3.4.1 Constraints on the Avionics Subsystem

Because the design of the CLL is being undertaken with no information about the payloads (other than maximum allowable mass), it is not possible to precisely predict important GNC parameters such as spacecraft principal axes or moments of inertia. Most spacecraft are designed such that these parameters are well-specified, and the GNC systems are designed to meet those specifications.

In contrast, the lander's preferred GNC system must be able to adapt to a range of configurations inside an operational envelope determined by physical constraints. One may determine a range of allowable center of gravity (CG) locations for which the reaction control system (RCS) is strong enough to correct for the moment developed by a main engine (either the solid capture motor or liquid descent engine) when its thrust does not pass through the spacecraft CG. Moments of inertia are another possible constraint on allowable payload configurations related to the GNC system (to ensure reasonable rates of rotation when changes in attitude are required). Once these constraints are well-defined, an adaptive GNC system could be designed to handle configurations which are inside the allowable ranges. Appendix E includes information on spacecraft mass distribution and some estimations of allowable spacecraft CG locations.

Adaptive guidance systems are currently evolving for certain applications, such as Rockwell's IntelliSTAR™ spacecraft control architecture¹. However, there is some question as to whether a system capable of controlling an arbitrarily-loaded spacecraft such as the CLL will be available within the three to five year projected development time. If such a system is unavailable, an alternate system could be developed which would require customization for each mission, once the spacecraft configuration was known. This would decrease the flexibility of the CLL, and potentially increase recurring operational costs.

3.4.2 Operation of the Avionics Subsystem

The avionics subsystem will operate in three relatively distinct modes during the three main phases of the CLL's mission: launch to LEO, lunar transit, and lunar descent and landing. During the launch phase, the avionics subsystem will be quiescent; it will monitor position and attitude without attempting to control the motion. All GNC functions during this phase of the mission will be handled by the launch system itself. Once the CLL separates from the Centaur, the legs will extend, placing the RCS jets in their operational configuration. Three-axis stabilization will begin at this point.

During lunar transit, the GNC subsystem will begin to actively control the attitude and velocity of the spacecraft. During this phase of the mission, attitude and position determination will be made using a battery of sensors, including at least one Sun sensor, Earth/Moon sensors, and at least one star tracker, in conjunction with an on-board ephemeris. These determinations will be backed up by Earth-based tracking information, and on-board gyros and dynamic mathematical models. Small perturbations from the desired CLL attitude will be eliminated using the fine RCS jets. Larger or quicker attitude changes, as well as corrections for moments generated by misalignment of main engine thrust with the spacecraft CG will be made using the coarse RCS jets^{2,3,4}.

During the landing phase of the mission, an additional function of the avionics subsystem will be to determine altitude above the lunar surface. This will be done using a radar altimeter, which will be backed up by inertial devices. Radar altimeters are not a new instrument on explorer spacecraft -- Surveyor used its radar altimeter to signal the engines to shut down 14 feet above the surface for the final free-fall to impact⁵. The CLL will follow a similar descent profile, zeroing out all transverse motion and coming to hover directly above the landing site at a height of about 10 feet before engine shut-off and final impact. Another function of the avionics which will be required during descent is autonomous evaluation of landing sites. A certain amount of fuel may be included for hover time (the fuel tanks were sized to allow 30 seconds of hover time with a 500 kg payload). The lander must evaluate the terrain and determine a suitable landing site. During the initial phases of the design, there was some interest in the use of terrain-following

systems for pinpoint landing accuracy; however, not enough information was available to evaluate that possibility. Research into real-time landing site determination and evaluation is currently being conducted by Ken Baker at NASA's Johnson Space Center; conclusions from that study could probably be adapted to the CLL as well.

Avionics Subsystem References

1. Barry, John, Linas Raslavicius, and Thomas P. Gathmann, "IntelliSTARTM - An Emerging Spacecraft Control Architecture to Improve Autonomous Control and Operation (AAS 91-048)," **Guidance and Control 1991** vol. 74 of *Advances in the Astronautical Sciences*, Univelt, Inc., San Diego, 1991, pp. 187-194.
2. Kaplan, Marshall H, **Modern Spacecraft Dynamics and Control**, John Wiley and Sons, New York, 1976.
3. Wertz, James R. **Spacecraft Attitude Determination and Control**, D. Reidel Publishing Company, Kluwer Academic Publishers, Dordrecht, The Netherlands, 1984.
4. Zermuehlen, Robert and Harold Zimbelman, "Guidance, Navigation, and Control," **Spacecraft Mission Analysis and Design** (ed. James Wertz and Wiley Larson), Kluwer Academic Publishers, Dordrecht, The Netherlands, 1991, pp. 303-328.
5. **Surveyor Project Final Report Part I: Project Description & Performance, Vol II. Technical Report 32-1265.** JPL, California Institute of Technology. Pasadena, California. July 1969. p. 363.

6. Stevenson, John, Teresa Morrison, and Timothy Murphy, "Autonomous Landing on Mars (AAS 90-050)," **Guidance and Control 1990** (ed. Robert Culp and Arlo Gravseth) vol. 72 of *Advances in the Astronautical Sciences*, Univelt, Inc., San Diego, 1990, pp. 363-368.

3.5 Communications Subsystem

The communications subsystem includes all necessary antennas, receivers, and transmitters required to maintain contact with the Earth during flight and after the CLL is on the surface. This subsystem is the only subsystem in which it is desirable that all components be completely shared between the lander and the payload(s). This decision was made because it was thought that requiring payloads to provide for their own communication was too big a burden to place on payload designers, and would be prohibitively inefficient if the lander were carrying multiple payloads from independent parties.

Additionally, the CLL will have no use for its communications equipment after landing, so its transmitters, receivers, and antennas would be fully functional and completely unused after a successful landing. The logical solution is to design the communication subsystem for re-allocation from the CLL to the payload(s) after landing. This re-allocation would involve switching the feeds to the communications subsystem from the CLL power supply to the payload power source, as well as switching the communication links themselves from the CLL to the payload(s).

Two different loads are expected for the CLL communications system. During the lunar transit phase, communications between the lander and the Earth are expected to be minimal, primarily due to the independent mode of operation of the spacecraft. Communications during this phase of the flight should be manageable using two low-gain, omni-directional antennas (LGAs) on opposing sides of the craft. The use of omni antennas will reduce pointing requirements, at the expense of input power required for the transmitter. Once the CLL has landed, and all the communications system controls have been passed to the payloads, the high-gain antenna (HGA) will probably be required to handle higher transmission rates, although the LGAs would still

be available as backups in case of an HGA failure. This will constrain lander orientation on the surface of the Moon. The CLL must be in a position where the HGA can track the Earth. Of course, until some type of communications satellite is placed at the Moon (either in orbit around the Moon itself or in a "halo" orbit around the Lagrange point behind the Moon), there will be no way to communicate with a CLL on the far side of the Moon.

No missions have been flown to the Moon since the end of the Apollo program in the mid-1970s, so information on actual Earth-Moon communications systems using recent technology is unavailable. Because of this, it was decided to model a "worst case" communications system for the CLL by using Surveyor data, since the missions are similar. The "worst case" designation refers to the probability that an actual system utilizing more recent technology could be designed to be lighter weight, require less power and space, and have better overall performance.

The communications system will probably operate in the S-band, like most other explorer spacecraft. Mass estimates of the entire communications subsystem (two transmitter units, two receiver units, two LGAs and one HGA), based on data from the 1960s Surveyor missions, are on the order of 20 to 30 kg; power requirements are estimated to be on the order of 10-15 W during low-power (HGA) communication and about 75-100 W for high-power (LGA) communication¹.

Communications Subsystem Reference

1. **Surveyor Project Final Report Part I: Project Description & Performance, Vol II. Technical Report 32-1265.** JPL, California Institute of Technology. Pasadena, California. July 1969. pp. 401-411.

3.6 Propulsion Subsystem

The CLL propulsion subsystem is required to provide orbit change capability and attitude control. Table 3.6.1 shows the CLL propulsion requirements (determined through trajectory analysis) used in designing the propulsion

subsystem. The total velocity change (ΔV) required from low Earth orbit (LEO) to lunar landing is 5.95 km/s, of which 2.80 km/s is provided by the CLL propulsion subsystem. Leaving low-Earth orbit (LEO) requires the largest velocity change and will be provided by the Centaur upper stage. For attitude control, the CLL must provide three-axis stabilization after separation from the Centaur upper stage until touchdown on the lunar surface. Three-axis stabilization requires control during three orbit change ΔV 's, attitude maneuvering, and for limit cycling in the control system¹. Thrust vector misalignment with the center of mass during lunar parking orbit (LPO) insertion, LPO descent, and landing ΔV 's also requires attitude control. The CLL must maneuver 180 degrees for correct positioning prior to ΔV for entering LPO; in addition, the CLL must make two approximately 90 degree maneuvers twice during landing. A thrust to weight ratio of 0.5 earth g is necessary for descent from LPO, while a thrust to weight ratio of 1 lunar g (1/6 earth g) is required to hover above the lunar surface.

Table 3.6.1. CLL Propulsion Subsystem Requirements

ΔV	
LEO Departure	3.146 km/s (provided by Centaur)
LPO Insertion	.7942 km/s
LPO Descent	.0329 km/s
Landing	1.973 km/s
Attitude Control	
Three-axis Control During ΔV	
Three-axis Attitude Maneuvering	360 deg
Limit Cycling	0.5 deg dead zone

Of the various propulsion system types available, chemical rockets are the best choice for low cost and high thrust. Chemical rocket engines can be separated into three broad categories: solid, liquid, and hybrid. Furthermore, liquid engines can be monopropellant or bipropellant. Monopropellant engines have lower specific impulse than bipropellant engines, but only one set of fuel tanks and lines are needed. Bipropellant engines are the most common type of liquid fuel rocket². The propellants used in liquid engines can be classified as storable or cryogenic. Cryogenic propellant loss due to boil-off becomes a factor in longer missions. Storable propellant has a higher

boiling point than cryogenic propellant and remains liquid without requiring cooling.

Table 3.6.2 shows the decision matrix used for determining the best engine. Engines are rated from 1 (poor) to 5 (good); the highest total is the best choice. The selection criteria used to determine engine type are propellant storability, safety, density, specific impulse, and engine simplicity. Specific impulse is a measure of performance and propellant density reflects fuel tank volume concerns. Solids are the best choice for lunar capture where variable thrust is not necessary. The variable thrust requirement during landing prevents the use of solids during landing since the thrust profile of solids is fixed when the motor is manufactured. As a result, storable bipropellant is the best choice for landing and descent from LPO.

Table 3.6.2. Selection of Engine Type

Category	Weight Factor*	Possible Selections**				
		Solid	Storable Mono-propellant	Storable Bipropellant	Cryogenic Bipropellant	Cold Gas
Storability	10	5	4	4	1	1
Safety	4	3	1	1	5	5
Density	6	5	3	3	1	2
Isp	9	3	2	4	5	1
Simplicity	8	4	3	2	1	5
Total		151	104	114	89	91

*Weight scale: 10-important, 1-not important

**Performance scale: 5-good, 1-poor

A three stage configuration has been chosen for the lunar lander propulsion subsystem. The first and second stages provide the ΔV 's necessary to leave LEO parking orbit and enter LPO. The third stage provides ΔV for descent and landing from LPO. The CLL's propulsion system is sized for a dry mass of 264 kg.

The Centaur upper stage is the CLL's first stage. Cryogenic LOX and LH₂ provide a specific impulse of 440 seconds necessary for the largest ΔV at LEO departure. High specific impulse reduces propellant mass.

The CLL's second stage is a Morton Thiokol STAR 30E (TE-M-700-19) solid motor. Figure 3.6.1 shows a schematic of the STAR 30E. This solid motor has been fired in three flights and tests. It has been chosen as the apogee motor for the BAe Skynet 4 satellite³, and is currently in production.

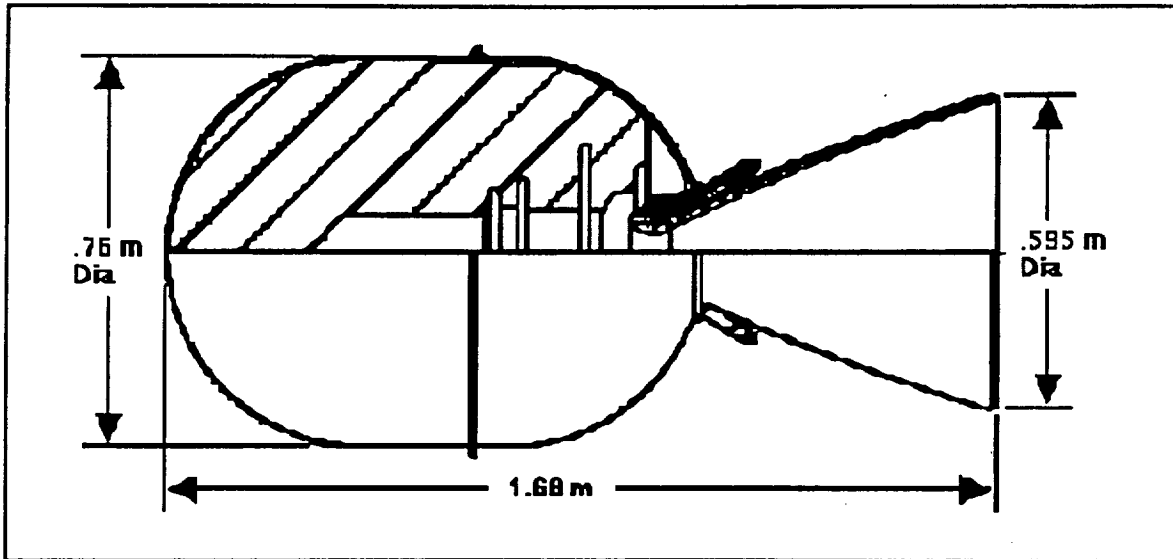


Figure 3.6.1. STAR 30E Schematic

Table 3.6.3 presents performance characteristics of the STAR 30E. The cylindrical length of the motor case can be increased to provide a larger propellant load; also, the length can be decreased for a smaller propellant load. By increasing or decreasing the cylindrical case length, the STAR 30E motor mass and propellant mass increase or decrease 809 kg/m and 784 kg/m, respectively.

Table 3.6.3. LPO Insertion Motor Specifications³

Manufacturer	Morton Thiokol
Model	STAR 30E
Motor Performance	
Burn Time/Action Time	49 / 50 sec
Ignition Delay Time	0.10 sec
Total Impulse	1781 kN-sec
Propellant Specific Impulse	291.9 sec
Effective Specific Impulse	289.2 sec

Burn Time Average Thrust	35400 N
Action Time Average Thrust	35200 N
Maximum Thrust	41000 N
Weights	
Total Loaded	667.3 kg
Propellant (Including 0.27 kg Igniter Propellant)	621.7 kg
Case Assembly	17.5 kg
Nozzle / Igniter Assembly (Excluding Igniter Propellant)	17.4 kg
Internal Insulation	9.30 kg
Liner	0.726 kg
Miscellaneous	0.726 kg
Total Inert (Excluding Igniter Propellant)	45.63 kg
Burnout	39.83 kg
Propellant Mass Fraction	0.932
Propellant	
Propellant Designation and Formula	TP-H-3340 AP - 71%, Al - 18%, HTPB Binder - 11%
Current Status	Production

The CLL's third stage consists of a pressure-fed, hypergolic propulsion system using a single Marquardt R-40A engine for descent and landing. Specifications for the R-40A are shown in Table 3.6.4.

Table 3.6.4. Descent and Landing Engine Specifications⁴

Manufacturer	Marquardt
Model	R-40A
Fuel	Monomethyl hydrazine (MMH)
Oxidizer	Nitrogen Tetroxide (N ₂ O ₄)
Fuel Flow Rate	.526 kg/s
Oxidizer Flow Rate	.838 kg/s
Tank Pressure	1640 kPa
Length	.67 m
Nozzle Exit Diameter	.653 m
Mass	9.5 kg
Max Thrust (vacuum)	3870 N
Chamber Pressure	1050 kPa
Specific Impulse	306 sec
Area Ratio	120

The R-40A is qualified as a Space Shuttle RCS engine and is currently used on the U.S. Navy's Shuttle Launch Dispenser.⁴ The engine and nozzle extension is constructed of silicide coated columbium. The engine's exterior is insulated for buried installation; the engine uses internal film cooling. The nozzle extension increases specific impulse which reduces the propellant load. The use of hypergolic propellants increases reliability and allows for multiple restarts. The attitude control thrusters use the same propellant as the descent and landing engine. Two different attitude control thrusters are used: 445 N coarse thrusters and 21 N fine thrusters. The coarse thrusters are necessary for rapid maneuvering during the landing phase, while the fine thrusters are necessary because lower thrust levels are necessary for attitude corrections. Specifications for the coarse thrusters are shown in Table 3.6.5; specifications for the fine thrusters are presented in Table 3.6.6.

Table 3.6.5. Coarse Attitude Control Thruster Specifications⁵

Manufacturer	Aerojet
Model	Satellite Engine
Fuel	Monomethyl hydrazine (MMH)
Oxidizer	Nitrogen Tetroxide (N ₂ O ₄)
Thrust	445 N
Specific Impulse	309 sec
Mass	1.9 kg

Table 3.6.6. Fine Attitude Control Thruster Specifications⁵

Manufacturer	Aerojet
Model	Satellite Engine
Fuel	Monomethyl hydrazine (MMH)
Oxidizer	Nitrogen Tetroxide (N ₂ O ₄)
Thrust	21 N
Specific Impulse	285 sec
Mass	0.59 kg

Propellant mass is calculated after engine selection by using specific impulse, ΔV requirements, and attitude control requirements. Table 3.6.7 shows propellant allocations for the CLL.

Table 3.6.7. Propellant Summary

	Propellant (kg)
ΔV 's	
LPO Descent	16
Landing	709
Attitude Control	
Three-axis Control During ΔV	31
Three-axis Attitude Maneuvering	5
Limit Cycling	1
Nominal Propellant Load	762
Allowance for Off-nominal Performance (1%)	8
Allowance for Off-nominal Operations (1%)	8
Mission Margin (10%)	76
Total Required Propellant	854
Residual Propellant (1.5%)	13
Loading Uncertainty (.5%)	4
Total Propellant Load	871

Extra propellant for off-nominal performance and operations, mission margin (10%), residual (trapped), and loading uncertainty is included in the propellant mass calculation. By knowing propellant mass and density, propellant volume is calculated. The tanks are sized once propellant volume is known. Extra volume is included in sizing the fuel tanks (10% ullage) in order to leave room for vapor and helium pressurant. Spherical tanks can't be placed in the space between the CLL and the launch vehicle payload shroud; therefore, cylindrical tanks are used. The cylindrical tank diameter is constrained by the space between the CLL and the launch vehicle. Tank thickness of 1 mm is determined from material and tank pressure requirements. Both fuel and oxidizer tanks are constructed from 6Al-4V titanium with a safety factor of 2. Table 3.6.8 presents propellant tank specifications. The propellant tanks use positive expulsion with the propellant contained in teflon bladders; the propellant tanks are similar to Surveyor.

Table 3.6.8. Propellant Tanks

Fuel Tank	
Length	1.0 m
Diameter	0.5 m
Mass	7.0 kg
Oxidizer Tank	
Length	0.97 m
Diameter	0.5 m
Mass	6.8 kg

As shown in Figure 3.6.2, the CLL third stage is a regulated pressurization system using helium stored at 41.4 MPa. The helium mass required is 1 kg. Surveyor used the same amount of helium pressurant at 35.8 MPa; CLL uses Surveyor's helium tank constructed out of 6Al-4V titanium with a mass of 15 kg.⁶ Helium passes through a filter before entering a pressure regulator. The pressure regulator reduces helium pressure from storage pressure (41.4 MPa) to propellant tank pressure (1.64 MPa). A dump-valve is included to vent the remaining helium once the CLL has landed. A relief valve is installed after the pressure regulator to prevent propellant tank over-pressurization. Squib-actuated release valves keep the system safe until after launch. Check valves prevent propellant mixing anywhere except combustion chambers. Single fault tolerant redundancy is provided where possible to ensure operational capability in case a single squib-actuated valve does not open. Relief valves, squib-actuated release valves, check valves, and propellant tanks should be similar to Surveyor designs.⁷ For variable thrust, a throttling valve is needed to keep combustion chamber pressure constant while reducing the flow of propellant to the R-40A engine. A throttling valve based on the Surveyor design would probably suffice.⁸

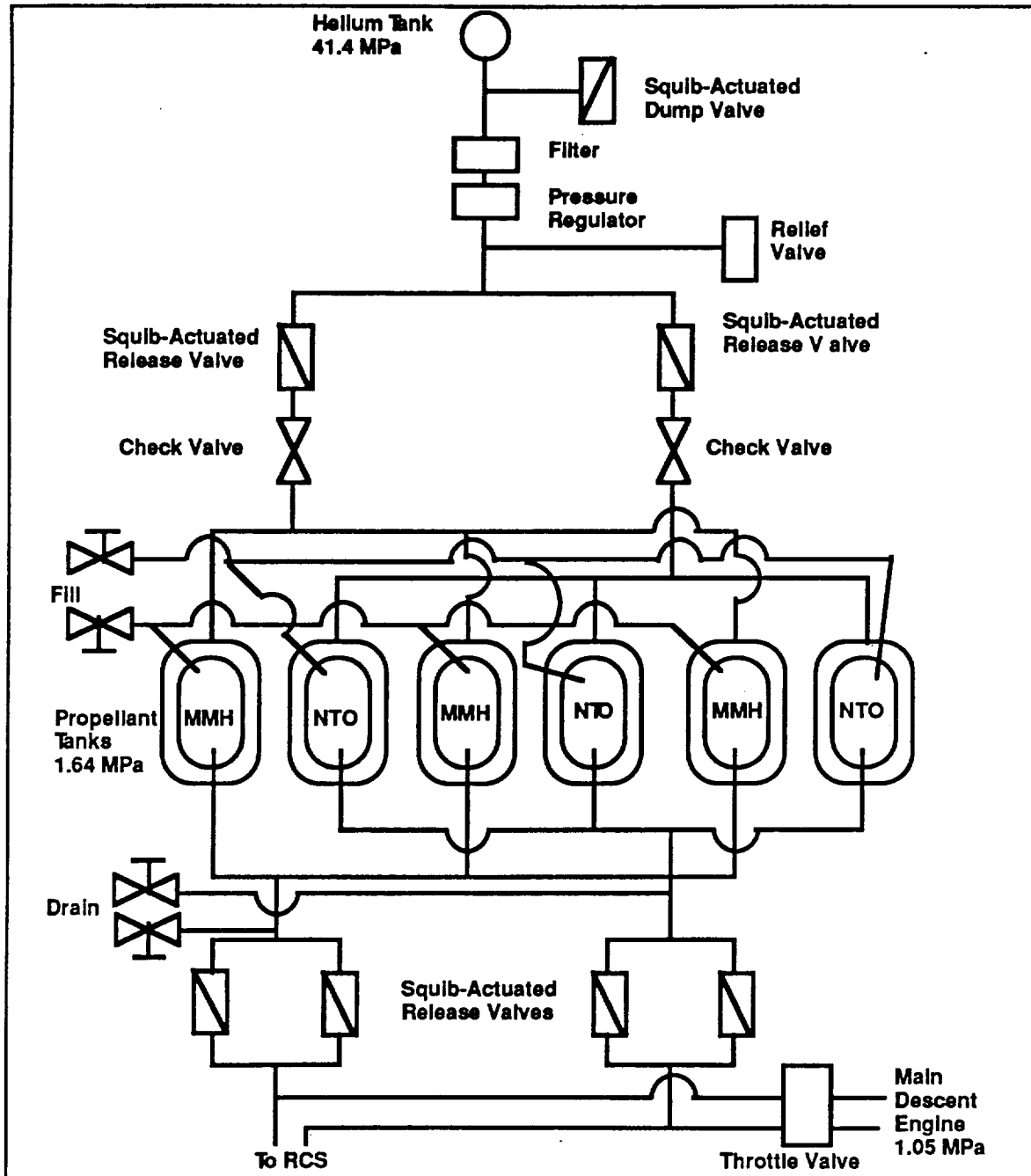


Figure 3.6.2. CLL Third Stage Propulsion System Schematic

Table 3.6.9 presents a mass statement for the CLL propulsion subsystem. The total dry mass of the propulsion subsystem is 776 kg; with propellant, the total mass of the propulsion subsystem is 1648 kg. The CLL propulsion subsystem

uses flight proven engines and a bipropellant feed system based on Surveyor technology and design experience.

Table 3.6.9. CLL Propulsion Subsystem Mass Summary

Component	Quantity	Component Mass (kg)	Total Mass (kg)
Fuel Tank	3	7.0	21
Oxidizer Tank	3	6.8	20
Helium Tank	1	15	15
Fittings, Misc.			8.7
R-40A Engine	1	14	14
Aerojet (445 N)	12	1.9	23
Aerojet (21 N)	12	0.59	7
STAR 30E	1	667	667
Propellant			871
Helium			1
Total			1648

Appendix F presents the propulsion subsystem sizing methods and a database of additional engines.

Propulsion References

1. Wertz, James R. and Wiley J. Larson, **Space Mission Analysis and Design**, Kluwer Academic Publishers, Dordrecht, The Netherlands, 1991, p. 273.
2. **Spacecraft Subsystems, Propulsion Subsystem Report and Database**, UT Austin, January 1991, p. 6.
3. Morton Thiokol STAR Handbook.
4. **Jane's All the World's Aircraft 1990-91**, Jane's Information Group Limited, United Kingdom, 1990, p. 745.
5. **Jane's All the World's Aircraft 1984-85**, Jane's Information Group Limited, United Kingdom, 1990, pp. 855-856.

6. Surveyor Project Final Report, Part I. Project Description and Performance, Volume II, Jet Propulsion Laboratory, 1969, p. 240.

7. Surveyor Final Report, pp. 242-252.

8. Surveyor Final Report, p. 228.

3.8 Final Design Configuration

The last task undertaken in this phase of the design was the integration of the various subsystems as they are currently envisioned. This process was undertaken by the entire group, and involved not only the placement of the various subsystems, but also the confirmation of mass estimates and power requirements. An illustration of the actual lander in its fully configured state is shown in Figure 3.8.1 (a discussion of the evolution of the CLL design is presented in Appendix D). A mass summary of the entire, fully loaded lander is listed in Table 3.8.1.

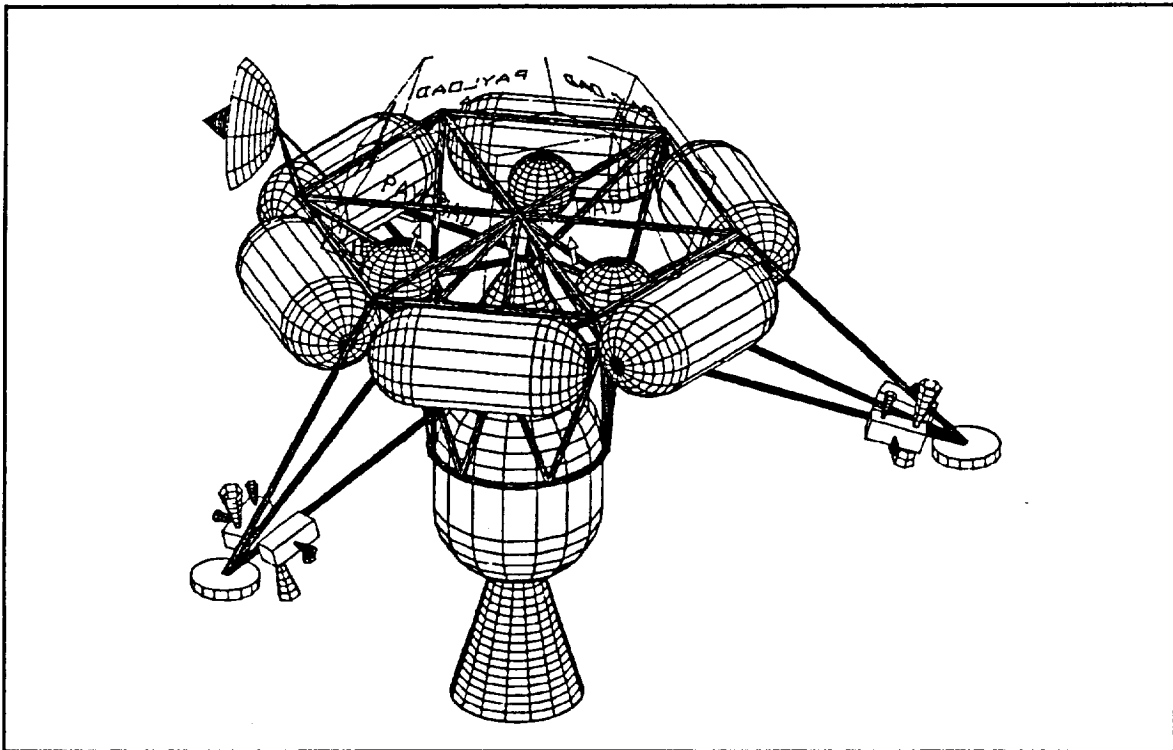


Figure 3.8.1. Final Common Lunar Lander Design (Fully Configured)

Table 3.8.1. CLL Mass Summary

Lander Components:	
Propulsion Hardware	109
Avionics	20
Communications	14
Thermal Control	43
Power	17
Structure	<u>65</u>
Subtotal	268
Payload	<u>500</u>
Spacecraft Dry Mass	768
Propellants and Consumables	<u>874</u>
Loaded Mass	1642
<u>LPO Insertion Motor</u>	<u>667</u>
Fully-loaded CLL Mass:	2309 kg

The short time available for completion of this design required that certain issues raised during the course of the project did not receive as much attention as we would have liked. For instance, the structure of the CLL was tested mathematically, but only under certain static loads. Further static tests should be performed. Time constraints prevented any dynamic analysis of the structure; the truly critical loads on the structure will be the dynamic loads which occur during launch, transfer orbit entry and landing, and these loads need to be studied. Also, further trajectory analysis needs to be done. With more refined estimates of the ΔV s required, especially if estimates were made for several possible mission scenarios, more accurate estimates of fuel mass could be made. Further, some estimates of the fuel required for RCS operation when the thrust vector does not pass through the center of mass (see Appendix E for information on CG analysis) would be useful; with a large misalignment between the thrust vector and the CG, large amounts of fuel could be required to correct for adverse moments. While there are other issues which deserve further attention as well, these are some of the most important issues which we feel need to be addressed.

4.0 Conceptual Payload Design

The Corporation has been tasked with development and integration of four to six conceptual payloads to be carried by the lander. Ideally, the payloads should operate independently of the lander, with the exception of the communications subsystem and the possible exception of using the lander as a radiator for heat transfer. Payload missions which have received attention include a common power system to supply other payloads, an experiment package, a sample return module with tethered micro-rover, materials utilization and testing systems, and families of containers (including options for pressure, power, unloading, etc.) for future payload packaging. These missions were selected using the results of a survey of the potential CLL user community¹. Other ideas which have been forwarded include such payloads as modular building components, a ground communications relay station, and a ballistic distribution system for smaller payloads requiring placement away from the lander; however, the main focus of this design effort remains the CLL itself, and time and resources do not allow for an in-depth study of all of the ideas proposed.

4.1 Common Payload Power Supply

It was stated in the request for proposal that each of the payloads should be as independent of the lander as possible. At the same time, it would be advantageous if each payload were not required to provide its own power. One possible solution to this problem would be a common power supply which could be used by all payloads on a mission. It is difficult, however, to design one single power supply which would be acceptable for a large variety of payloads or payload combinations. Modular power packs would allow each payload to tie into a single power source, which could be tailored to fit specific mission needs. Two modular power subsystems which seemed the most promising are deployable solar arrays for short-term, relatively low-power equipment, and a small radioisotope thermal generator (RTG) for equipment requiring power for longer durations. This second option would be ideal for experimental packages that would operate from one to ten years after

touchdown on the moon. RTG's can be manufactured for power output as small as 14 watts, and can deliver this power for over 10 years.

4.2 Sample Return Mission

In order to facilitate exploration and research, a Sample Return Module (SRM) has been conceptualized which would be capable of sending a 38 kg sample from the lunar surface to LEO, where it would be retrieved. The SRM incorporates a propulsion subsystem and GNC into a one-half meter diameter by one meter tall package. The mass of the SRM including propellant is 400 kg.

Loading of the SRM will be accomplished by means of a tethered micro-rover. Currently, NASA's Jet Propulsion Laboratory is experimenting with a 55 pound micro-rover to incorporate into future Mars missions². The micro-rover's dimensions are 24x20x16 inches, and information on power consumption is not yet available. An expandable ramp will allow the micro-rover to exit and return to the payload platform of the lander, allowing the SRM to be loaded with gathered materials. The micro-rover, including the tether and related electronic navigational equipment, has a mass of 100 kg. The SRM and the micro-rover together fit within the limit of the CLL's 500 kg payload capacity.

As an alternative to the micro-rover, a soil auger could be mounted to the lander's frame which would allow for soil sampling. Figure 4.2.1 shows a schematic of an auger which could be utilized. A benefit to using a micro-rover instead of an auger is that a wider variety of soil samples can be obtained due to increased mobility.

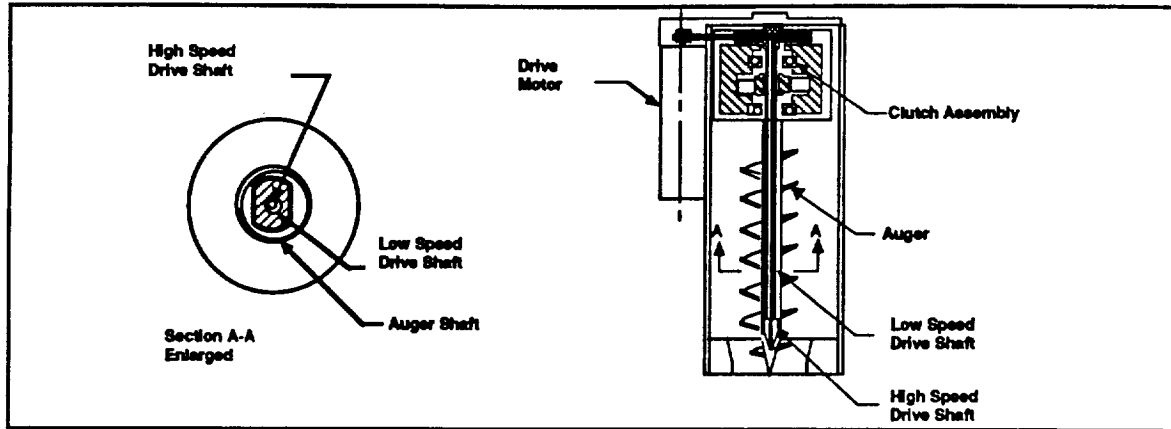


Figure 4.2.1. Soil Sample Auger

4.3 Experimental Packages

To enable advancement in lunar research, several experimental packages are being examined for use on future lander missions. These packages include gamma-ray and X-ray spectrometers, ion mass spectrometer, multi-spectral photography, microwave radiometers, and solidification experiments. The microwave radiometer fell within the weight constraints; however, the dimensions of 4x4x4 meters would fit neither the two meter diameter platform nor any payload fairing available for the Atlas launch vehicle. On the other hand, the solidification experiment (1x1x2 meters) fits on the lander, but its weight of 1100 kilograms exceeds the payload weight limit of the lander.

The X-ray spectrometer measures the composition of the lunar surface from the lunar parking orbit, as well as measuring the galactic X-ray flux during the trans-lunar coast period. Once on the lunar surface, the X-ray spectrometer will continue to analyze solar X-ray interaction. The estimated mass of the X-ray spectrometer is 465 kilograms, with an operating power of 30 watts³.

The gamma-ray spectrometer measures the chemical composition of the lunar surface in conjunction with the X-ray experiment. The device can measure energy ranges from 0.1 to 10 million electron volts, and is capable of operation on the Moon's light and dark sides⁴.

The mass spectrometer measures the composition and distribution of the lunar atmosphere, identifies possible sources of volatiles, and detects contamination in the lunar atmosphere. The mass spectrometer uses two ion counters to detect species from 12 to 28 atomic mass units (AMU), and from 28 to 66 AMU. Its dimensions are 0.5 x 0.5 x 0.4 meters and it weighs 80 kilograms. The power requirement of the mass spectrometer is 334 watts.⁴

Payload References

1. National Aeronautics and Space Administration/Johnson Space Center, **Workshop on the Concept of a Common Lunar Lander**, July 1991.
2. **Aviation Week & Space Technology**, McGraw-Hill Publication, Vol 135, No 13, September 30, 1991, p. 71.
3. Wertz, James R. and Wiley J. Larson, **Space Mission Analysis and Design**, Kluwer Academic Publishers, Dordrecht, The Netherlands, 1991, p. 219.
4. National Aeronautics and Space Administration, **Press Kit**, Washington, D.C., March 22, 1972, p. 86.

5.0 Corporate Structure and Cost Status

5.1 Management Overview

Figure 5.1.1 shows the corporate structure of the Austin Cynthesis Corporation. The program is headed by a Project Manager, with a Technical Manager and an Administrative Manager as assistants in project coordination.

The Administrative Manager is tasked with the collection and organization of timekeeping and cost data, and scheduling. His duties also include preparing weekly summaries of project progress, current problems, and projected accomplishments to provide the Project Manager with information for briefings to the Contract Monitor. All scheduling problems, including projected schedule slips and recovery plans, are addressed by the Administrative Manager.

Because of the small size of our corporation, only one technical management position has been created to oversee the several smaller design task groups. The responsibilities of the Technical Manager include directing the technical course of the design effort, ensuring the validity of major assumptions made during analysis, and verifying the major results of the analysis. If problems arise which cannot be resolved inside a design task group, they are brought to the attention of the Technical Manager for resolution. Problems or suggestions which require a significant change in either the current design configuration (i.e., a change affecting other design task groups) or the projected project schedule will be dealt with by the Technical Manager, Administrative Manager, and Project Manager in committee. There have not been any problems that could not be resolved by the management committee.

Figure 5.1.1 also indicates the various individual design task groups in the Corporation. Each group has one to three members assigned to perform the necessary research and analysis required during the design process. The first name listed in each group is the nominal leader of the group; his

responsibilities are to maintain contact with the Technical Manager and submit weekly group status reports to the Administrative Manager.

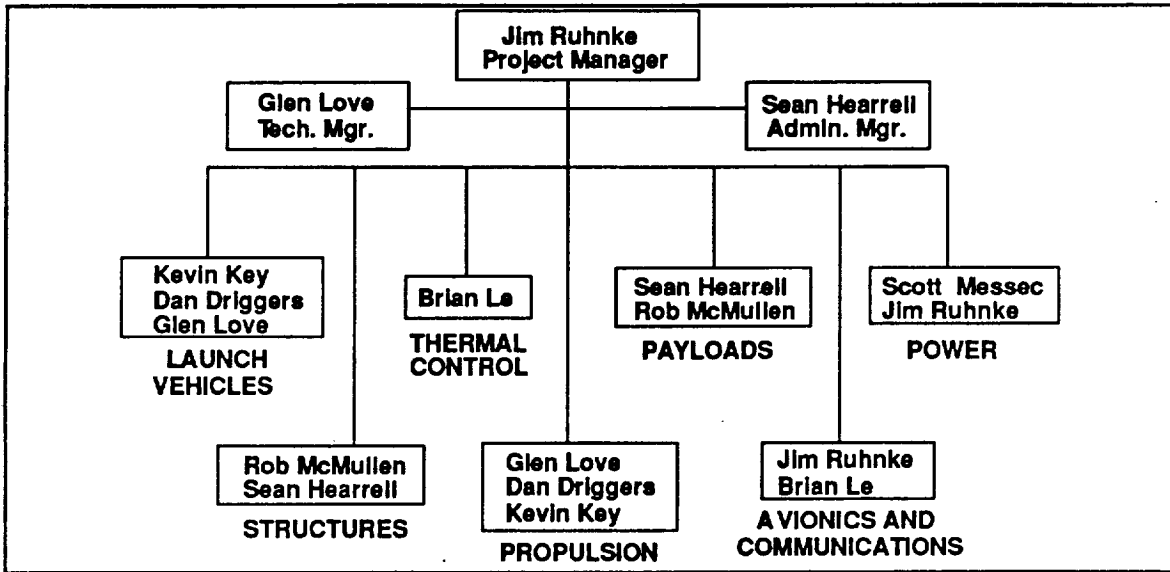


Figure 5.1.1. Corporate Structure

For the final phases of the design, one more group was required to address the integration of the various subsystems. Due to the small size of the overall design team, it was possible for this problem to be addressed by the entire group at once.

5.2 Critical Design Path and Scheduling

Figure 5.2.1 shows the Critical Design Path which was followed over the course of the design. Major milestones lie directly on the path and are identified by hexagons. Both major and minor milestones are indicated in the Project Schedule Gantt chart in Figure 5.2.2.

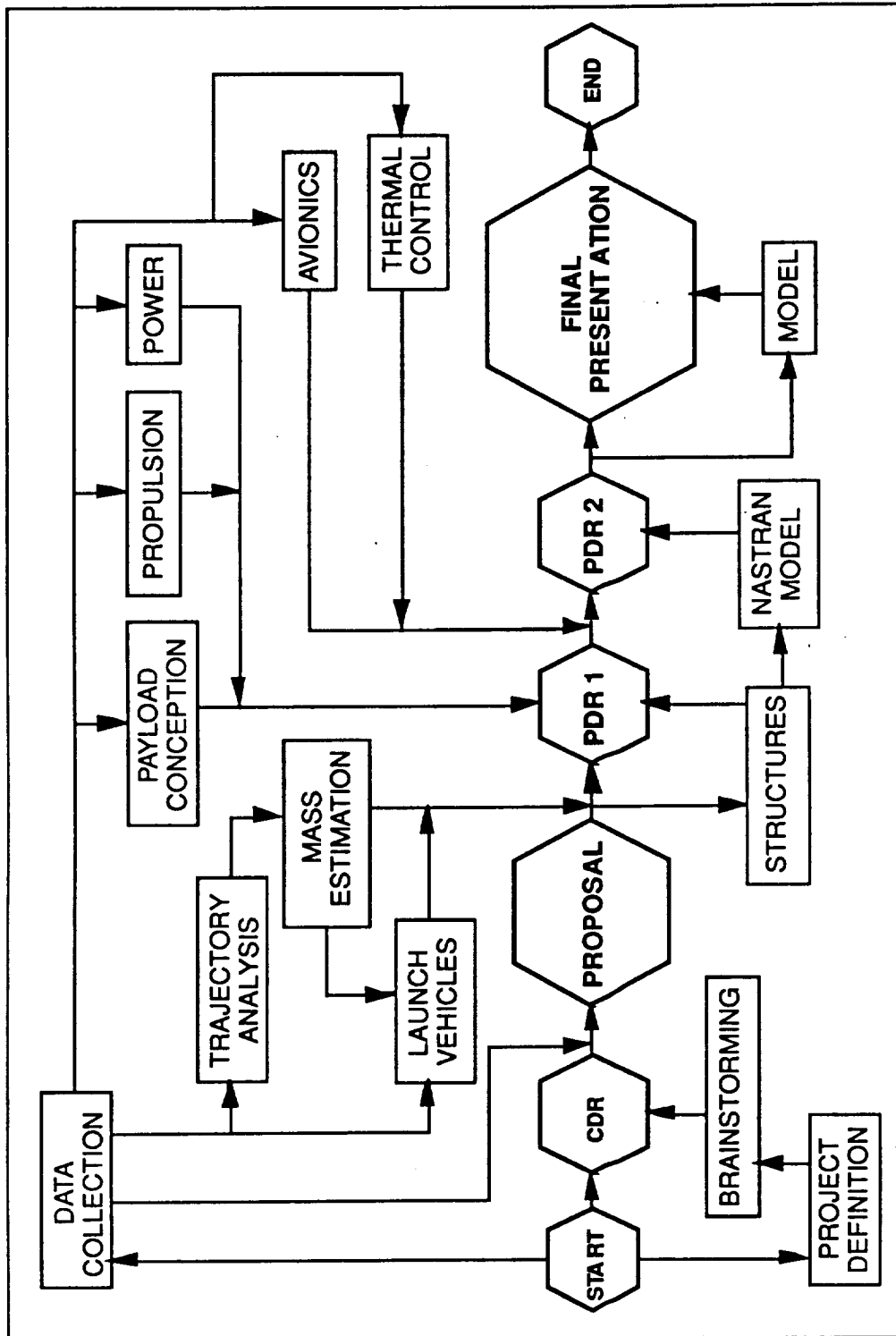


Figure 5.2.1. Critical Design Path

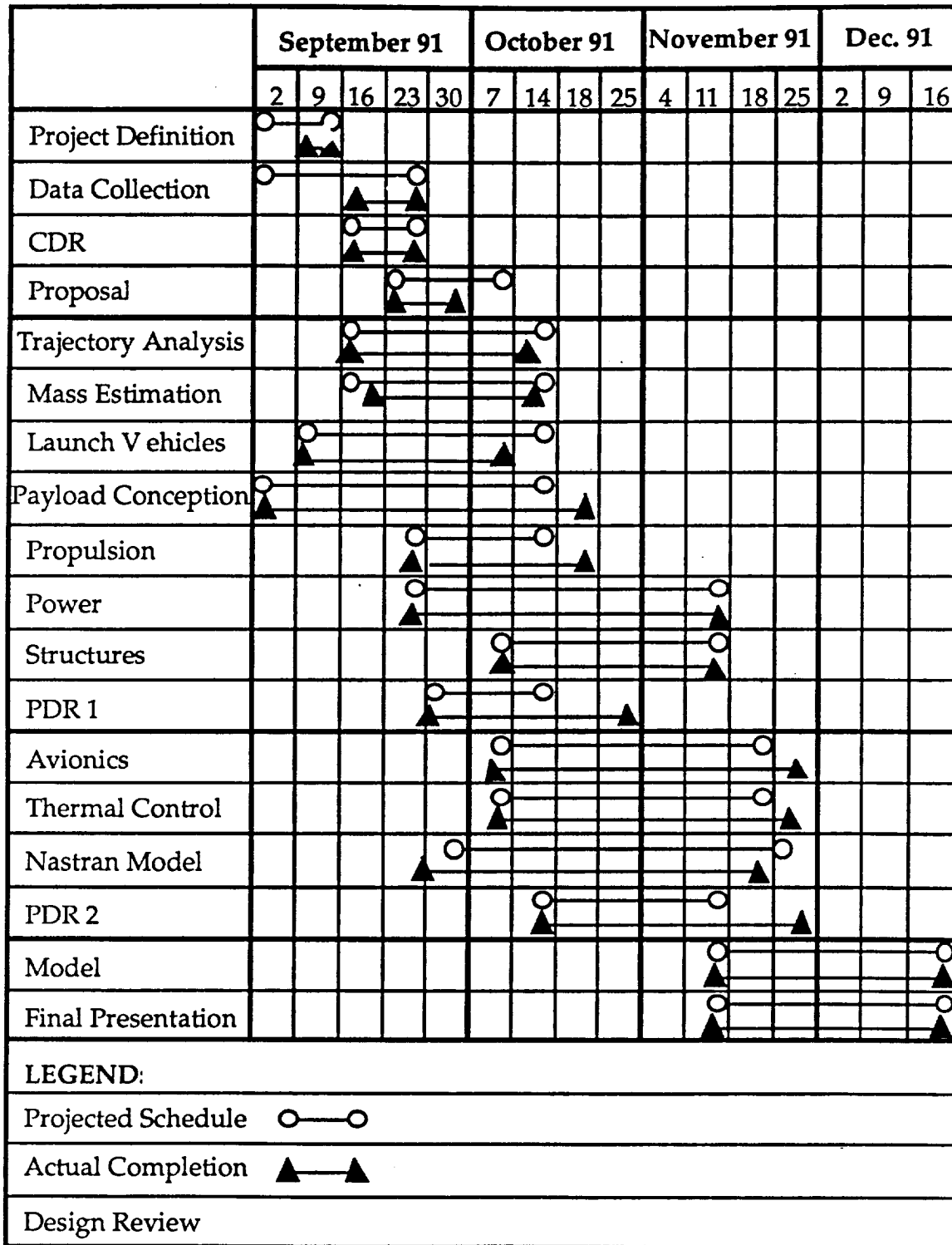


Figure 5.2.2. Schedule of Project Milestones

5.3 Cost Information

5.3.1 Personnel Cost

Salaries associated with various job titles were provided in the Request for Proposal. The number of hours per employee per week are based on a total group meeting time of nine hours per week and an additional six to nine hours of individual time. Actual time spent on the project closely follows the estimated weekly time estimates that were made in the proposal. Figure 5.3.1.1 shows how actual hours compare to estimated hours. A summary of the projected personnel costs are shown in Table 5.3.1.1.

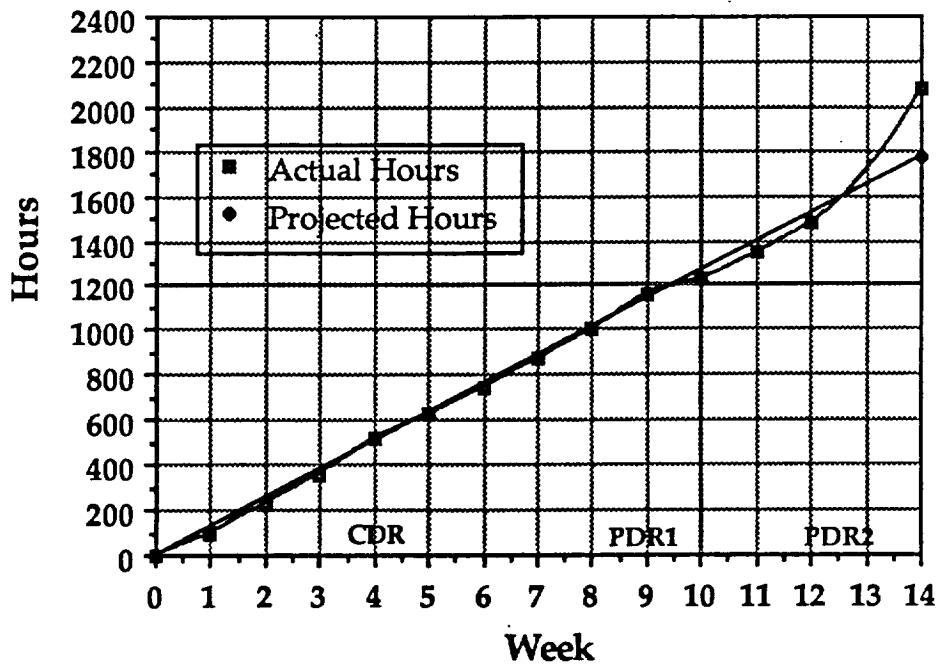


Figure 5.3.1.1. Actual Hours and Projected Hours Through Completion

Table 5.3.1.1. Summary of Personnel Costs

Position	Cost/hr.	# hrs/wk.	Weekly Total
1 Project Manager	\$25.00	18	\$ 450.00
1 Technical Manager	\$22.00	18	\$ 396.00
1 Admin. Manager	\$22.00	16	\$ 352.00
5 Engineers	\$15.00	15	\$1125.00
Graphics	\$ 6.00	4	\$ 24.00
<hr/>			
Subtotal:	\$2497.00		
	Cost for 14 Weeks:		\$34,958.00

5.3.2 Material and Hardware Cost

The material and hardware cost estimates are based on 1991 rates for computer rentals and mainframe time, and the expenses incurred. The current expenses are listed in Table 5.3.2.1.

Table 5.3.2.1. Material and Hardware Costs

14 Weeks Rent for IBM 386-33 and Peripherals:	\$1000.00
14 Weeks Rent for Mac IIsi and Peripherals:	1500.00
Software rental:	100.00
Mainframe Time:	250.00
300 Copies (@ \$0.05/copy)	15.00
100 Transparencies (@ \$0.50/copy)	50.00
Miscellaneous Supplies:	50.00
Long-Distance Calls:	30.00
Model and Poster:	40.00
<hr/>	
Total:	\$ 3035.00

5.3.3 Total Costs

The total cost for work completed on the contract for the design of the Common Lunar Lander is \$37,993.00 (1991 dollars). Table 5.3.3.1 contains the current cost associated with the project.

Table 5.3.3.1. Total Costs

Personnel Costs	\$ 34,958.00
Material and Hardware Costs	\$ 3,035.00
<hr/>	
Current Total	\$ 37,993.00

6.0 Bibliography

Many references other than those listed in the main body of the report were consulted during the course of this project. The following list includes sources which provided information considered useful during the course of the design, but which were not directly referenced in the final report.

Advanced Nuclear Systems for Portable Power in Space, National Academy Press: Washington, D.C., 1983.

Agraway, Brij N, **Design of Geosynchronous Spacecraft**, Prentice-Hall Inc., Englewood Cliffs, New Jersey, 1986.

Anderson, John D., **Introduction to Flight**, McGraw-Hill, New York, 1985.

Apollo 11 Lunar Landing Mission Press Kit 20th Anniversary Souvenir Edition, NASA, 1989.

Atlas Mission Planners Guide, General Dynamics Commercial Launch Services, San Diego, CA.

Aviation Week & Space Technology, McGraw-Hill Publication, Vol. 135, March 18, 1991.

Aviation Week & Space Technology, McGraw-Hill Publication, Vol. 135, No. 13, September 30, 1991.

Barry, John, Linas Raslavicius, and Thomas P. Gathmann, "IntelliSTAR™ - An Emerging Spacecraft Control Architecture to Improve Autonomous Control and Operation (AAS 91-048)," **Guidance and Control 1991** (ed. Robert Culp and James McQuerry) vol. 74 of **Advances in the Astronautical Sciences**, Univelt, Inc., San Diego, 1991.

Bate, Roger, Donald Mueller, and Jerry White, **Fundamentals of Astrodynamics**, Dover Publications, Inc., New York, 1971, Chapter 7: The Earth-Moon System.

Botbyl/Fowler, **Spacecraft Subsystems**, Fall 1991.

Boyd, William C. and Warren L. Brasher, **A Perspective on the Use of Storable Propellants for Future Space Vehicle Propulsion**, Johnson Space Center, Houston, TX, N90-18473.

Burgess, Eric, **To the Red Planet**, Columbia University Press, New York, 1978.

Curtis, Anthony, **Space Almanac**, Arcsoft Publishers, Woodsboro, MD, 1990.

Dubrawsky, Ido, Jeff Kline, John Neff, and Steve Hirshorn, "Thermal Control System Design," **Space Systems Design/Spacecraft Mission Design**, University of Texas at Austin, Fall, 1991.

Eagle Engineering Inc., **Lander Program Manual**, NASA Contract Number NAS9-17878, EEI Report 88-195, 1988.

Final Report Space Shuttle Hypergolic Bipropellant RCS Engine Design Study Bell Model 8701, Report Number 8701-910041, Johnson Space Center, Houston, TX, May 1974.

Gatland, Kenneth, **The Illustrated Encyclopedia of Space Technology: Second Edition**, Orion Books, New York, 1989.

Jane's All the World's Aircraft 1984-85, Jane's Information Group Limited, United Kingdom, 1990.

Jane's All the World's Aircraft 1990-91, Jane's Information Group Limited, United Kingdom, 1990.

Kaplan, Marshall H, **Modern Spacecraft Dynamics and Control**, John Wiley and Sons, New York, 1976.

- Kit, Boris and Douglas S. Evered, **Rocket Propellant Handbook**, The Macmillan Company, New York, 1960.
- Lunar Lander Conceptual Design**, Lunar Base Systems Study Task 2.2, Nasa Contract NAS9-17878, EEI Report No. 88-181, Eagle Engineering, Houston Division, March 30, 1988.
- McMordie, Dr. Robert K., "Thermal [Subsystem]," **Spacecraft Mission Analysis and Design** (ed. James Wertz and Wiley Larson), Kluwer Academic Publishers, Dordrecht, The Netherlands, 1991.
- Mondt, Jack F., "An Overview of the SP-100 Space Reactor Power System for NASA-OAST S TAC", March 10, 1987.
- Morton Thiokol STAR Handbook.
- National Aeronautics and Space Administration, **Aeronautics and Space Report of the President**, Washington DC, 1991.
- National Aeronautics and Space Administration/Johnson Space Center, **Workshop on the Concept of a Common Lunar Lander**, July 1991.
- National Aeronautics and Space Administration, **Press Kit**, Washington, D.C., March 22, 1972.
- Othon, Bill, "Moonport: Transportation Node In Lunar Orbit", The University of Texas at Austin, 1987.
- "Session 7: Propulsion and Power Space Shuttle Electrical Power Generation and Reactant Supply System," (Space Shuttle Technical Conference Part II).
- Spacecraft Mass Estimation, Relationships, and Engine Data**, Lunar Base Systems Study Task 1.1, Nasa Contract NAS9-17878, EEI Report No. 87-171, Eagle Engineering, Houston Division, April 6, 1988.

- Spacecraft Subsystems, Propulsion Subsystem Report and Database, UT Austin, January 1991.**
- Stevenson, John, Teresa Morrison, and Timothy Murphy, "Autonomous Landing on Mars (AAS 90-050)," Guidance and Control 1990 (ed. Robert Culp and Arlo Gravseth) vol. 72 of Advances in the Astronautical Sciences, Univelt, Inc., San Diego, 1990.**
- Surveyor Project Final Report Part I: Project Description & Performance, Vol II, Technical Report 32-1265, JPL, California Institute of Technology, Pasadena, California, July 1969.**
- United States Congress, Office of Technology Assessment, Access to Space: The Future of U.S. Space Transportation Systems, U.S. Government Printing Office, Washington DC, April 1990.**
- The Viking Mission to Mars, Martin Marietta Corporation, Denver, Colorado, 1979.**
- Wertz, James R. Spacecraft Attitude Determination and Control, D. Reidel Publishing Company, Kluwer Academic Publishers, Dordrecht, The Netherlands, 1984.**
- Wertz, James R. and Wiley J. Larson, Space Mission Analysis and Design, Kluwer Academic Publishers, Dordrecht, The Netherlands, 1991.**
- Zermuehlen, Robert and Harold Zimbelman, "Guidance, Navigation, and Control," Spacecraft Mission Analysis and Design (ed. James Wertz and Wiley Larson), Kluwer Academic Publishers, Dordrecht, The Netherlands, 1991.**

7.0 Appendix A: Background and History of Other Lunar and Martian Landers

The proposed lunar lander will not be the first vehicle designed to soft land on planetary or lunar surfaces. The first lunar landers were the unmanned Surveyor missions from 1966 to 1968; Apollo lunar landers transported astronauts to the lunar surface starting in 1969. The Viking missions to Mars included landers to place experiments on the Martian surface in 1976.

7.1 Surveyor

The Surveyor program sent seven unmanned soft landers, Surveyors I through VII, to the lunar surface before the manned Apollo missions. The Surveyor program had the following objectives: to perform successful landings, to gather data in support of Apollo, and to gather scientific data about the moon. The Surveyor program fulfilled the three objectives listed above.

The Surveyor spacecraft were launched on Atlas launch vehicles with Centaur upper stages. With the Surveyor payload, the total weight of the Atlas/Centaur combination was 325000 lbs at lift-off. The spacecraft were sent directly into lunar transfer orbit or into parking orbit around the Earth. At LEO injection, the Surveyor spacecraft weighed approximately 2200 lbs. The Centaur upper stage was developed for the Surveyor missions; the first Centaur operational flight was for Surveyor I in 1966. The Atlas launch vehicle had been used for the Ranger and Mariner missions.

The Surveyor landers had the following main design constraints: operation for 90 days, landing on lunar surface visible to Earth, and average landing accuracy (depending on mid-course correction) of 100 km. Surveyor's structure consisted of a pyramid shaped, open frame constructed of aluminum. During launch, the lander's legs were designed to be folded inside the Atlas/Centaur payload shroud and extended after shroud separation. The spacecraft had a low center of gravity to provide stability over a range of landing conditions.

Surveyor spacecraft had the following subsystems: structures and mechanisms; thermal control; power; propulsion; flight control and radar, radio, signal processing, and command; and scientific payload. The structure subsystem had three legs with hydraulic shock absorbers and crushable footpads. Thermal control was based on active systems such as heaters and passive systems such as Mylar insulation and coatings. The power subsystem consisted of a solar panel and batteries. Propulsion was provided by a solid retrorocket and three throttleable, bipropellant vernier engines. Three sets of fuel and oxidizer tanks pressurized with helium contained propellant for the vernier engines. The solid retrorocket provided most of the deceleration and was separated from the spacecraft prior to touchdown. Cold gas jets made up the reaction control system (RCS). The flight control and radar subsystem used an inertial reference provided by gyros and accelerometers. The inertial reference was updated with sun and star sensors during transfer. For lunar reference during landing, a radar altimeter and a doppler velocity radar were included. The radio, signal processing, and command subsystem contained a S-band radio system and a signal processor. All Surveyor landers contained a television camera, while Surveyors III, IV, and VII contained a surface sampler as part of the scientific instrument payload subsystem. The total scientific payload subsystem weight was 71 lbs.

Side and top views of the Surveyor spacecraft are presented below. Figure 1B shows the spacecraft stowed inside the Atlas/Centaur payload shroud. The legs are folded upward to fit inside a frustum shaped shroud 104.704 inches in diameter at the base and 32.774 inches in diameter at the top. The solar panel and antenna is also folded. Figure 2B shows a side view of Surveyor after landing.

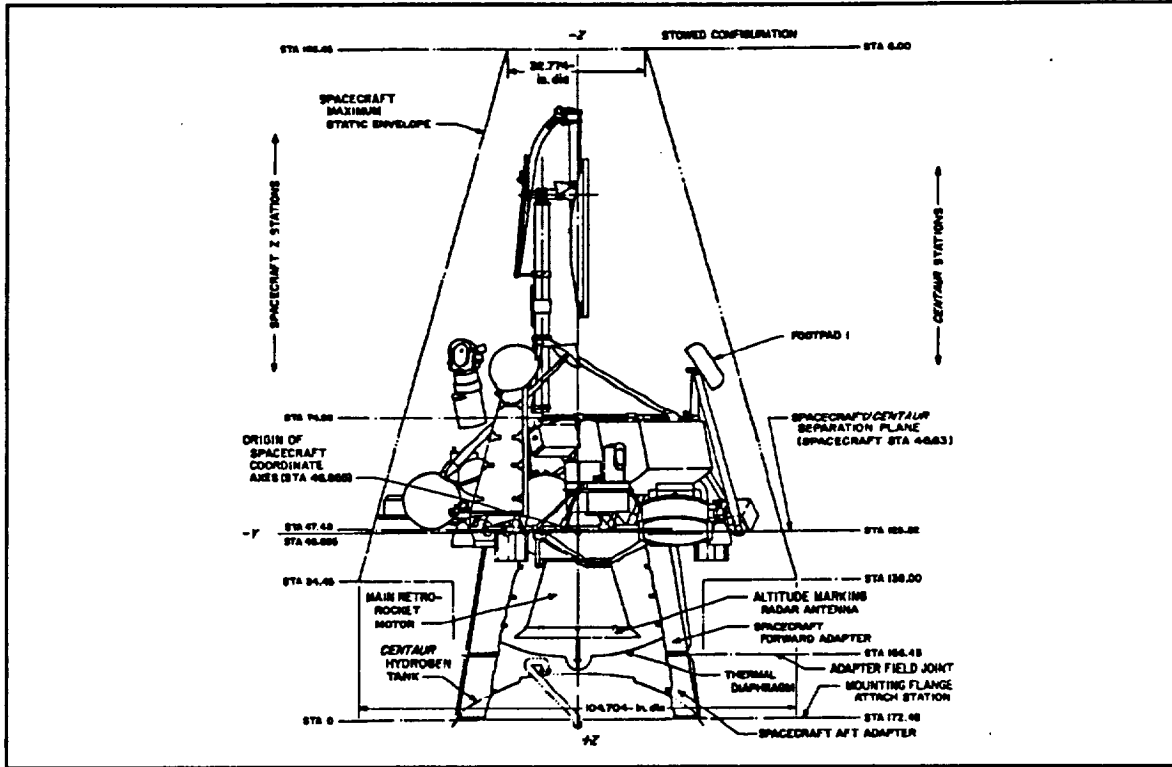


Figure A1. Surveyor in Stored Configuration

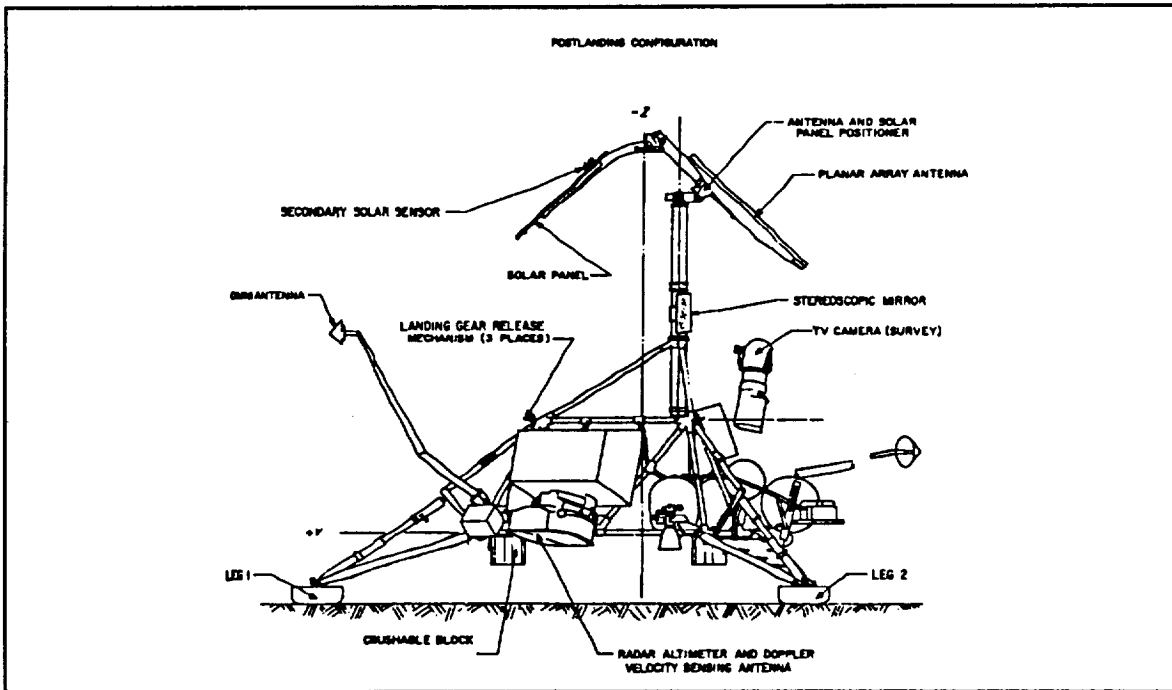


Figure A2. Surveyor in Operational Configuration

7.2 Apollo

The Apollo program was born when President John F. Kennedy said, "I believe that this nation should commit itself to achieving the goal, before this decade is out, of landing a man on the Moon and returning him safely to Earth . . .", in a public speech. Eight years of national effort culminated on the manned lunar landing of astronauts Neil A. Armstrong and Edwin "Buzz" Aldrin on July 20, 1969. The lunar module (LM) transported two astronauts between the lunar surface and a command module in lunar orbit.

The launch vehicle for the lunar module and command module was the Saturn V. The Saturn V was 281 feet long and weighed approximately 6.5 million pounds at lift-off; the Saturn V had the capability of launching 50 tons of payload to lunar orbit. The Saturn V consisted of three stages. The first stage had five F-1 engines burning RP-1 and LOX, while the second stage had five J-2 engines burning LH2 and LOX. The third stage had one J-2 engine burning the same fuel as the other J-2 engines.

The lunar module consisted of two stages: an ascent stage and a descent stage. Both stages functioned together during descent; however, the ascent stage separated from the descent stage before lift-off from the lunar surface. The ascent stage's structure consisted of an external beam system to remove loads from the crew compartment. The descent stage had four legs explosively extended before descent. To provide impact load attenuation, the landing gear struts contained energy absorbing crushable aluminum honeycomb. The total lunar module weight at launch was 33205 lbs.

The lunar module had the following subsystems: electrical power; environmental control; communication; guidance, navigation, and control; and propulsion. Silver zinc batteries produced all the lunar module's power. The environmental control subsystem supplied water and oxygen; this subsystem also provided thermal control. S-band and VHF radio systems provided communications. The guidance, navigation, and control system contained an inertial measurement unit updated with optical sightings and radar data. The ascent engine, descent engine, and RCS engines were the propulsion subsystem. The descent engine was throttleable between 1050 and

6300 lbs thrust; in addition, the descent engine was gimbaled. The ascent engine was fixed and not throttleable. All the engines burned hypergolic Aerozine 50 and nitrogen tetroxide supplied from tanks pressurized with helium. The payload carried by the lander consisted of the fueled ascent stage which weighed 10622 lbs. Figure 3B shows the fully configured lunar module.

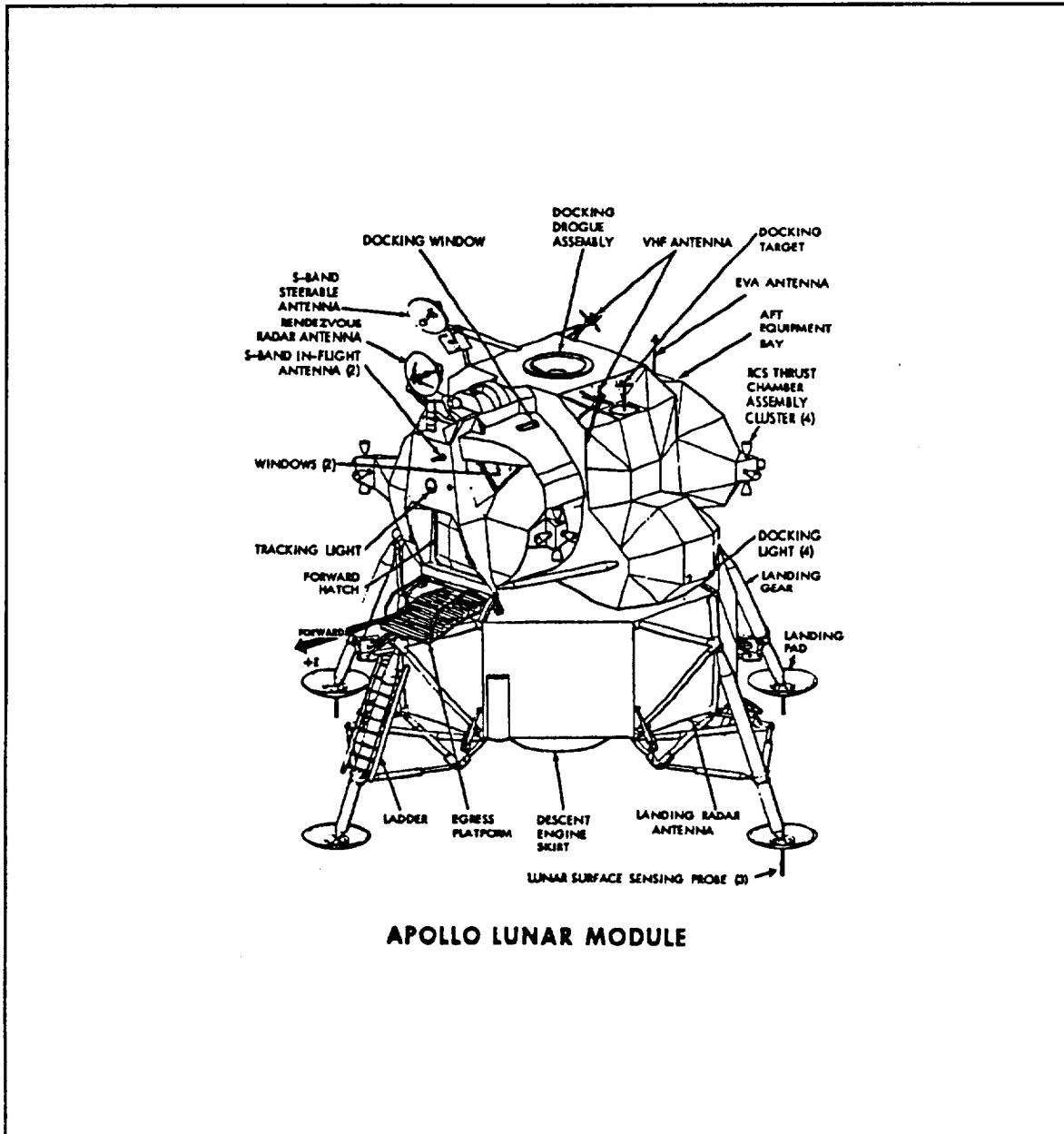


Figure A3. The Apollo Lunar Module

7.3 Viking

The Viking program was developed as a follow-on to the Mariner missions. Viking would land and sample the surface to provide better and more detailed data on Mars. The primary objective was to search for life on Mars through several scientific payloads on the lander. The launch vehicles for the 3400-kg Viking 1 and 2 were Titan III boosters with Centaur upper stages.

Each Viking spacecraft consisted of an orbiter and a soft lander. The orbiter would enter orbit around Mars and search for landing sites with its cameras; after finding a suitable landing site, the orbiter would release the lander. Atmospheric braking using an aeroshell and a parachute would slow the lander's descent. Before touchdown, rocket engines would provide the final deceleration. The lander operated autonomously during descent and landing. The orbiter served as a communications relay between Earth and the lander. The landers were designed to remain operational on the Martian surface for 90 days. During transfer to Mars, the orbiter was powered by a combination of solar panels and batteries. Upon landing, the lander was powered by RTGs. Rocket engines had multiple nozzles to avoid disturbing the surface while landing. Figure A4 shows an isometric view of a Viking lander.

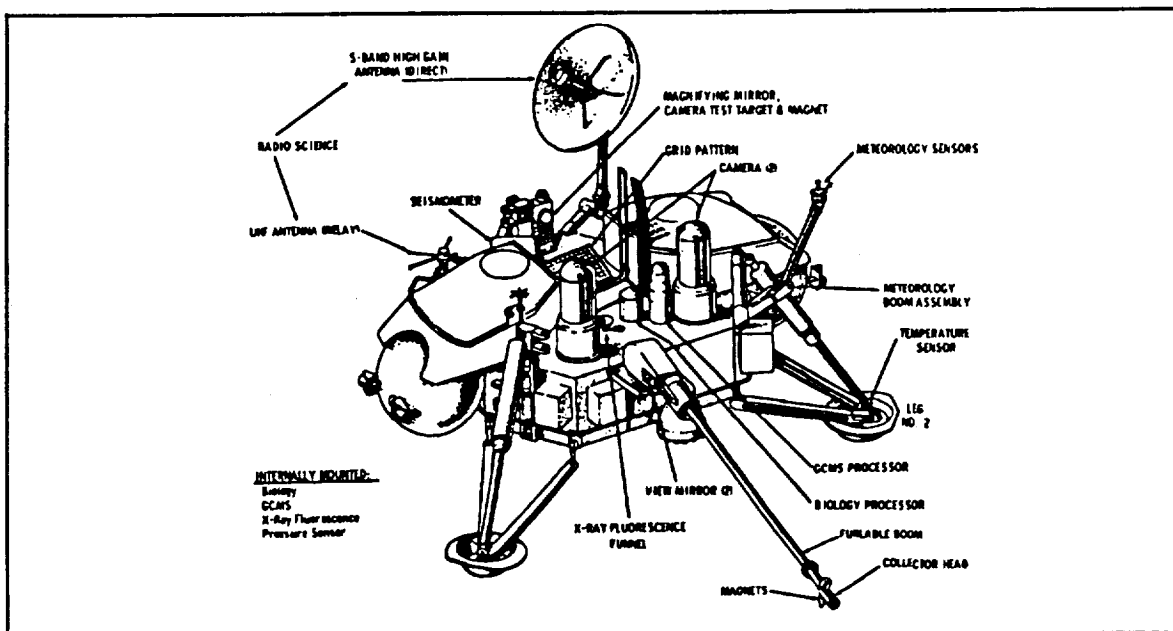


Figure A4. The Viking Lander

7.4 References

Anderson, John D., **Introduction to Flight**, McGraw-Hill, New York, 1985.

Apollo 11 Lunar Landing Mission Press Kit 20th Anniversary Souvenir Edition, NASA, 1989.

Botbyl/Fowler, **Spacecraft Subsystems**, Kinko's, Fall 1991.

Burgess, Eric, **To the Red Planet**, Columbia University Press, New York, 1978.

Surveyor Project Final Report Part 1: Project Description and Performance,
Volumes 1 and 2, JPL, 1969.

8.0 Appendix B: TK! Solver Models and Output Used for Trajectory Analysis

This TK! Solver model was used to get estimates for velocity changes required for the different phases of the mission. This information was used for fuel tank sizing and overall mass estimation. The model uses the patched-conic approximation method as a first-order approximation of the trajectory.

8.1 TK! Solver Patched Conic Model Variables

<u>Input</u>	<u>Variable</u>	<u>Output</u>	<u>Units</u>	<u>Comments</u>
	Rc	6544.145	Km	GEOCENTRIC CIRCULAR ORBIT Initial circular radius
	Vc	7.80444798	Km/s	Velocity of circular orbit
	delVe	3.14555202	Km/s	Delta V for the Centaur stage
	ENE0	-0.9581583	Km ² /s ²	GEOCENTRIC ELLIPTICAL ORBIT Energy of geocentric orbit
10.95	V0		Km/s	Injection Vel. provided by Centaur
	lowV	10.9355466	Km/s	The lowest delta V is determined by both R0 and lamda1
398600	MUe		Km ³ /s ²	Gravitational parameter of the Earth
166	alt		Km	Altitude of injection
	R0	6544.145	Km	Radius of injection
	H0	71658.3878	Km ² /s	Angular momentum of geocentric orbit
0	phi0		rad	Flight path angle at injection
	R1	357066.691	Km	Arrival radius at Rs
384400	D		Km	Distance between the Earth and moon
66300	Rs		Km	Radius of sphere of influence of moon
1.06575	lamda1		rad	Specifies the pt. at which the geocentric trajectory crosses Rs
	V1	0.56242286	Km/s	Arrival velocity at Rs
	phi1	1.20592987	rad	Arrival flight path angle at Rs
	gamma1	0.16322166	rad	The angle R1 makes with D
	p0	12882.3997	Km	CALC. OF TIME OF FLIGHT FOR GEO Semi-latus rectum of elliptical orbit
	a0	208003.201	Km	Semi-major axis of elliptical orbit
	e0	0.96853825		Eccentricity of elliptical orbit
	AA	1	rad	
	BB	-0.9952334	rad	
	nu0	0	rad	Injection true anomaly
	nu1	3.04391543	rad	Arrival true anomaly

	E0	0	rad	Injection eccentric anomaly
	E1	2.40374706	rad	Arrival eccentric anomaly
	TOF1	263283.706	s	TOF for geocentric elliptical orbit
	gamma0	2.18325523	rad	The phase angle at injection
2.6E-06	Wm		rad/s	Angular velocity of the moon in its geocentric orbit
				CONDITIONS AT PATCH POINT
	R2	66300	Km	Initial radius relative to the moon
0	FF		Km/s	Delta V at arrival to change IC's
	V2A	0.88071039	Km/s	
	V2	0.88071039	Km/s	Initial velocity relative to the moon
1.018	Vm		Km/s	Vel of Moon relative to Earth
	cc	0.55927266		
	cd	0.63843185		
	eps2	-0.0792421	rad	Defines the direction of I.C.'s
				SELENOCENTRIC HYPERBOLIC ORBIT
	ENE2	0.31387624	Km ² /s ²	Energy of selenocentric orbit
	MUm	4902.82903	Km ³ /s ²	Gravitational parameter of the moon
	H2	-4622.1921	Km ² /s	Angular momentum of seleno orbit
	p2	4357.61884	Km	Semi-latus rectum of seleno orbit
	e2	1.24817643		Eccentricity of selenocentric orbit
	Rp2	1938.29042	Km	Radius of closest approach to the moon
	Vp2	2.38467471	Km/s	Velocity at closest approach of moon
	a2	-7810.1308	Km	Semi-major axis of seleno orbit
	csnu2	-0.7485113		
	F2	2.71724006	rad	Hyperbolic eccentric anomaly
	TOF2	65939.2045	s	Time of flight in hyperbolic orbit
				SELENOCENTRIC CIRCULAR PARKING ORBIT
	Rcm	1938.29042	Km	Final radius of circular parking orbit
	Vcm	1.59042777	Km/s	Velocity of circular orbit
	delVm	0.79424694	Km/s	Delta V required to change from the hyperbolic orbit to the circular orbit
				ENGINEERING DESIGN CRITERIA
	ALTm	200.29042	Km	Altitude of circular parking orbit
	delV	0.79424694	Km/s	Total delta V for the lander
	TOF	91.4508084	Hr	Total time of flight

8.2 Equations used in the TK! Solver Patched-Conic Approximation Model

```

Rc = R0
Vc = sqrt(MUe/Rc)
delVe = sqrt(Vc*Vc+V0*V0-2*Vc*V0*cos(phi0))
R0 = 6378.145 + alt
ENE0 = (V0*V0)/2 - MUe/R0
H0 = R0 * V0 * cos(phi0)
R1 = sqrt(D*D+Rs*Rs-2*D*Rs*cos(lamda1))
lowV = sqrt(2*MUe*(1/R0-1/R1))
V1 = sqrt(2*(ENE0 + MUe/R1))
phi1 = acos(H0/R1/V1)
gamma1 = asin((Rs/R1)*sin(lamda1))
p0 = (H0*H0)/MUe
Vcm = sqrt(MUm/Rcm)
a0 = -MUe/(2*ENE0)
delVm = abs(Vp2-Vcm)
e0 = sqrt(1-(p0/a0))
delV = abs(FF) + delVm
AA = (p0-R0)/R0/e0
TOF = (TOF1 + TOF2)/60/60
BB = (p0-R1)/(R1*e0)
ALTM = Rcm - 1738
if AA=>1 then nu0=0.0 else nu0=acos(AA)
if BB=>1 then nu1=0.0 else nu1 = acos(BB)
E0 = acos((e0+AA)/(1+e0*AA))
E1 = acos((e0+BB)/(1+e0*BB))
TOF1 = ((E1-e0*sin(E1))-(E0-e0*sin(E0))) * sqrt((a0*a0*a0)/MUe)
gamma0 = nu1 - nu0 - gamma1 - Wm*TOF1
R2 = Rs
V2A = sqrt(V1*V1 + Vm*Vm -2*V1*Vm*cos(phi1-gamma1))
V2 = V2A + FF
cc = (Vm/V2)* cos(lamda1)
dd = (V1/V2)*cos(lamda1+gamma1-phi1)
eps2 = asin(cc-dd)

```

$$\text{ENE2} = (\text{V2}^2 \cdot \text{V2}) / 2 - (\text{MUm} / \text{R2})$$

$$\text{MUm} = \text{MUe} / 81.3$$

$$\text{H2} = \text{R2}^2 \cdot \text{V2}^2 \cdot \sin(\text{eps2})$$

$$\text{p2} = (\text{H2} \cdot \text{H2}) / \text{MUm}$$

$$\text{e2} = \sqrt{1 + ((2 \cdot \text{ENE2} \cdot \text{H2} \cdot \text{H2}) / (\text{MUm} \cdot \text{MUm}))}$$

$$\text{Rp2} = \text{p2} / (1 + \text{e2})$$

$$\text{Vp2} = \sqrt{2 \cdot (\text{ENE2} + \text{MUm} / \text{Rp2})}$$

$$\text{a2} = \text{Rp2} / (1 - \text{e2})$$

$$\text{csnu2} = (\text{p2} / \text{R2} - 1) / \text{e2}$$

$$\text{F2} = \text{acosh}((\text{e2} + \text{csnu2}) / (1 + \text{e2} \cdot \text{csnu2}))$$

$$\text{TOF2} = (\text{e2} \cdot \sinh(\text{F2}) - \text{F2}) \cdot \sqrt{(-\text{a2}) \cdot (-\text{a2}) \cdot (-\text{a2}) / (\text{MUm})}$$

$$\text{Rcm} = \text{Rp2}$$

8.3 Trajectory Analysis Diagrams

The following diagrams illustrate some of the many variables used in the above model and in the Trajectory Analysis section of the main report.

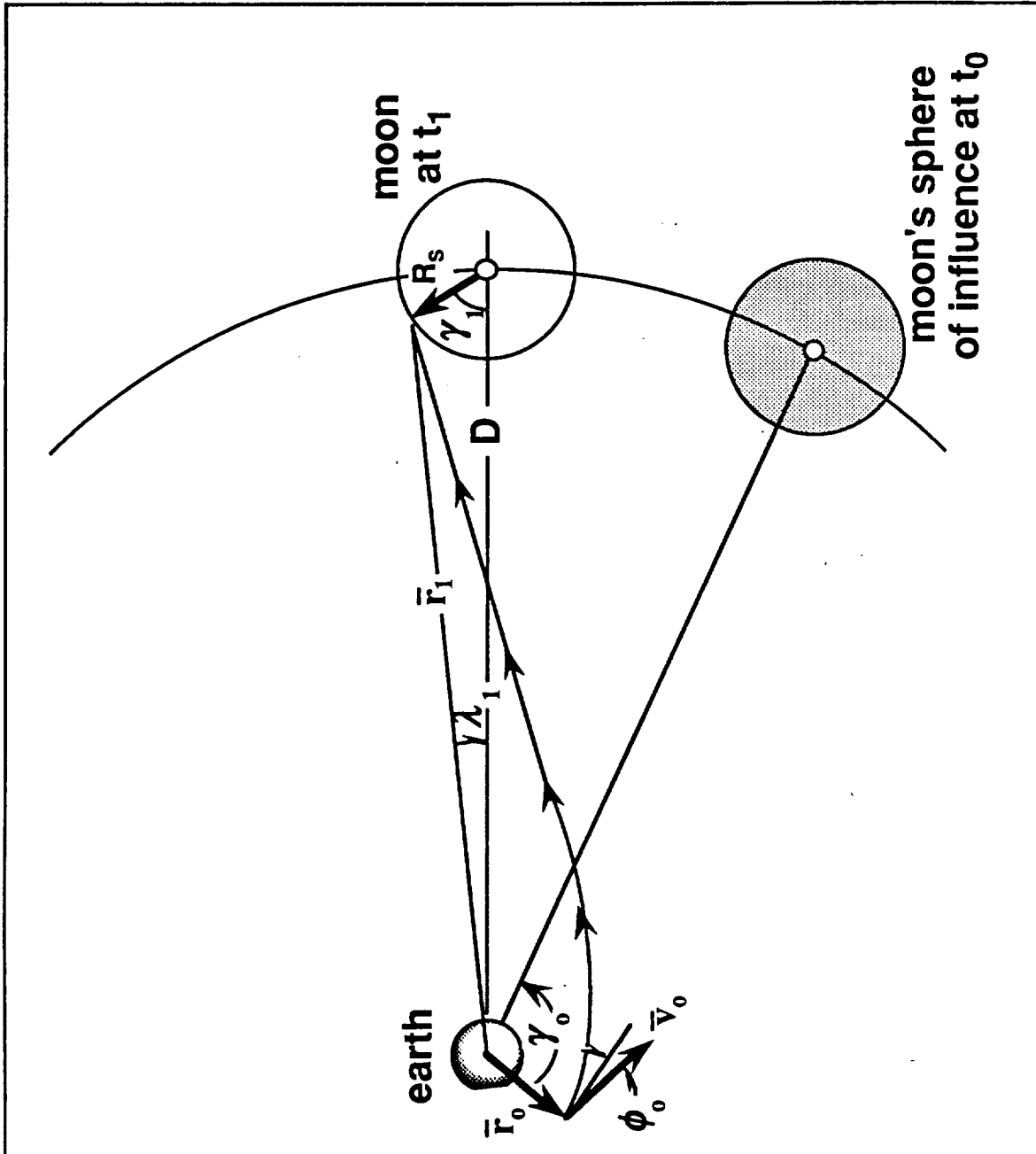


Figure B1. Geocentric Transfer Orbit

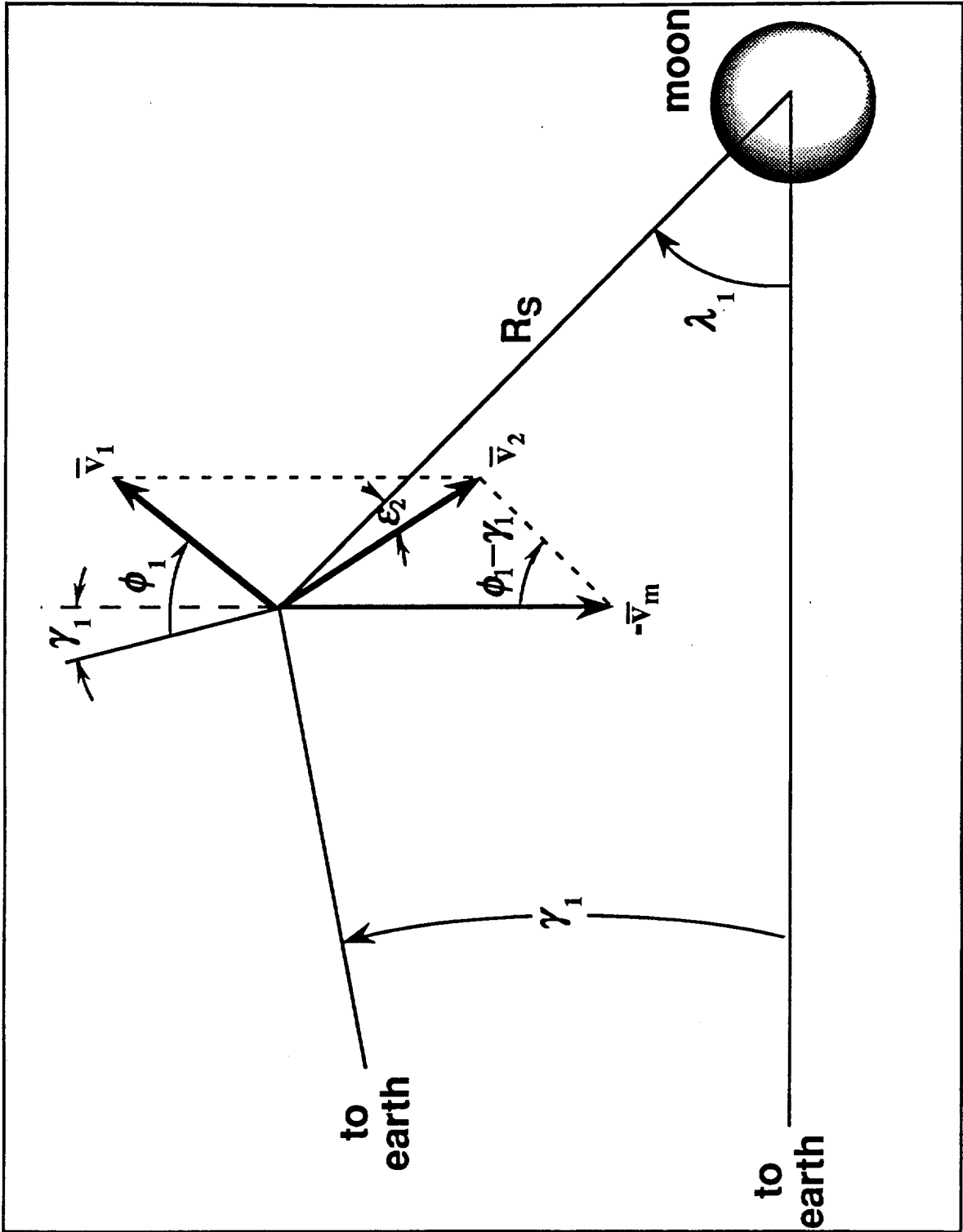


Figure B2. Patch Conditions

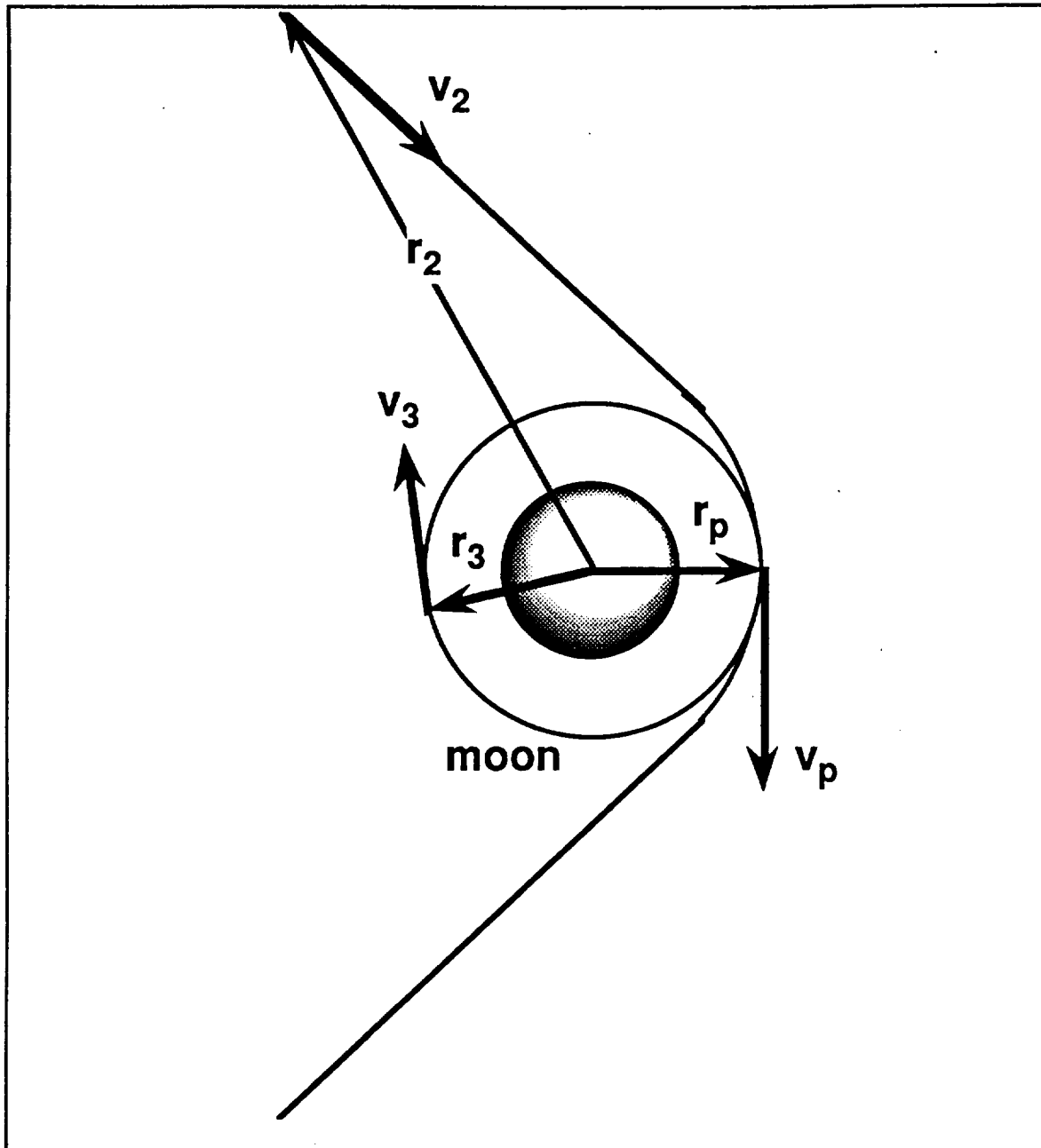


Figure B3. Selenocentric Orbit

8.4 Input and Output from LANDER Sample Run

The following is the input and output information from a sample run of Eagle Engineering's LANDER lunar landing descent trajectory modeling program, written by Chris Varner. This run used a CLL dry mass of about 265 kg (~582 lb), a payload mass of 500 kg (~1102 lb), an equatorial parking orbit, and a desired landing site on the equator.

***** INPUT *****

Landing site latitude 0 <deg>
 Landing site longitude 0 <deg>

Inert weight 582 <lb>
 Payload weight 1102 <lb>
 Propellant weight 0 <lb>
 Thrust 70 <lbf>
 Specific Impulse 306 <s>
 Hover time 30 <s>

Holding orbit (108 x 108) <nm>
 The inclination of the holding orbit is 0

Initial guesses:

Flight path angle at pitch-over 85 <deg>
 Time to main engine cut-off (MECO) 800 <s>

***** OUTPUT *****

Weight Prior to Deorbit Burn <lb> : 3283.122

Delta Velocity Required to Deorbit
 to the Initial Descent Orbit <ft/s> : 107.8892

Fuel Required for the Deorbit Burn <lb>: 35.76962

Initial Descent Orbit:

Apocynthion <nm> -- 109.2681
 Pericynthion <nm> -- 25.58479
 Inclination <deg> -- 0
 Longitude of the Ascending Node <deg> -- 179.9787
 Argument of Pericynthion <deg> -- 164.9085
 Eccentricity <n.d.> -- 4.16E-02

Time <s>	Altitude <ft>	Range <nm>	Velocity <ft/s>	Gamma <deg>	Heading <deg>	Thrust <lbf>	Weight <lb>
0	155508	244	5542	-0.01	90	870	3242
5	155515	240	5499	-0.02	90	870	3227
10	155525	236	5455	-0.02	90	870	3213
15	155535	231	5412	-0.02	90	870	3199
20	155543	227	5368	-0.01	90	870	3185
25	155548	223	5324	0	90	870	3171
30	155548	218	5280	0.01	90	870	3156

35	155539	214	5235	0.03	90	870	3142
40	155521	210	5191	0.05	90	870	3128
45	155491	206	5146	0.08	90	870	3114
50	155449	202	5101	0.11	90	870	3100
55	155391	198	5055	0.15	90	870	3085
60	155316	194	5010	0.19	90	870	3071
65	155222	190	4964	0.24	90	870	3057
70	155108	186	4919	0.29	90	870	3043
75	154972	182	4873	0.35	90	870	3028
80	154812	178	4826	0.41	90	870	3014
85	154627	174	4780	0.48	90	870	3000
90	154414	170	4734	0.55	90	870	2986
95	154173	166	4687	0.63	90	870	2972
100	153901	163	4640	0.71	90	870	2957
105	153597	159	4593	0.8	90	870	2943
110	153261	155	4545	0.89	90	870	2929
115	152889	152	4498	0.99	90	870	2915
120	152482	148	4450	1.1	90	870	2900
125	152037	145	4402	1.21	90	870	2886
130	151553	141	4354	1.33	90	870	2872
135	151029	138	4306	1.45	90	870	2858
140	150464	134	4258	1.58	90	870	2844
145	149856	131	4209	1.71	90	870	2829
150	149204	127	4160	1.86	90	870	2815
155	148508	124	4111	2	90	870	2801
160	147766	121	4062	2.16	90	870	2787
165	146977	118	4013	2.32	90	870	2773
170	146140	114	3963	2.49	90	870	2758
175	145255	111	3913	2.67	90	870	2744
180	144320	108	3863	2.85	90	870	2730
185	143335	105	3813	3.04	90	870	2716
190	142298	102	3763	3.24	90	870	2701
195	141209	99	3712	3.44	90	870	2687
200	140067	96	3662	3.66	90	870	2673
205	138873	93	3611	3.88	90	870	2659
210	137624	90	3560	4.11	90	870	2645
215	136322	87	3509	4.35	90	870	2630
220	134964	85	3457	4.59	90	870	2616
225	133552	82	3406	4.85	90	870	2602
230	132085	79	3354	5.12	90	870	2588
235	130562	76	3302	5.39	90	870	2574
240	128984	74	3250	5.67	90	870	2559
245	127350	71	3198	5.97	90	870	2545
250	125660	69	3145	6.27	90	870	2531
255	123915	66	3093	6.58	90	870	2517
260	122115	64	3040	6.91	90	870	2502
265	120259	61	2987	7.24	90	870	2488
270	118349	59	2934	7.59	90	870	2474
275	116385	57	2880	7.95	90	870	2460
280	114367	54	2827	8.32	90	870	2446
285	112296	52	2773	8.7	90	870	2431
290	110173	50	2719	9.09	90	870	2417
295	107998	48	2666	9.5	90	870	2403
300	105773	46	2611	9.92	90	870	2389

305	103498	44	2557	10.36	90	870	2374
310	101176	42	2503	10.81	90	870	2360
315	98806	40	2448	11.27	90	870	2346
320	96391	38	2393	11.75	90	870	2332
325	93932	36	2339	12.25	90	870	2318
330	91431	34	2284	12.76	90	870	2303
335	88889	32	2228	13.29	90	870	2289
340	86309	31	2173	13.84	90	870	2275
345	83692	29	2118	14.4	90	870	2261
350	81041	27	2062	14.99	90	870	2247
355	78359	26	2006	15.6	90	870	2232
360	75647	24	1951	16.23	90	870	2218
365	72910	23	1895	16.87	90	870	2204
370	70149	21	1839	17.55	90	870	2190
375	67368	20	1782	18.25	90	870	2175
380	64570	18	1726	18.97	90	870	2161
385	61758	17	1670	19.72	90	870	2147
390	58938	16	1613	20.49	90	870	2133
395	56111	15	1557	21.3	90	870	2119
400	53284	13	1500	22.14	90	870	2104
405	50459	12	1443	23.01	90	870	2090
410	47643	11	1386	23.92	90	870	2076
415	44839	10	1330	24.86	90	870	2062
420	42054	9	1273	25.85	90	870	2048
425	39292	8	1216	26.88	90	870	2033
430	36560	8	1159	27.95	90	870	2019
435	33864	7	1102	29.07	90	870	2005
440	31210	6	1045	30.24	90	870	1991
445	28605	5	987	31.47	90	870	1976
450	26057	5	930	32.77	90	870	1962
455	23573	4	873	34.13	90	870	1948
460	21160	3	816	35.56	90	870	1934
465	18828	3	759	37.08	90	870	1920
470	16586	2	702	38.69	90	870	1905
475	14442	2	645	40.4	90	870	1891
480	12407	2	588	42.22	90	870	1877
485	10492	1	532	44.18	90	870	1863
490	8707	1	475	46.28	90	870	1848
495	7063	1	418	48.57	90	870	1834
500	5573	1	362	51.08	90	870	1820
505	4251	0	306	53.85	90	870	1806
510	3108	0	250	56.95	90	870	1792
515	2161	0	194	60.52	90	870	1777
520	1418	0	142	64.72	90	786	1764
525	867	0	99	69.67	90	702	1752
530	484	0	63	75.4	90	618	1741
535	244	0	36	85.8	90	534	1732
540	113	0	17	90	90	450	1723
545	60	0	6	90	90	367	1717
550	45	0	2	90	90	283	1711
555	38	0	2	90	90	282	1707
560	30	0	2	90	90	281	1702
565	23	0	2	90	90	280	1698
570	15	0	2	90	90	280	1693

575	8	0	2	90	90	279	1689
580	0	0	2	90	0	278	1684

Ideal Performance Delta Velocity is 6467.278 <ft/s>
1972.52 <m/s>

9.0 Appendix C: Static Structural Modeling

9.1 Sample NASTRAN model

This listing is the NASTRAN code representing the CLL space frame design. Specifically, this code tests the case where a reaction control jet (located on a footpad) thrusts with a side force of 100 Newtons. This section of code provides a basis that other, future tests can use.

```
NASTRAN SYSTEM(5)=39
ID STATICS,TEST
SOL 24
TIME 3
CEND
TITLE=FIRST GRID COMPUTATION FOR LANDER FRAME
DISP=ALL
ELFORCE=ALL
ELSTRESS=ALL
LOAD=999
OLOAD=ALL
SUBCASE 1
SPC=1001
OUTPUT (PLOT)
PLOTTER NAST
SET 1=ALL
AXES Z,X,Y
VIEW 0.,0.,0.
FIND SCALE,ORIGIN 1,SET 1
PLOT SET 1,ORIGIN 1,LABEL BOTH
PLOT STATIC DEFORMATION 0, SET 1, ORIGIN 1, LABEL BOTH
BEGIN BULK
GRID 1 0. 0. 0.
GRID 2 1. 0. 0.
GRID 3 .5 -.866 0.
GRID 4 -.5 -.866 0.
GRID 5 -1 0. 0.
GRID 6 -.5 -.866 0.
GRID 7 .5 -.866 0.
GRID 8 .433 .25 -.866
GRID 9 0. .5 -.866
GRID 10 -.433 .25 -.866
GRID 11 -.433 -.25 -.886
GRID 12 0. -.5 -.866
GRID 13 .433 -.25 -.866
GRID 14 1.5 0. -1.
GRID 15 -.75 1.299 -1.
GRID 16 -.75 -1.299 -1.
MAT1 997 7.2+10 .345
LOAD 999 1. 1. 1000
```

PLOAD1	1000	1	FZ	FR	0.	-500.	1.	-500.
PLOAD1	1000	2	FZ	FR	0.	-500.	1.	-500.
PLOAD1	1000	3	FZ	FR	0.	-500.	1.	-500.
PLOAD1	1000	4	FZ	FR	0.	-500.	1.	-500.
PLOAD1	1000	5	FZ	FR	0.	-500.	1.	-500.
PLOAD1	1000	6	FZ	FR	0.	-500.	1.	-500.
PLOAD1	1000	7	FZ	FR	0.	-500.	1.	-500.
PLOAD1	1000	8	FZ	FR	0.	-500.	1.	-500.
PLOAD1	1000	9	FZ	FR	0.	-500.	1.	-500.
PLOAD1	1000	10	FZ	FR	0.	-500.	1.	-500.
PLOAD1	1000	11	FZ	FR	0.	-500.	1.	-500.
PLOAD1	1000	12	FZ	FR	0.	-500.	1.	-500.
FORCE	1000	14		FR	100.0	0.	-1.	0.
PBAR	1	997	1.129-4			2.65-8	2.65-8	
CBAR	1	1	1	2	0.	1.		
CBAR	2	1	1	3	1.	0.		
CBAR	3	1	1	4	1.	0.		
CBAR	4	1	1	5	0.	1.		
CBAR	5	1	1	6	1.	0.		
CBAR	6	1	1	7	1.	0.		
CBAR	7	1	2	3	1.	0.		
CBAR	8	1	3	4	0.	1.		
CBAR	9	1	4	5	1.	0.		
CBAR	10	1	5	6	1.	0.		
CBAR	11	1	6	7	0.	1.		
CBAR	12	1	7	2	1.	0.		
CBAR	13	1	1	8	-.5	.866		
CBAR	14	1	1	9	-1.	0.		
CBAR	15	1	1	10	-.5	-.866		
CBAR	16	1	1	11	.5	-.866		
CBAR	17	1	1	12	1.	0.		
CBAR	18	1	1	13	.5	.866		
CBAR	19	1	8	9	.5	.866		
CBAR	20	1	9	10	-.5	.866		
CBAR	21	1	10	11	-1.	0.		
CBAR	22	1	11	12	-.5	-.866		
CBAR	23	1	12	13	.5	-.866		
CBAR	24	1	13	8	1.	0.		
CBAR	25	1	2	8	.5	.866		
CBAR	26	1	8	3	1.	0.		
CBAR	27	1	3	9	-.5	.866		
CBAR	28	1	9	4	.5	.866		
CBAR	29	1	4	10	-1.	0.		
CBAR	30	1	10	5	-.5	.866		
CBAR	31	1	5	11	-.5	-.866		
CBAR	32	1	11	6	-1.	0.		
CBAR	33	1	6	12	.5	-.866		
CBAR	34	1	12	7	-.5	-.866		
CBAR	35	1	7	13	1.	0.		
CBAR	36	1	13	2	.5	-.866		
CBAR	37	1	8	14	0.	1.	0.	
CBAR	38	1	13	14	0.	1.	0.	
CBAR	39	1	2	14	0.	1.	0.	
CBAR	40	1	10	15	-.433	-.25		
CBAR	41	1	9	15	-.433	-.25		
CBAR	42	1	4	15	-.433	-.25		
CBAR	43	1	12	16	.433	-.25		
CBAR	44	1	11	16	.433	-.25		

```

CBAR  45    1    6    16    .433  -.25
SPC   1001  14    3
SPC   1001  15    3
SPC   1001  16   123
ENDDATA

```

9.2 Sample Output

The following output was compiled from a NASTRAN run of the preceding code.

Table C1. Gridpoint Displacements (Meters)

Gridpoint	X	Y	Z
1	0	0	-1.07E-03
2	-1.22E-04	-1.14E-02	-7.89E-04
3	9.88E-03	-5.65E-03	-1.09E-03
4	9.92E-03	5.58E-03	-7.90E-04
5	-5.01E-05	1.14E-02	-1.08E-03
6	-9.79E-03	5.79E-03	-7.87E-04
7	-9.83E-03	-5.73E-03	-1.09E-03
8	2.88E-03	-4.92E-03	-1.03E-03
9	5.68E-03	2.73E-05	-1.03E-03
10	2.82E-03	4.95E-03	-1.02E-03
11	-2.87E-03	4.90E-03	-1.02E-03
12	-5.70E-03	-2.52E-05	-1.03E-03
13	-2.81E-03	-4.93E-03	-1.03E-03
14	4.35E-04	-2.28E-02	0
15	1.95E-02	1.18E-02	0
16	-1.98E-02	1.10E-02	0

Table C2. Load Vector (Newtons)

POINT ID	X	Y	Z	Rotate X	Rotate Y	Rotate Z
1	0	0	-4.08E+02	0	0	0
2	0	0	-1.59E+02	0	-1.83E+01	0
3	0	0	-1.59E+02	1.58E+01	-9.66E+00	0
4	0	0	-1.59E+02	1.58E+01	9.66E+00	0
5	0	0	-1.59E+02	0	1.83E+01	0
6	0	0	-1.59E+02	-1.58E+01	9.66E+00	0
7	0	0	-1.59E+02	-1.58E+01	-9.66E+00	0
8	0	0	-1.29E+00	0	0	0
9	0	0	-1.29E+00	0	0	0
10	0	0	-1.29E+00	0	0	0
11	0	0	-1.29E+00	0	0	0
12	0	0	-1.29E+00	0	0	0
13	0	0	-1.29E+00	0	0	0
14	0	-1.00E+01	-1.23E+00	0	0	0
15	0	0	-1.23E+00	0	0	0
16	0	0	-1.23E+00	0	0	0

Table C3. Stresses in ROD Elements (N/m²)

ID.	STRESS
50	-8.34E+06
51	-8.40E+06
52	-8.29E+06

**Table C4. Stresses in BAR Elements (N/m²)
(Part 1)**

Element ID	Station (%)	AXIAL	S-MAX	S-MIN
1	0	-8.72E+06	-8.72E+06	-8.72E+06
1	1	-8.72E+06	-8.72E+06	-8.72E+06
2	0	3.65E+06	3.65E+06	3.65E+06
2	1	3.65E+06	3.65E+06	3.65E+06
3	0	-8.75E+06	-8.75E+06	-8.75E+06
3	1	-8.75E+06	-8.75E+06	-8.75E+06
4	0	3.59E+06	3.59E+06	3.59E+06
4	1	3.59E+06	3.59E+06	3.59E+06
5	0	-8.61E+06	-8.61E+06	-8.61E+06
5	1	-8.61E+06	-8.61E+06	-8.61E+06
6	0	3.71E+06	3.71E+06	3.71E+06
6	1	3.71E+06	3.71E+06	3.71E+06
7	0	-2.49E+06	-2.49E+06	-2.49E+06
7	1	-2.49E+06	-2.49E+06	-2.49E+06
8	0	-2.55E+06	-2.55E+06	-2.55E+06
8	1	-2.55E+06	-2.55E+06	-2.55E+06
9	0	-2.55E+06	-2.55E+06	-2.55E+06
9	1	-2.55E+06	-2.55E+06	-2.55E+06
10	0	-2.42E+06	-2.42E+06	-2.42E+06
10	1	-2.42E+06	-2.42E+06	-2.42E+06
11	0	-2.63E+06	-2.63E+06	-2.63E+06
11	1	-2.63E+06	-2.63E+06	-2.63E+06
12	0	-2.50E+06	-2.50E+06	-2.50E+06
12	1	-2.50E+06	-2.50E+06	-2.50E+06
13	0	-6.90E+05	-6.90E+05	-6.90E+05
13	1	-6.90E+05	-6.90E+05	-6.90E+05
14	0	-1.00E+06	-1.00E+06	-1.00E+06
14	1	-1.00E+06	-1.00E+06	-1.00E+06
15	0	-9.64E+05	-9.64E+05	-9.64E+05
15	1	-9.64E+05	-9.64E+05	-9.64E+05
16	0	-6.27E+05	-6.27E+05	-6.27E+05
16	1	-6.27E+05	-6.27E+05	-6.27E+05
17	0	-1.15E+06	-1.15E+06	-1.15E+06
17	1	-1.15E+06	-1.15E+06	-1.15E+06
18	0	-1.03E+06	-1.03E+06	-1.03E+06
18	1	-1.03E+06	-1.03E+06	-1.03E+06
19	0	7.21E+06	7.21E+06	7.21E+06
19	1	7.21E+06	7.21E+06	7.21E+06
20	0	1.70E+06	1.70E+06	1.70E+06
20	1	1.70E+06	1.70E+06	1.70E+06
21	0	7.19E+06	7.19E+06	7.19E+06
21	1	7.19E+06	7.19E+06	7.19E+06

**Table C4: Stresses in BAR Elements (N/m²)
(Part 2)**

Element ID	Station (%)	AXIAL	S-MAX	S-MIN
22	0	1.52E+06	1.52E+06	1.52E+06
22	1	1.52E+06	1.52E+06	1.52E+06
23	0	6.85E+06	6.85E+06	6.85E+06
23	1	6.85E+06	6.85E+06	6.85E+06
24	0	1.43E+06	1.43E+06	1.43E+06
24	1	1.43E+06	1.43E+06	1.43E+06
25	0	3.67E+06	3.67E+06	3.67E+06
25	1	3.67E+06	3.67E+06	3.67E+06
26	0	-9.99E+05	-9.99E+05	-9.99E+05
26	1	-9.99E+05	-9.99E+05	-9.99E+05
27	0	-8.34E+05	-8.34E+05	-8.34E+05
27	1	-8.34E+05	-8.34E+05	-8.34E+05
28	0	3.72E+06	3.72E+06	3.72E+06
28	1	3.72E+06	3.72E+06	3.72E+06
29	0	3.73E+06	3.73E+06	3.73E+06
29	1	3.73E+06	3.73E+06	3.73E+06
30	0	-7.57E+05	-7.57E+05	-7.57E+05
30	1	-7.57E+05	-7.57E+05	-7.57E+05
31	0	-1.07E+06	-1.07E+06	-1.07E+06
31	1	-1.07E+06	-1.07E+06	-1.07E+06
32	0	3.36E+06	3.36E+06	3.36E+06
32	1	3.36E+06	3.36E+06	3.36E+06
33	0	3.97E+06	3.97E+06	3.97E+06
33	1	3.97E+06	3.97E+06	3.97E+06
34	0	-7.69E+05	-7.69E+05	-7.69E+05
34	1	-7.69E+05	-7.69E+05	-7.69E+05
35	0	-1.07E+06	-1.07E+06	-1.07E+06
35	1	-1.07E+06	-1.07E+06	-1.07E+06
36	0	3.71E+06	3.71E+06	3.71E+06
36	1	3.71E+06	3.71E+06	3.71E+06
37	0	3.42E+06	3.42E+06	3.42E+06
37	1	3.42E+06	3.42E+06	3.42E+06
38	0	2.84E+06	2.84E+06	2.84E+06
38	1	2.84E+06	2.84E+06	2.84E+06
40	0	3.15E+06	3.15E+06	3.15E+06
40	1	3.15E+06	3.15E+06	3.15E+06
41	0	3.15E+06	3.15E+06	3.15E+06
41	1	3.15E+06	3.15E+06	3.15E+06
43	0	2.63E+06	2.63E+06	2.63E+06
43	1	2.63E+06	2.63E+06	2.63E+06
44	0	3.59E+06	3.59E+06	3.59E+06
44	1	3.59E+06	3.59E+06	3.59E+06

10.0 Appendix D: Structural Design Evolution

10.1 Early Conceptual Designs

During the brainstorming phase of the project, several ideas were proposed for the possible configuration of the lander. There were four main variables, namely the structure of the legs (if any), the payload-carrying platform, the number and placement of engines, and the number and placement of fuel tanks. As part of the brainstorming, several ideas were proposed for how each of the four listed categories might look or be arranged. The following pages depict several conceptual ideas for the lander configuration.

10.1.1 Conceptual Lander Configuration 1

These two pictures show a rather conventional type of lander: three legs, one centrally mounted descent engine, and a tubular grid for a payload-carrying platform.

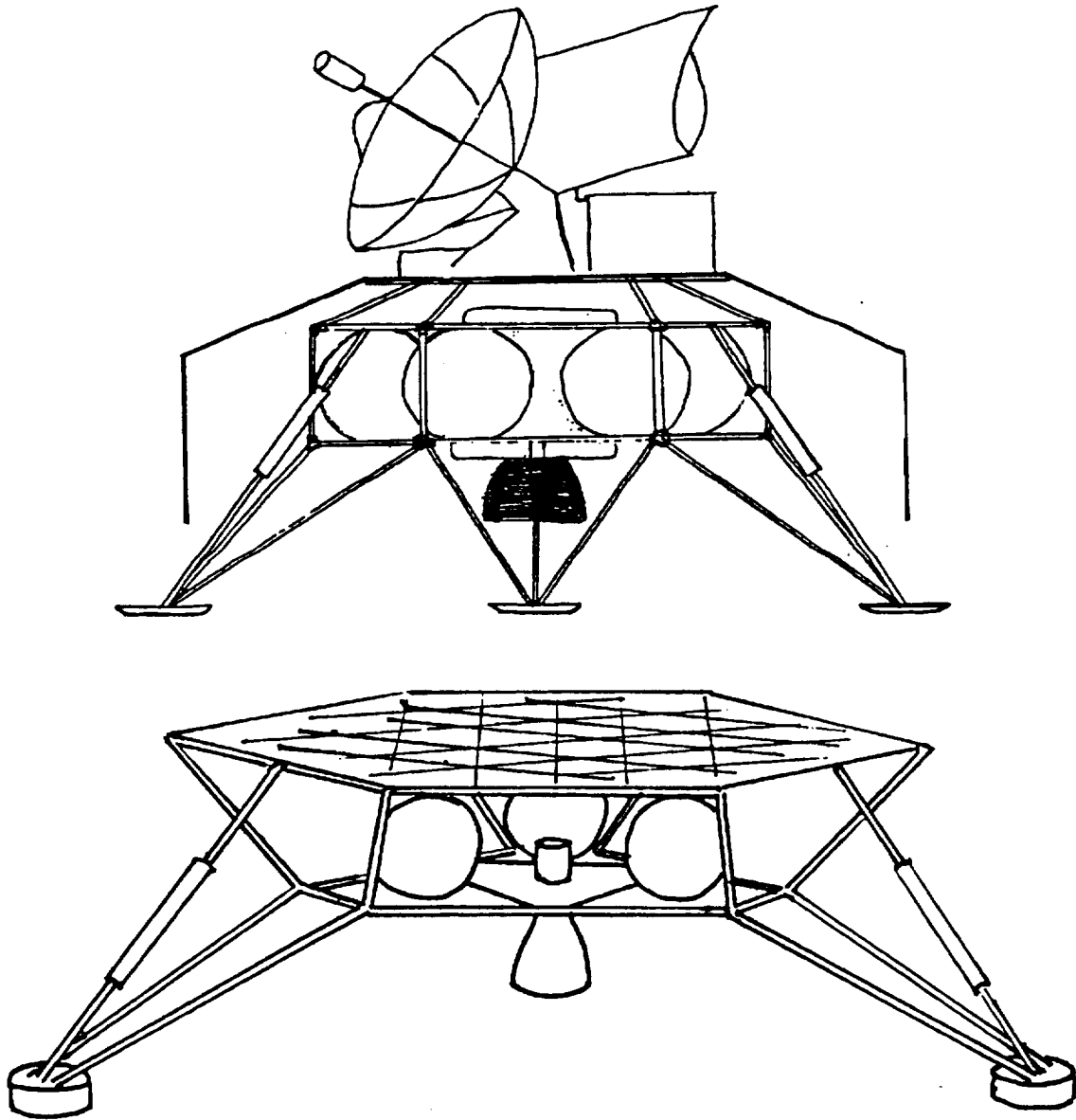


Figure D1. Conceptual Lander Configuration 1

10.1.2 Conceptual Lander Configuration 2

These two figures represent one idea of the appearance of a lander which uses a crushable skirt or pad for impact attenuation. This design incorporates six circumferentially-mounted smaller engines for propulsion during descent.

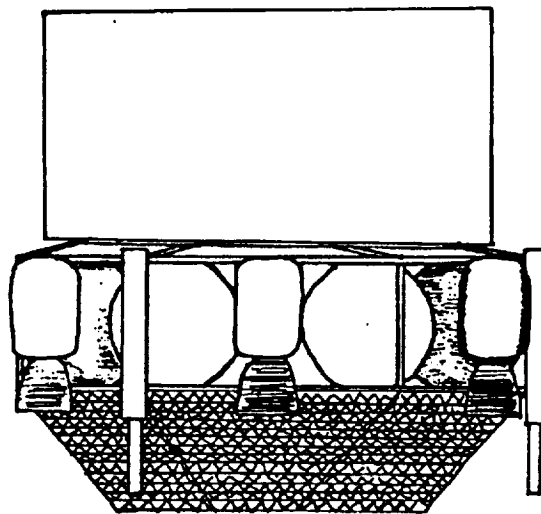
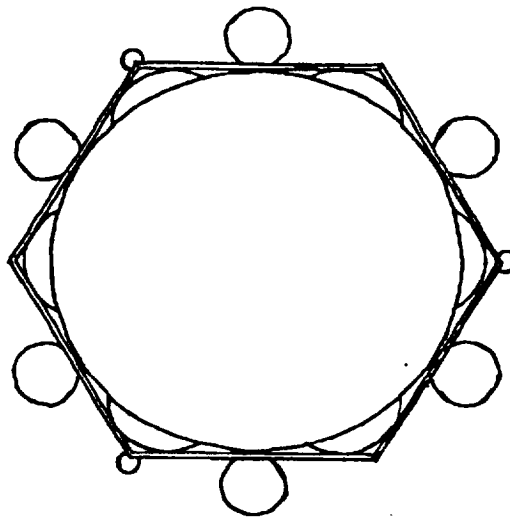


Figure D2. Conceptual Lander Configuration 2

10.1.3 Conceptual Lander Configuration 3

Pictured here is an idea of how a lander configured with airbags for impact attenuation might look. Three airbags almost surrounding the lander would serve in a leg-like fashion; some additional structure would be necessary to support the craft after landing.

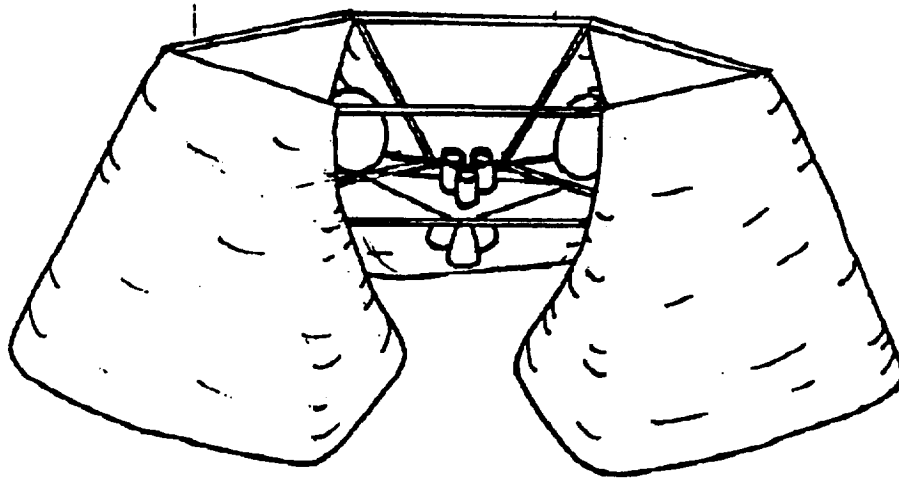


Figure D3. Conceptual Lander Configuration 3

10.1.4 Conceptual Lander Configuration 4

This final figure is a conceptual drawing of a lander configured with crushable legs and illustrating the perforated plate for payload attachment.

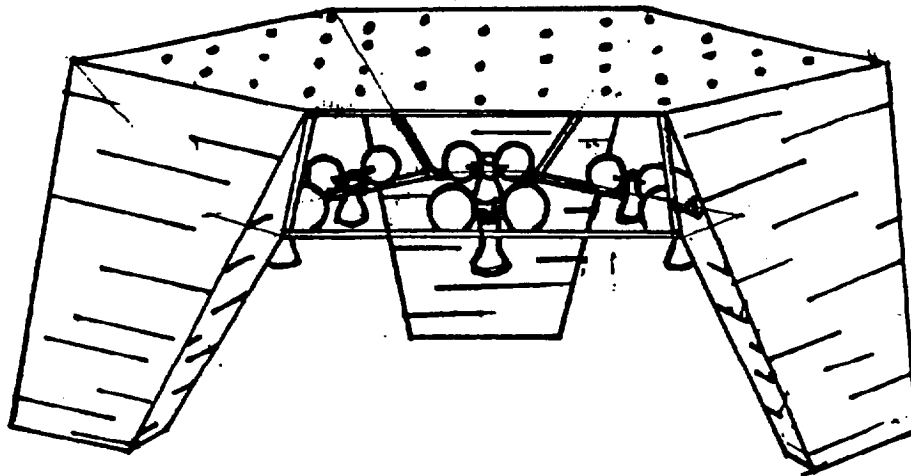


Figure D4. Conceptual Lander Configuration 4

10.2 Evolution of Final Design

Early in the design, several impact attenuation systems were studied. The crushable legs/skirt idea was rejected due to its high weight. The idea of using airbags continued for some time; it was thought that a system incorporating bags at the feet, possibly pressurized with helium from the propulsion system, could be a lightweight method of absorbing impact energy. This was eventually rejected due to the unfavorable energy absorption characteristics of airbags. Eventually, traditional legs with feet constructed of crushable aluminum honeycomb were chosen for use with the CLL. Three legs were chosen for stability reasons.

10.2.1 Engine and Fuel Tank Placement

Through the course of the design, descent engine and corresponding fuel tank configurations varied with changing mass estimates and new information on thrust requirements. Originally, three vernier engines mounted along the perimeter of the payload platform were considered. Six spherical fuel tanks would be mounted below the outer bars of the payload platform (see Figure D5). This configuration was discarded when lunar landing simulations indicated that higher thrust levels would be required for a stable descent trajectory.

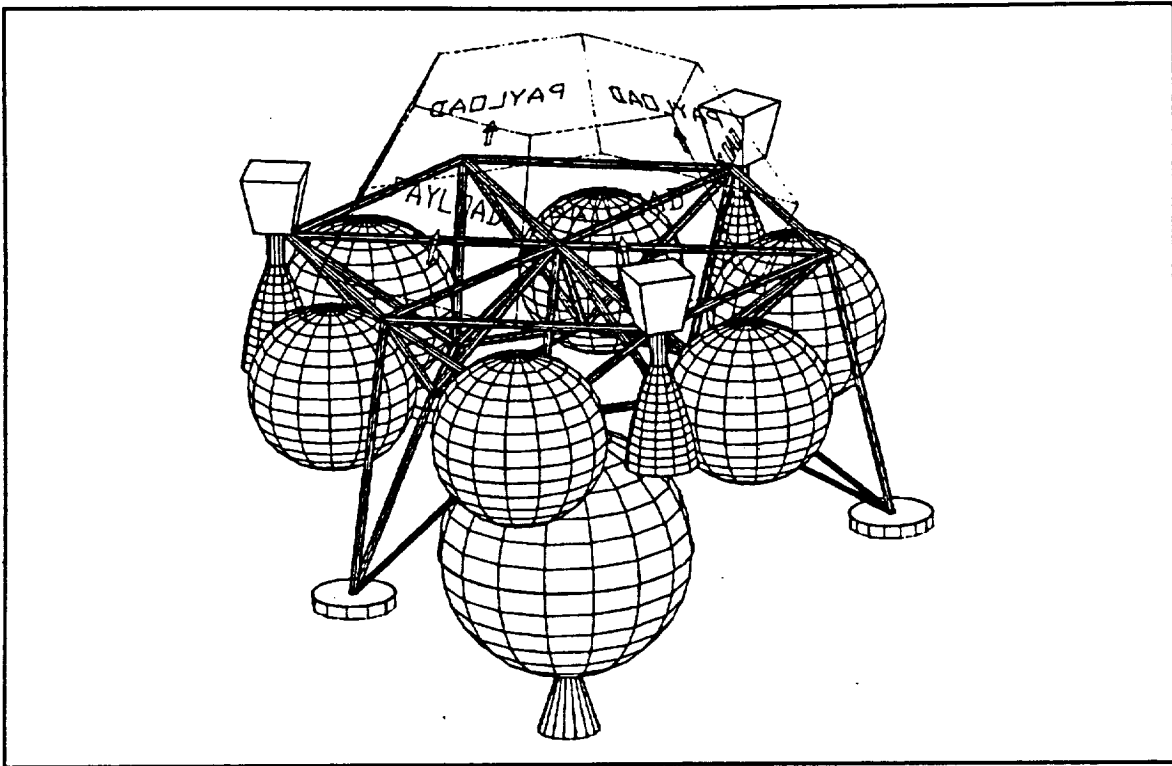


Figure D5. Three Outboard Vernier Engines with Spherical Fuel Tanks

To obtain the greater thrust, a single main descent engine was selected. This engine would be mounted directly below the center of the platform. Fuel requirements also went up with the better descent information; spherical tanks would no longer fit on the lander structure. Cylindrical tanks solved the problem, and they were sized to fit along the perimeter of the payload platform, as shown in Figure D6. The solid rocket used for lunar capture is also visible.

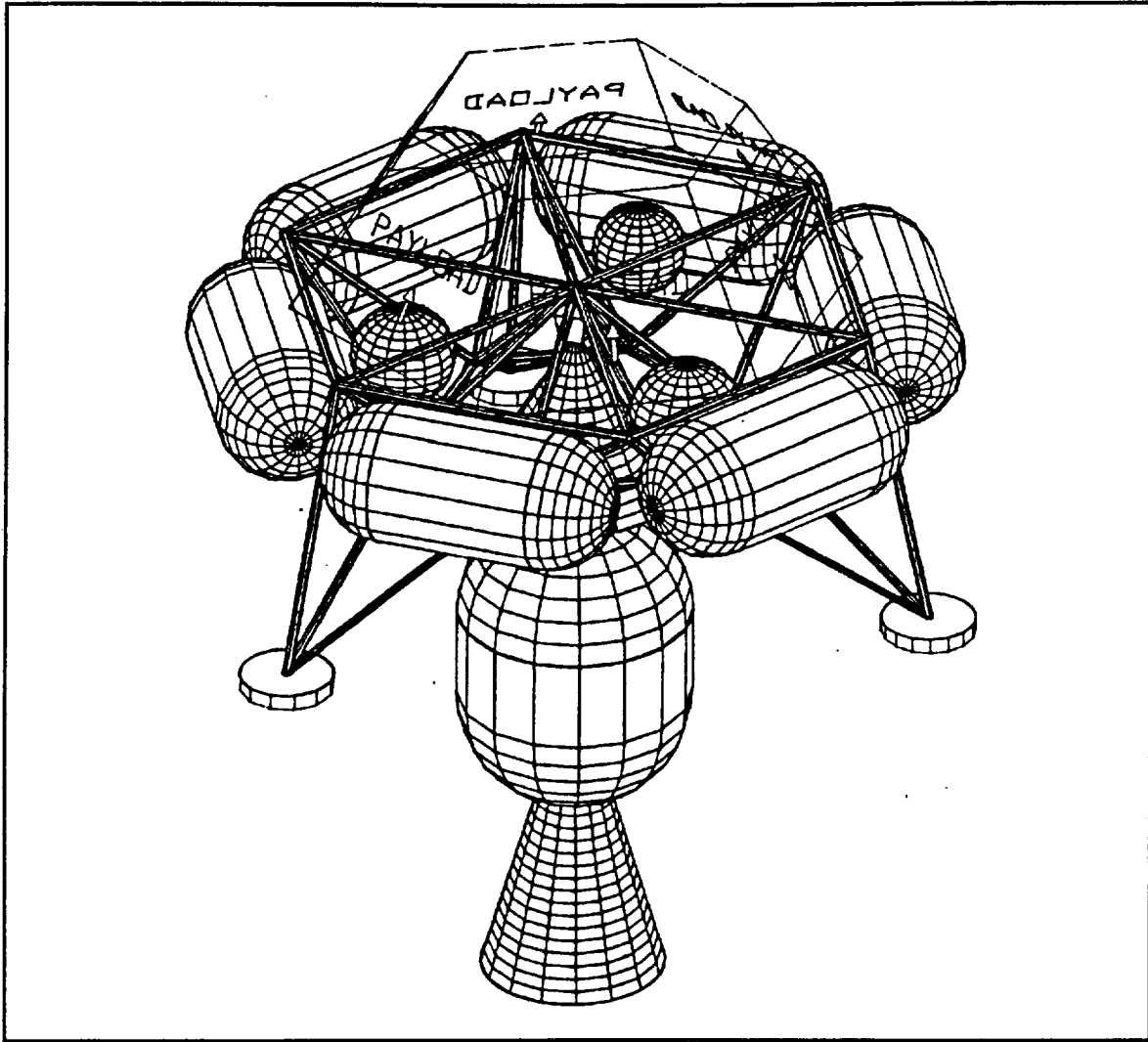


Figure D6. One Central Descent Engine and Cylindrical Fuel Tanks

10.2.2 CLL Footprint Considerations

The next issue which arose was the length of the legs, which determined the "footprint" of the CLL. Originally, as seen in the previous two figures, the lander had a relatively small footprint. This was done to allow the legs to fit inside the medium Atlas payload fairing without having to bend or fold. After some simple analysis, however, it was determined that the small footprint made the CLL potentially "top-heavy" and unstable. It was decided to extend the feet to provide more stability, but this also required that the legs be able to bend. The solution to this design problem may be seen in Figures D7 and D8.

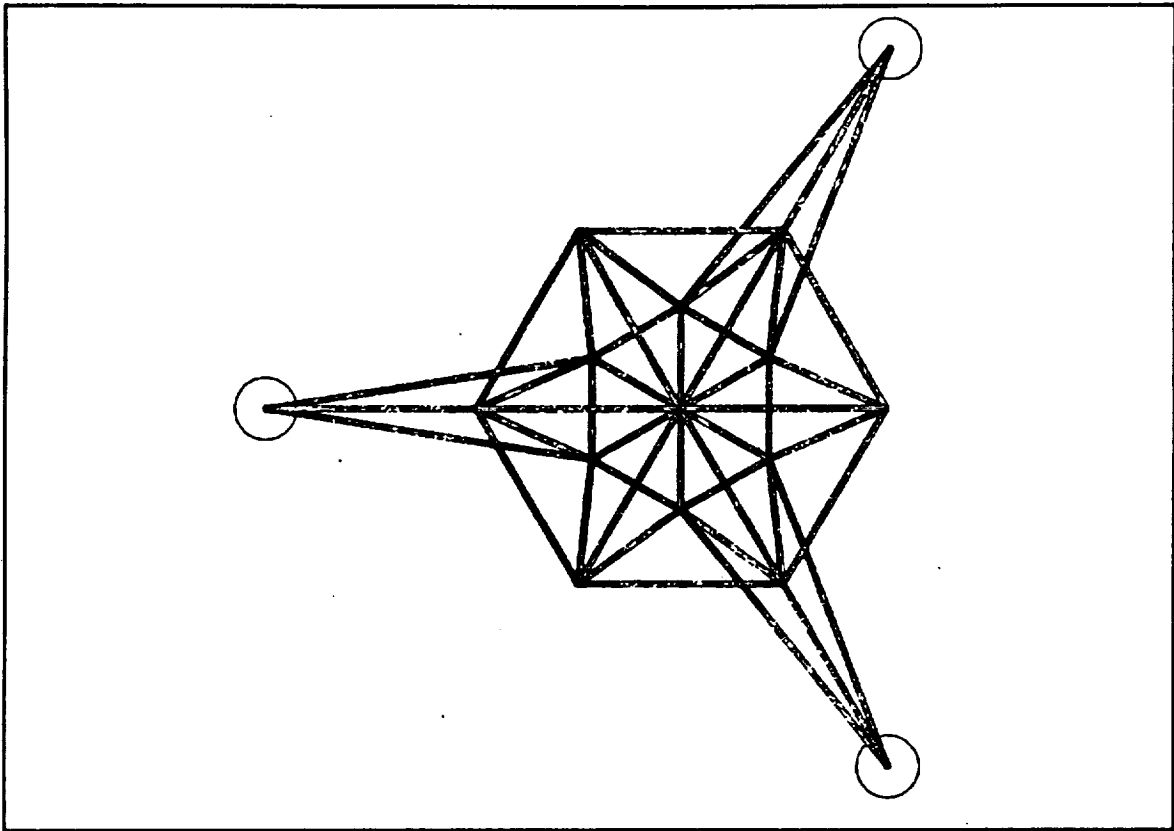


Figure D7. Top View of CLL Showing 4-Meter Footprint

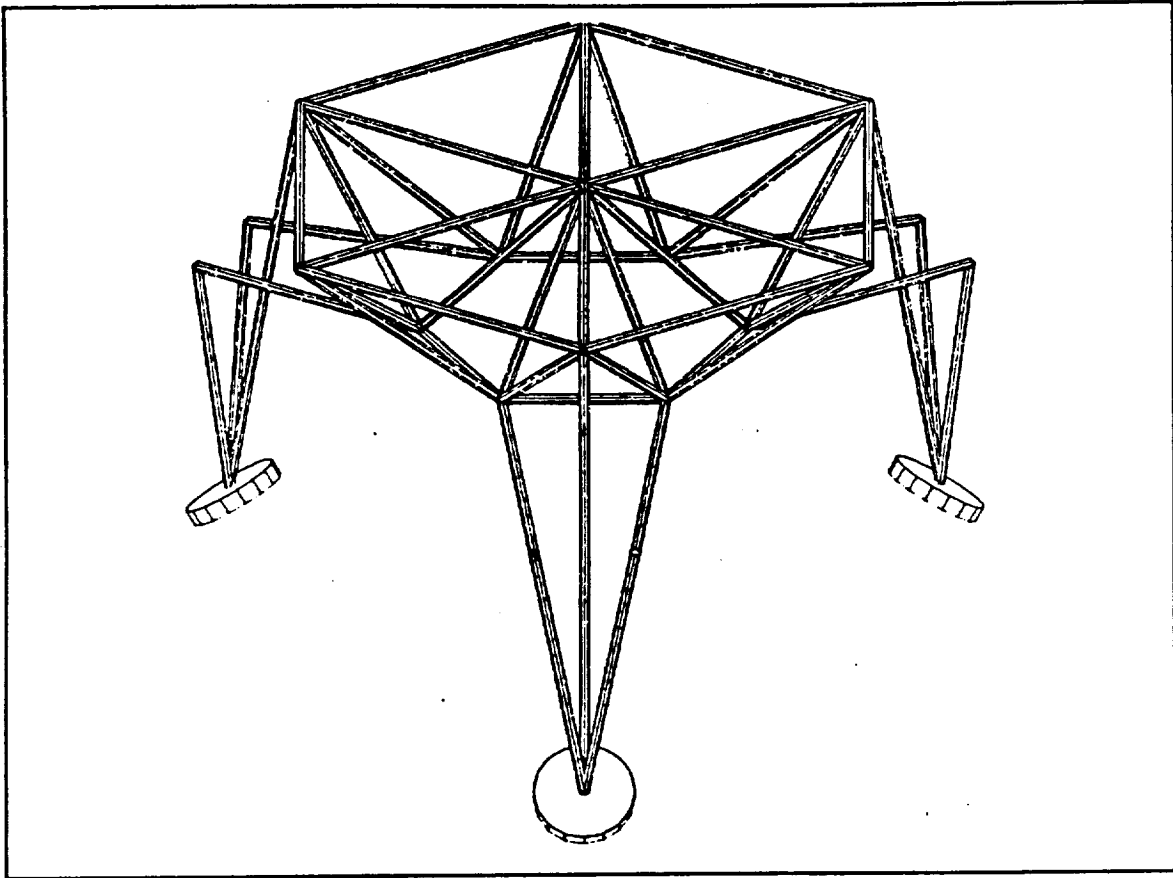


Figure D8. Legs in Folded Configuration

10.2.3 Final Configuration

The last two images depict the Common Lunar Lander in the final configuration chosen by the Austin Cynthesis Corporation. The lander has a solid motor for lunar parking orbit insertion, a single centrally-mounted liquid-fueled descent engine, six cylindrical fuel tanks mounted around the perimeter of the payload platform, and three legs which extend one meter from the edge of the platform to create a four-meter diameter footprint. The payload platform sits one meter above the plane of the feet when legs are extended. Note the placement of the reaction control jets on the legs, near the feet. The increased moment arm available from longer legs with such placement of the RCS jets was another reason for extending the legs.

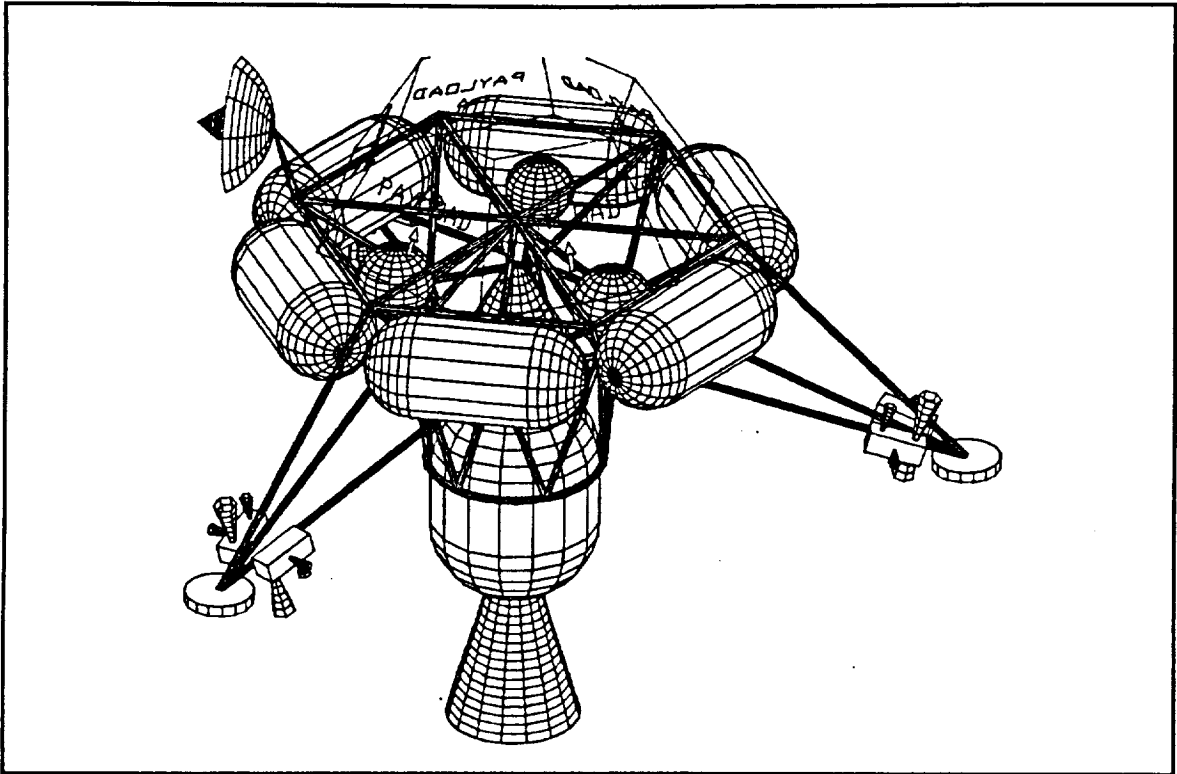


Figure D9. Final Common Lunar Lander Design (Fully Configured)

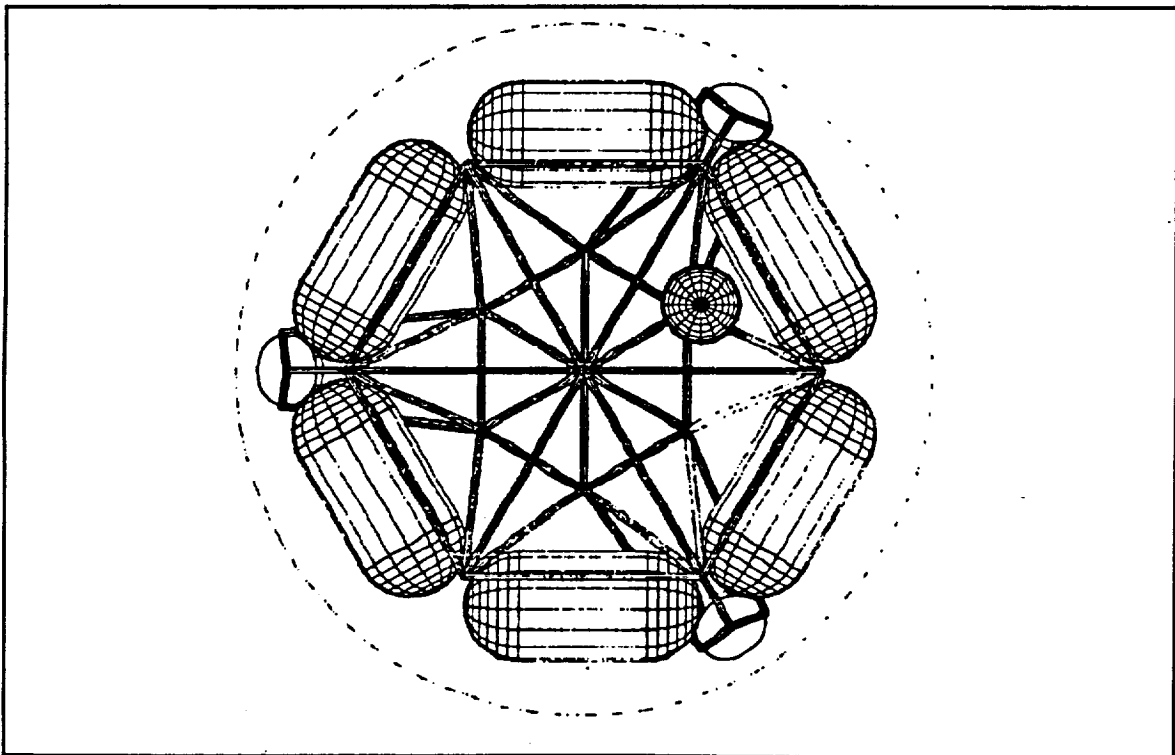


Figure D10. CLL Clearance Inside Atlas Medium Payload Fairing

11.0 Appendix E: Center of Gravity Analysis

One of the criteria constraining possible CLL configurations is the allowable center of gravity (CG) location. While the CLL is designed to carry arbitrary payloads of 500 kg or less, some restrictions are necessary on where those payloads may be placed. The solid capture motor and the liquid descent engine are fixed with respect to the spacecraft frame and are not gimballed. As a result, the potential exists for the thrust vector from the main engines to be offset from the spacecraft center of mass, resulting in a moment which needs to be nulled by the RCS jets. The size of the moments for which the RCS jets may correct is determined by the size and placement of the jets themselves. Figure E1 shows the orientation of the spacecraft-fixed coordinate system, with the origin at the center of the payload platform (the Z-axis completes a right-handed coordinate system). Due to the placement of the RCS jets on the legs near the feet (see the diagram of the fully configured lander, Figure D10, for the exact location of the RCS jets), they are capable of creating larger moments around the Y-axis than the X-axis (perturbations around the Z-axis are expected to be negligible and are not considered here).

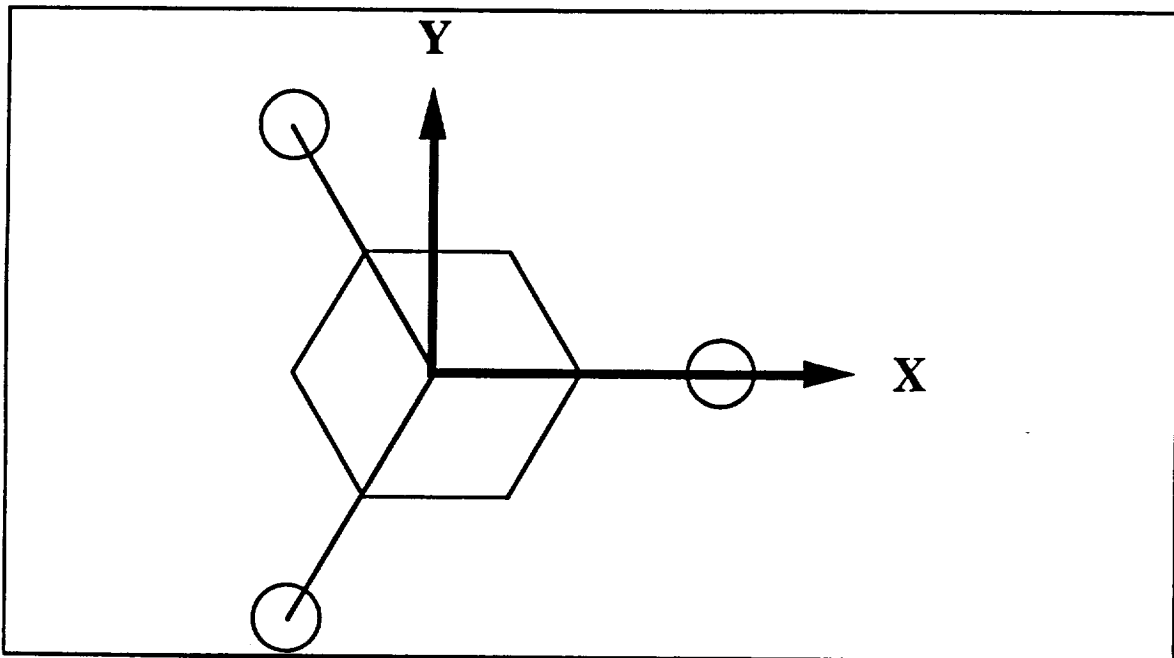


Figure E1. Spacecraft Coordinate System.

To make a first-cut approximation at an allowable range for the CG, some simple moment calculations were performed. It was assumed that the CG would lie in the plane of the payload platform; while this is not realistic, it should provide a conservative CG range. Since the actual CG will lie below the platform until most of the fuel is expended, an angled thrust vector will be closer to the CG the lower the CG lies, and a smaller adverse moment will result. It was also assumed that the direction the thrust vector would be offset was known, so that payloads could be placed accordingly.

For the "best" case, providing a control moment around the Y-axis, thrust from the RCS jets parallel to the Z-axis can contribute about 1450 N·m; thrust parallel to the X-axis can contribute about 380 N·m. The total moment available to control rotation around the Y-axis is therefore about 1830 N·m. Similarly, the smallest control moment may be provided around the X-axis. RCS thrust parallel to the Z-axis contributes 785 N·m and thrust parallel to the Y-axis contributes 255 N·m, for a total available moment of 1040 N·m.

Since the solid motor generates more thrust than the liquid, it will be the limiting factor on allowable CG locations. Based on the available control moments stated in the previous paragraph, the solid thrust vector (magnitude 41,000 N) can be offset no more than 2.5 cm along the X-axis; the vector could be offset by 4.5 cm along the Y-axis. Figure E2 illustrates the allowable range for the spacecraft center of gravity based on these calculations.

Table E1 is a spreadsheet showing the mass and location of most of the CLLs components, and estimates of the spacecraft CG based on these figures. The largest contributions, of course, come from the masses of the fuel and oxidizer (about 900 kg), and the LPO insertion motor (667 kg). Due to the symmetry of the lander about the Z-axis, the CG of the CLL without a payload is very close to the Z-axis, but depending on how much of the propulsion consumables are loaded, may vary between about 15 and 60 cm below the payload platform. Payloads may be included in the spreadsheet to easily estimate how the spacecraft CG will be affected. Sample placements show that the CG may still fall within the allowable range with a 500 kg point mass placed about 10 cm away from the Z-axis, or a 100 kg point mass placed near the edge of the

platform. These are reasonable restrictions, and most payloads could probably meet them without difficulty.

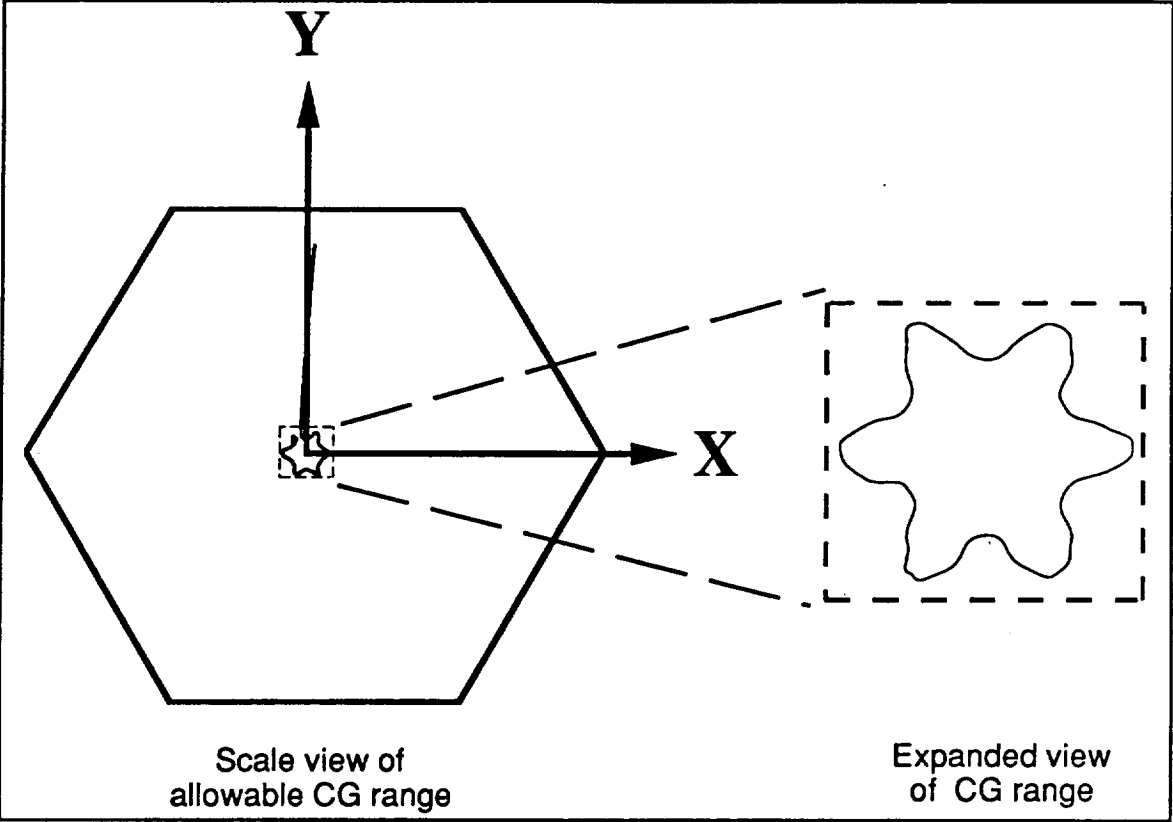


Figure E2. Allowable Center of Gravity Range for the CLL

Table E1. Mass Distribution / Center of Gravity Spreadsheet

Item Description	Location	Mass (kg)	X (m)	Y (m)	Z (m)
DRY LANDER ELEMENTS:					
Fuel Tank (empty)		7	1.08	0.625	-0.25
Fuel Tank (empty)		7	-1.08	0.625	-0.25
Fuel Tank (empty)		7	0	-1.25	-0.25
Oxidizer Tank (empty)		6.8	0	1.25	-0.25
Oxidizer Tank (empty)		6.8	-1.08	-0.625	-0.25
Oxidizer Tank (empty)		6.8	1.08	-0.625	-0.25
Structural Element	Top hexagon	0.69	0.933	0.433	0
Structural Element	Top hexagon	0.69	0	0.866	0
Structural Element	Top hexagon	0.69	-0.933	0.433	0
Structural Element	Top hexagon	0.69	-0.933	0.433	0
Structural Element	Top hexagon	0.69	0	-0.866	0
Structural Element	Top hexagon	0.69	0.933	-0.433	0
Structural Element	Top hex spoke	0.69	0.5	0	0
Structural Element	Top hex spoke	0.69	0.25	0.433	0
Structural Element	Top hex spoke	0.69	-0.25	0.433	0
Structural Element	Top hex spoke	0.69	-0.5	0	0
Structural Element	Top hex spoke	0.69	-0.25	-0.433	0
Structural Element	Top hex spoke	0.69	0.25	-0.433	0
Structural Element	Bottom hexagon	0.345	0.433	0	-0.5
Structural Element	Bottom hexagon	0.345	0.2165	0.375	-0.5
Structural Element	Bottom hexagon	0.345	-0.2165	0.375	-0.5
Structural Element	Bottom hexagon	0.345	-0.433	0	-0.5
Structural Element	Bottom hexagon	0.345	-0.2165	-0.375	-0.5
Structural Element	Bottom hexagon	0.345	0.2165	-0.375	-0.5
Structural Element	Interior (inside)	0.4876	0.2165	0.125	-0.25
Structural Element	Interior (inside)	0.4876	0	0.25	-0.25
Structural Element	Interior (inside)	0.4876	-0.2165	0.125	-0.25
Structural Element	Interior (inside)	0.4876	-0.2165	-0.125	-0.25
Structural Element	Interior (inside)	0.4876	0	-0.25	-0.25
Structural Element	Interior (inside)	0.4876	0.2165	-0.125	-0.25
Structural Element	Interior (outside)	0.5842	0.283	-0.125	-0.25
Structural Element	Interior (outside)	0.5842	0.283	0.125	-0.25
Structural Element	Interior (outside)	0.5842	0.4467	0.5613	-0.25
Structural Element	Interior (outside)	0.5842	0.25	0.6838	-0.25
Structural Element	Interior (outside)	0.5842	-0.25	0.6838	-0.25
Structural Element	Interior (outside)	0.5842	-0.4467	0.5613	-0.25
Structural Element	Interior (outside)	0.5842	-0.283	0.125	-0.25
Structural Element	Interior (outside)	0.5842	-0.283	-0.125	-0.25
Structural Element	Interior (outside)	0.5842	-0.4467	-0.5613	-0.25
Structural Element	Interior (outside)	0.5842	-0.25	-0.6838	-0.25
Structural Element	Interior (outside)	0.5842	0.25	-0.6838	-0.25
Structural Element	Interior (outside)	0.5842	0.4467	-0.5613	-0.25
Leg 1 Element	0° +	1.165	1.2165	0.125	-0.75
Leg 1 Element	0° middle	0.975	1.5	0	-0.5
Leg 1 Element	0° -	1.165	1.2165	-0.125	-0.75
Leg 2 Element	120° +	1.165	-0.5	1.116	-0.75
Leg 2 Element	120° middle	0.975	-0.75	1.299	-0.5
Leg 2 Element	120° -	1.165	-0.7166	0.9911	-0.75
Leg 3 Element	240° +	1.165	-0.7166	-0.9911	-0.75
Leg 3 Element	240° middle	0.975	-0.75	-1.299	-0.5
Leg 3 Element	240° -	1.165	-0.5	-1.16	-0.75

Table E1. Mass Distribution / Center of Gravity Spreadsheet

Item Description	Location	Mass (kg)	X (m)	Y (m)	Z (m)
Foot 1	0°	0.5	2	0	-1
Foot 2	120°	0.5	-1	1.732	-1
Foot 3	240°	0.5	-1	-1.732	-1
RCS assembly 1	0° +	5	1.723	0.0656	-0.9041
RCS assembly 1	0° -	5	1.723	-0.0656	-0.9041
RCS assembly 2	120° +	5	-0.8047	1.525	-0.9041
RCS assembly 2	120° -	5	-0.9182	1.459	-0.9041
RCS assembly 3	240° +	5	-0.9182		-0.9041
RCS assembly 3	240° -	5	-0.8047	-1.459	-0.9041
High Gain Antenna	180°	5	-1.05	0	0.2
Low Gain Antenna	180°	0.15	-1.1		0.2
Low Gain Antenna	0°	0.15			
Liquid-fueled Descent Engine		14	0	0	-0.3
MASS OF DRY LANDER:		122.401			
CG Location of dry lander:			-0.044233568	0.066758278	-0.427831472
ADDITIONAL ELEMENTS PRESENT AT BEGINNING OF DESCENT BURN:					
Fuel		151	1.08	0.625	-0.25
Fuel		151	-1.08	0.625	-0.25
Fuel		151	0	-1.25	-0.25
Oxidizer		151	0	1.25	-0.25
Oxidizer		151	-1.08	-0.625	-0.25
Oxidizer		151	1.08	-0.625	-0.25
payload		500	-0.2	0	0
Helium Tank		3	-0.634	-0.296	-0.2
CG Location of lander with fuel:			-0.064890617	0.004403961	-0.168984558
ADDITIONAL ELEMENTS PRESENT ON FULLY LOADED LANDER:					
Solid Capture Motor (incl. mounting collar)		667	0	0	-1.5
CG Location of fully-fueled lander including solid motor:			-0.046241012	0.00313826	-0.551519259

12.0 Appendix F: Propulsion Sizing Information

Figure F1 shows the method used in sizing the bipropellant propulsion system on the CLL. The bipropellant system included the main landing engine and attitude control thrusters.

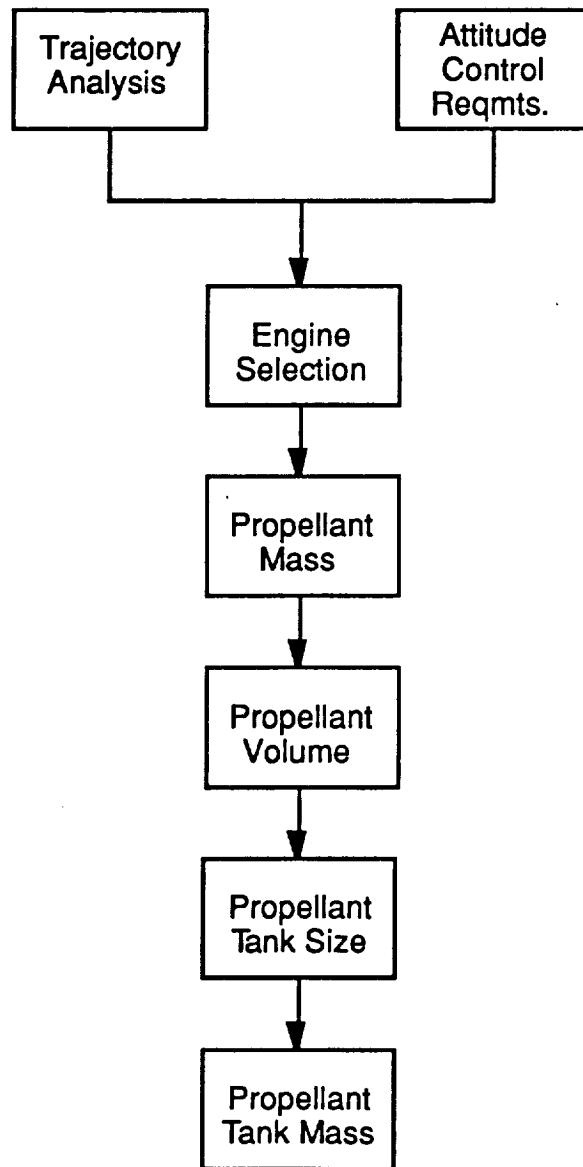


Figure F1. Bipropellant Propulsion System Sizing

Sizing the propulsion subsystem is an iterative process. Figure F2 shows the evolution of the the CLL descent and landing engine.

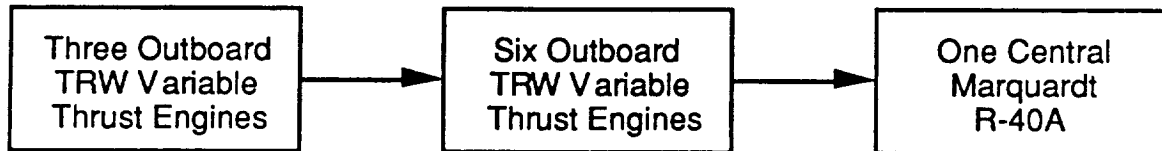


Figure F2. CLL Propulsion Subsystem Evolution

Sizing the propulsion system requires different methods for solid and liquid engines. Solid rocket motors are chosen by calculating the total impulse from¹

$$I = \int T dt = M_{prop} U_{eq} \quad (1)$$

where

I = total impulse
 T = thrust
 dt = time
 M_{prop} = propellant mass
 U_{eq} = equivalent velocity

Equivalent velocity is calculated from¹

$$U_{eq} = I_{sp} g \Delta V \quad (2)$$

where

U_{eq} = equivalent velocity
 I_{sp} = specific impulse
 g = Earth gravity
 ΔV = velocity change

Propellant mass is calculated using the ideal rocket equation which is based on impulsive velocity changes (ΔV s) without gravity losses²

$$\frac{M_o}{M_b} = e^{\frac{\Delta V}{I_{sp} g_e}} \quad (3)$$

where

M_o = total mass before burn
 M_b = mass at burnout
 ΔV = velocity change
 I_{sp} = specific impulse
 g_e = Earth gravity

The CLL is three-axis stabilized after separation from the Centaur upper stage until touchdown. The fuel required for three-axis stabilization during LPO insertion, LPO descent, and landing velocity changes is calculated by³

$$M_{\Delta V} = \frac{K_v M_{s/c} \Delta V L_v \alpha_v}{L_t g I_{sp}} \quad (4)$$

where

$M_{\Delta v}$ = propellant required
 K_v = control system effectivity (≈ 2)
 $M_{s/c}$ = spacecraft mass
 ΔV = velocity change due to main engine
 L_v = distance from main engine to center of mass
 α_v = angular offset of thrust vector from center of mass
 L_t = RCS jet lever arm
 g = Earth gravity
 I_{sp} = RCS jet specific impulse

The propellant required for three-axis controlled attitude maneuvering is given by³

$$M_{attman} = \frac{4 I_c \theta_m}{T L_t g I_{sp}} \quad (5)$$

where

M_{attman} = propellant required
 I_c = control axis moment of inertia
 θ_m = rotation angle of attitude maneuver (rad)
 T = attitude maneuver time
 L_t = RCS jet lever arm
 g = Earth gravity
 I_{sp} = RCS jet specific impulse

When the CLL attitude exceeds a set dead-zone limit the control system fires thrusters to reorient the CLL back to the correct attitude. The formula for fuel consumed during the mission for attitude control system cycling is³

$$IR = \frac{I_{min}^2 L_t}{4 \theta_d I_c} \quad (6)$$

where

IR = RCS jet impulse rate
 I_{min} = RCS jet minimum impulse capability
 L_t = RCS jet lever arm
 θ_d = dead - zone (rad)
 I_c = control axis moment of inertia

and

$$M_p = \frac{(IR)(\text{Mission Duration})}{I_{sp} g} \quad (7)$$

where

M_p = propellant required
IR = RCS jet impulse rate
 I_{sp} = RCS jet specific impulse
g = Earth gravity

The tanks are sized after material and tank pressure are known. The tanks are sized with a safety factor of 2; i.e., the allowable stress is twice the yield stress of the tank material. The formula for sizing cylindrical propellant tanks is for circumferential (hoop) stress⁴

$$\sigma = \frac{(p)(r)}{t} \quad (8)$$

σ = allowable stress of tank material
p = tank pressure
r = tank radius
t = tank thickness

Selection of specific engines depends on thrust-to-weight ratio. A decision was made to go with proven designs for increased reliability, low cost, and availability for launch in 1995. Engine data was gathered from several sources^{5,6,7} and placed in a database attached to the end of this Appendix. Figure F3 shows the thrust-to-weight ratios of flight-proven cryogenic engines.

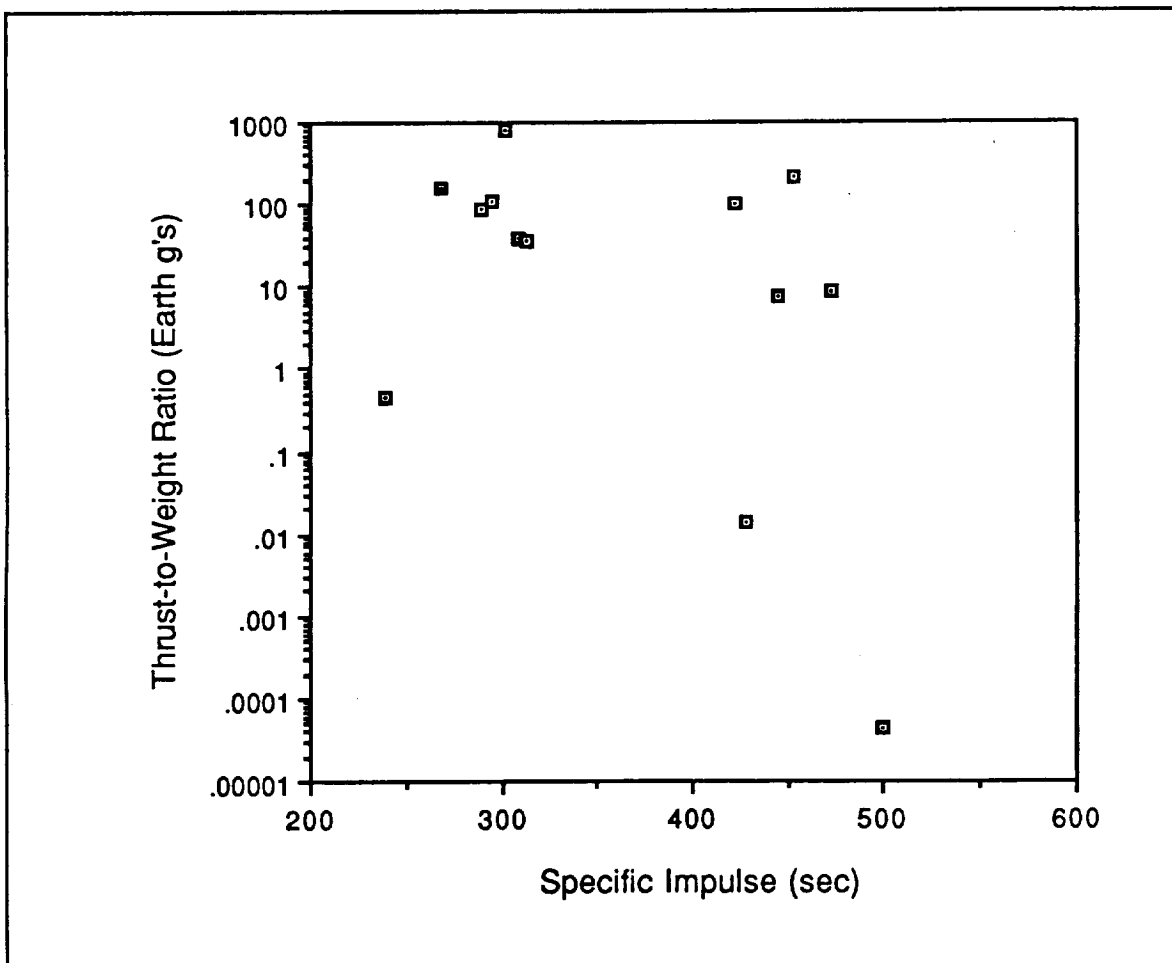


Figure F3. Flight-Proven Cryogenic Engines

The minimum thrust-to-weight ratio necessary for landing is .1667 Earth g. The only engine between .01 and 10 g's is the Rocketdyne MA-3A-C engine with a specific impulse of 239 seconds due to LOX/RP-1 fuel; high specific impulse engines reduce the amount of fuel for a fixed ΔV . Basically, no high specific impulse cryogenic engines exist within the thrust-to-weight ratio range necessary for use as a lunar landing engine. Figure F4 shows the thrust-to-weight ratios for bipropellant engines.

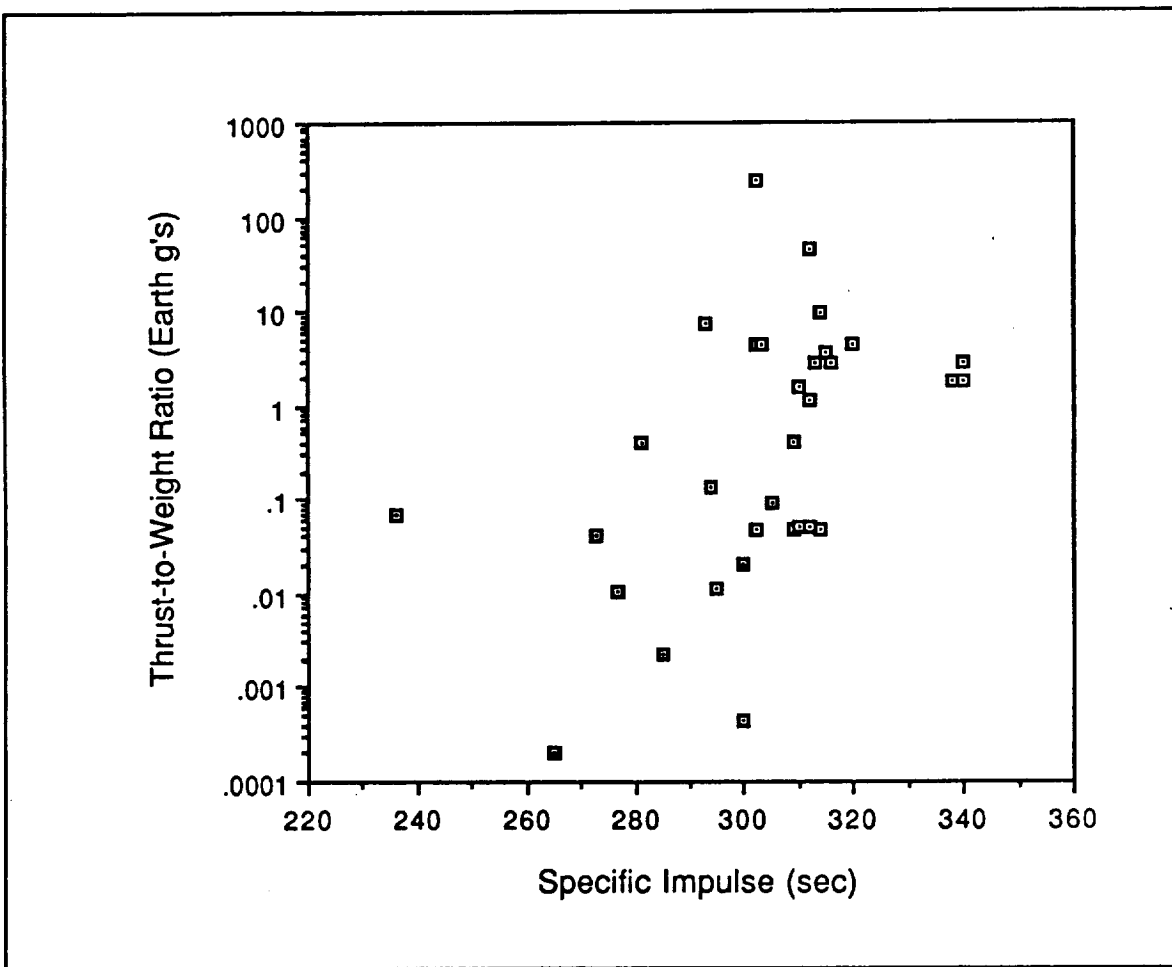


Figure F4. Storable Bipropellant Engines

The average specific impulse is around 300 seconds. Several engines are between .1667 and 1.667 which corresponds to a 10:1 throttling ratio. A solid

motor is used for insertion into lunar parking orbit. Since the thrust varies with time, the performance of solid motors is characterized by total impulse. Figure F5 shows the solid motor mass versus total impulse for current solids.

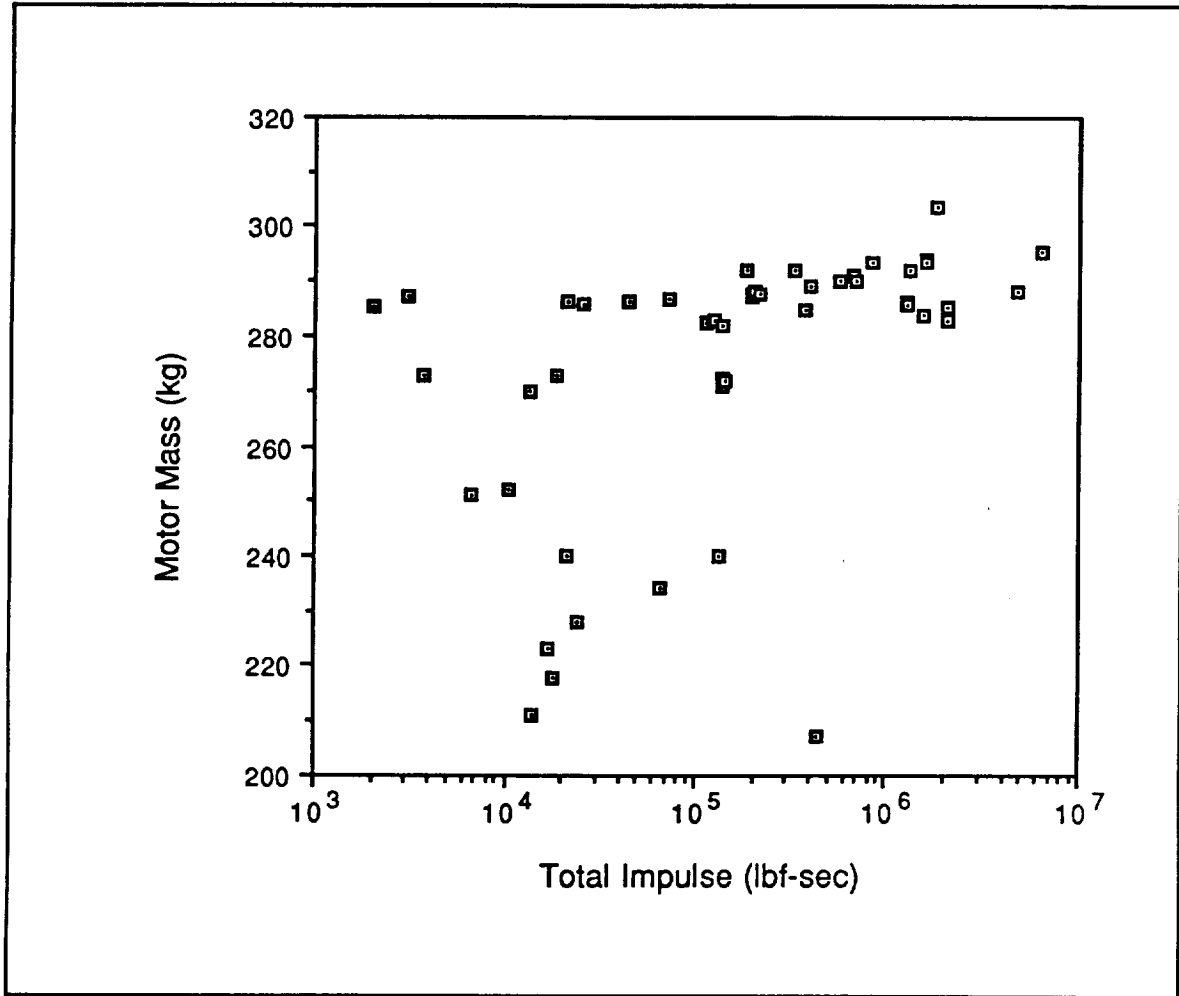


Figure F5. Solid Motors

Table F1 is the propulsion database which was used to select main descent engines and LPO insertion motors. It was taken from the propulsion section of the University of Texas Spacecraft Subsystems handbook.

Table F1. Database of Available Propulsion Systems

ID	Name	Manufacturer	Type	Use	E		G		H		J		K		L		M	N	
					Max Thrust	Nominal Thrust	Thrust Low Est	Thrust High Est	Total Impulse	Thrust High Est	Thrust Low Est	isp Vacuum	isp High Est	isp Low Est	isp High Est	Fuel			
1																			
2																			
3																			
4	Liquid Engines		Storable Liquid	Anti-Sub		23								277				Hydrazine	
5	SE-6 Gemini	Rocket International	Storable Liquid	Pitch/Yaw		45								300				Hydrazine	
6	SE-9 Transstage	Rocket International	Storable Liquid	Roll		25								285				Hydrazine	
7	SE-9 Transstage	Rocket International	Storable Liquid	Roll		93								273				Hydrazine	
8	Apollo Attitude Control System	Rocket International	Storable Liquid	Attitude		3500								309.9				Hydrazine	
9	Lunar Module Ascent Engine	Rocket International	Beryllium, Storable Liquid	Lunar Ascent		1								300				Hydrazine	
10	RS-45	Rocket International	Liquid, Multi-Start	Mariner/Viking Main Propulsion		300								294				Hydrazine	
11	Advanced Space Engine	Rocket International	Pump-Fed Liquid	Orbit Transfer		6000								313				Hydrazine	
12	Advanced Space Engine	Rocket International	Pump-Fed Liquid	Orbit Transfer		20000								473.4				LH2	
13	Space Station Resettler	Rocket International	Electrically Heated Platinum	Attitude, Stationkeeping		0.1								500				H2 N2, air, CO2, CH4, N2	
14	Rockwell Space Station Thruster	Rocket International	Electrically Heated Platinum	Station Boost		30								428				LH2	
15	RL-10	Pratt and Whitney	Restartable Liquid	Centaur Upper Stage		16500								444.4				LH2	
16	SSME	Rocket International	Throtttable Liquid	Shuttle, Shuttle-Derived Vehicle		470000								453				LH2	
17	Advanced Space Engine	Rocket International	Cryogenic Liquid	Saturn V Second Stage		230000								422				LH2	
18	J-2	Rocket International	Cryogenic Liquid	Orbit Transfer Vehicle		7500								485				LH2	
19	AJ10-199	Aerojet Liquid Rocket Co.	Cryogenic Liquid	RCS Systems		1250								427				LH2	
20	AJ10-197	Aerojet Liquid Rocket Co.	Cryogenic Liquid	Advances Orbital Transfer Vehicle		500								458				LH2	
21	LC-D-11	Pratt/Martin Marietta	Cryogenic Liquid	Space Propulsion/RCS Systems		25								409				LH2	
22	AJ23-139/138	Aerojet Liquid Rocket Co.	Storable Liquid	Triam III - C Booster		520000						254		302				A-50	
23	AJ23-137/140	Aerojet Liquid Rocket Co.	Storable Liquid	Triam III - Upper		100000								314				A-50	
24	AJ10-137	Aerojet Liquid Rocket Co.	Storable Liquid	Apollo CSM Propulsion		20500								263				Hydrazine	
25	Ball 8008	TRW	Storable Liquid	Agency Propulsion System		18000								263				A-50	
26	Lunar Module Descent Engine	Aerojet General Co.	Storable Liquid	Apollo LEM Descent		9750								303				Hydrazine	
27	Shuttle OMS	Aerojet General Co.	Storable Liquid	Shuttle Orbital Maneuvering System		6000								316				Hydrazine	
28	AJ10-195	Aerojet Liquid Rocket Co.	Storable Liquid	RCS System		1800								280				RP-1	
29	F-1	Aerojet Liquid Rocket Co.	LOX/Storable Liquid	Saturn V S-1C Stage		1740000								302				RP-5	
30	AJ23-144	Aerojet Liquid Rocket Co.	LOX/Storable Liquid	ALS		753300								264				RP-1	
31	AJ23-130	Aerojet Liquid Rocket Co.	LOX/Storable Liquid	Triam I Booster Stage		344400								320				RP-1	
32	AJ23-130	Aerojet Liquid Rocket Co.	LOX/Storable Liquid	Triam I Booster Stage		252								269				RP-1	
33	HL-1	Rocket - Rocketyne	LOX/Storable Liquid	Saturn I-B First Stage		236000								263				RP-1	
34	HL-3	Rocket - Rocketyne	LOX/Storable Liquid	Thor Delta		195100								296				RP-1	
35	AJ23-131	Aerojet Liquid Rocket Co.	LOX/Storable Liquid	Triam I Second Stage		80000								313				RP-1	
36	MA-3A-A	Rocket - Rocketyne	LOX/Storable Liquid	Triam I Second Stage		180950								290				RP-1	
37	MA-3A-B	Rocket - Rocketyne	LOX/Storable Liquid	Atlas Booster		85200								219				RP-1	
38	MA-3A-C	Rocket - Rocketyne	LOX/Storable Liquid	Atlas Sustainer		1003								239				RP-1	
39	XL-R-132	Rocket - Rocketyne	Storable Liquid	Atlas Veriers, Space Cycle (K-3)		3752.8								196				MMH	
40	Transfer	Aerojet	Storable Liquid			3752.8								340				MMH	
41	Transstage	Aerojet	Storable Liquid			8000								315				A-50	
42	Delta II	Aerojet	Storable Liquid			9797.8								320				MMH	
43	RA-40B	Marquardt	Storable Liquid			888.9								309				MMH	
44	OME/UR	Aerojet				6000								340				MMH	
45	DMA/LAE	TRW				100								314				MMH	
46	RL-D	Marquardt				100.9								310				MMH	
47	RA2	Marquardt				200								302				MMH	
48	MA/BE	Rocketyne				100								312				MON-3	
49	RS-31	ARCALPG				2494								312				MMH	
50	HS601 AKE	Aerojet				100.9								310.9				MMH	
51	Triam III Transstage	Aerojet	Storable Liquid			16000								265				MMH	
52	Aerojet Satellite Engine	Aerojet	Storable Liquid			0.45								285				MMH	
53	Aerojet Satellite Engine	Aerojet	Storable Liquid			4.8								309				MMH	
54	Aerojet Satellite Engine	Aerojet	Storable Liquid			100								281				MMH	
55	PL-40A	Marquardt	Storable Liquid			870								236				Hydrazine	
56	PL-30	Marquardt	Storable Liquid			155								302				A-50	
57	TH-201 (Delta)	TRW	Storable Liquid			9800								286.5					
58	Soled Rocket	Morton Thiokol	Solid			1680								210.50					
59	Star 13A	Morton Thiokol	Solid			2180								265.7					
60	Star 13B	Morton Thiokol	Solid			2775								445.00					
61	Star 17	Morton Thiokol	Solid			2590000								286.2					
62	Space Shuttle SRB	Morton Thiokol	Solid	Space Shuttle Booster		54594								267					
63	Star 75	Morton Thiokol	Solid	Pingree Kick Motor		18660								288					
64	Star 48	Morton Thiokol	Solid	Space Shuttle PAM		12298								290					
65	Star 37FM	Morton Thiokol	Solid	Upper Stage Motor		7060								287					
66	Star 20	Morton Thiokol	Solid	Altair III		4.98								189					
67	Star 5	Morton Thiokol	Solid	Apogee Kick Motor															

Table F1. Database of Available Propulsion Systems

A	B	C	D	E	F	G	H	I	J	K	L	M	N
68	IUS SRM-1 (ORBUS-21)			56536	44610			6314607					286.5
69	LEASAT PKM			43416	35375			2090999					285.4
70	Star 48A	Solid		22491	17900			1523596					283.9
71	Star 48B(S)	Morton Thiokol		15944	14945			1274157					286.2
72	Star 48B(L)	Morton Thiokol		16184	15160			1301124					282.2
73	Star 62	Morton Thiokol						1600000					283.5
74	Star 75	Morton Thiokol		54572	44608			4786517					288
75	IUS SRM-2 (ORBUS-6)			24680	18020			1822472					303.8
76	Star 30BP	Solid		7197	5960			328089					292
77	Star 30C	Morton Thiokol						370787					284.6
78	Star 30E	Morton Thiokol		9211	7910			400000					289.2
79	Star 37F	Morton Thiokol		11046	9911			678632					291
80	Star 6	Morton Thiokol						3077					287
81	Star 6A	Morton Thiokol						2063					285.3
82	Star 6B	Morton Thiokol						5686					273
83	Star 10	Morton Thiokol						6600					251
84	Star 12	Morton Thiokol						10350					252
85	Star 12A	Morton Thiokol						13745					270
86	Star 13	Morton Thiokol						18800					273
87	Star 13C	Morton Thiokol						18200					218
88	Star 13D	Morton Thiokol						17200					223
89	Star 13E	Morton Thiokol						14200					211
90	Star 13F	Morton Thiokol						21190					240
91	Star 15	Morton Thiokol						24500					228
92	Star 17A	Morton Thiokol						71800					286.7
93	Star 20 (Spherical)	Morton Thiokol						66600					234
94	Star 20A	Morton Thiokol						18400					201.9
95	Star 24	Morton Thiokol						128000					282.9
96	Star 24A	Morton Thiokol						112400					282.4
97	Star 24B	Morton Thiokol						128200					282.9
98	Star 24C	Morton Thiokol						138000					282.1
99	Star 25	Morton Thiokol						134720					240
100	Star 26	Morton Thiokol						138500					271
101	Star 26B	Morton Thiokol						142758					271.7
102	Star 26C	Morton Thiokol						138600					272.1
103	Star 27	Morton Thiokol						213780					287.9
104	Star 27A	Morton Thiokol						197780					287.7
106	Star 27B	Morton Thiokol						203590					288.2
106	Star 27C	Morton Thiokol						185300					287.5
107	Star 27D	Morton Thiokol						185550					287.5
108	Star 27E	Morton Thiokol						184740					287.4
108	Star 30BP	Morton Thiokol						328200					292
109	Star 30C	Morton Thiokol						371400					284.6
110	Star 30E	Morton Thiokol						400720					289.2
112	Star 31	Morton Thiokol						840000					293.5
113	Star 37FM	Morton Thiokol						685804					289.9
114	Star 37KEP	Morton Thiokol						570450					289.9
116	Star 40	Morton Thiokol						443028					207
116	Star 48A	Morton Thiokol						1525098					283.9
117	Star 48B	Morton Thiokol						1275740					286
118	Star 48S	Morton Thiokol						1303795					282.1
118	Star 62	Morton Thiokol						1800000					294
120	Star 63D	Morton Thiokol						2033000					283
131	Star 75	Morton Thiokol						4785730					288

Table F1. Database of Available Propulsion Systems

	A	O	P	O	H	S	Y	U	V	W	X	Y	Z	AA	AB	AC	
	Name	Outdr	O/Fuel Ratio	Length m	Diameter m	Engine Mass kg	Propellant Mass Fraction	Fuel Mass kg	Power Low Est kW	Power High Est kW	Power Required kW	Status	Resists Max No.	Lifeime hours	Relis	T/W Ratio	
1																	
2																	
3																	
4	Liquid Engines																
5	SE-6 Gemini	N2O4	1.3:1	0.246	0.064	1.07						Flight Proven				3	0.010433
6	SE-9 Transtage	N2O4	1.5:1	0.21	0.084	56.7						Flight Proven				3	0.020413
7	SE-9 Transtage	N2O4	1.5:1	0.21	0.084	56.7						Flight Proven				3	0.01134
8	Apollo Attitude Control System	N2O4	2.1:1	0.278	0.127	3.69						Flight Proven				3	0.042187
9	Lunar Module Ascent Engine	N2O4	1.6:1	1.321	0.813	19.8						Flight Proven				3	1.587666
10	RS-45	N2O4	1.6:1	0.139	0.064	0.125						Flight Proven				3	0.000454
11	RS-21	N2O4	1.5:1	0.554	0.229	8.39						Flight Proven				3	0.136086
12	Orbital Maneuvering Technology Engine	N2O4	1.6:1	1.83	1.27	88.9						Flight Proven				3	2.721713
13	Advanced Space Engine	LO2	6.0:1	1.283-2.3676	1.232	174.2					0.5-1.0		100000	300		3	0.072375
14	Space Station Resuscitant	O2	3.1:0.1			2.72							Yes			2	0.013609
15	Rockwell Space Station Thruster	LO2	5.0:1			138.4									4.8	7.484709	
16	RL-10	LO2	6.0:1			3175.2										8	213.2008
17	SSME	LO2	6.0:1			1578.2										8	104.3323
18	J-2	LO2	5.5:1			304.6						Proposed				8	3.402141
19	Advanced Space Engine	LO2	4.5:1			14.1						Proposed				8	0.567023
20	AJ10-199	LO2	6.0:1			20						Proposed				8	0.228009
21	C-D-III	LO2	3.0:1			1.7						Proposed				8	0.01134
22	AJ10-197	N2O4	1.9:1			1874.7						Flight Proven				8	255.8818
23	AJ23-139/138	N2O4	1.8:1			570.6						Flight Proven				8	45.38186
24	AJ23-137/140	N2O4	1.8:1			373.3						Flight Proven				8	9.299185
25	AJ10-137	N2O4	1.6:1			145.1						Flight Proven				8	7.2579
26	BH 8098	IRFNA	2.57:1			178.3						Flight Proven				8	4.422783
27	Lunar Module Descent Engine	N2O4	1.6:1			134.7						Proposed				8	0.72579
28	Shuttle OMS	N2O4	1.6:1			5.8						Flight Proven				8	791.1111
29	AJ10-185	LO2	2.0:1			8391.5						Proposed				8	333.5459
30	F-1	LO2	2.4:1			2420						Flight Proven				8	156.2283
31	AJ23-144	LO2	2.2:1			1228.5						Flight Proven				8	107.054
32	AJ23-130	LO2	2.2:1			908.5						Flight Proven				8	88.50102
33	H-1	LO2	2.15:1			943.5						Flight Proven				8	36.2805
34	MB-3	LO2	2.25:1			505.8						Flight Proven				8	86.21024
35	AJ23-131	LO2	2.25:1			631.4						Flight Proven				8	38.64832
36	MA-3A	LO2	2.27:1			482.2						Flight Proven				8	0.45408
37	MA-3A-B	LO2	1.8:1			23.1						Flight Proven				8	1.70234
38	MA-3A-C	LO2	1.8:1			51.28						In Development		5000		1.70234	
39	XLR-132	N2O4				57.15						In Development		5400		1.70234	
40	Transtape	N2O4				107.05						Flown		1000		3.82805	
41	Transtape	N2O4				90.79						Flown		1200		4.444466	
42	Delta II	N2O4				7.28						Qualified		25000		0.407758	
43	R-40B	N2O4				90.72						Modified OME		1200		2.721713	
44	OMEU/UR	N2O4				4.54						In Qualification		15000		0.045382	
45	DM/JAE	N2O4				3.78						Flown		20000		0.048853	
46	RA-D	N2O4				4.54						Qualified		15000		0.090724	
47	RA2	N2O4				5.22						Flight Qualified		20000		0.045382	
48	RA-BPE	N2O4				113.4						Flight Qualified		20000		1.131325	
49	RS-41	N2O4				4.08						In Development		10000		0.048853	
50	HS-601 AKE	N2O4				193.7						Flight		500		7.2579	
51	Transtape	N2O4				0.2722						Flight				0.002204	
52	Aerocet Baseline Engine	N2O4				0.5897						Flight				0.002177	
53	Aerocet Baseline Engine	N2O4				1.859						Flight				0.045382	
54	Aerocet Baseline Engine	N2O4				0.525						Flight				0.394648	
55	R-40A	N2O4				1.361						Flight				0.070311	
56	R-30	N2O4				113.4						Flight				4.445464	
57	TR-201 (Delta)	N2O4				0.4724						Flight				0.045382	
58	Solid Rockets					0.2731						Flight				0.045382	
59	Star 13A					0.579						Flight				0.045382	
60	Star 13B					0.837						Flight				0.045382	
61	Star 17					96.1						Flight				0.045382	
62	Space Shuttle SRB					47						Flight				0.045382	
63	Star 75					570201						Flight Proven				6	0
64	Star 48					8066						Flight Proven				6	0
65	Star 37FM					2113.3						Flight Proven				6	0
66	Star 20					1148.5						Flight Proven				6	0
67	Star 5					300.7						Flight Proven				6	0
						2						Flight Proven				6	0
						1.7						Flight Proven				6	0
						33.1						Flight Proven				6	0
						41.2						Flight Proven				6	0
						96.1						Flight Proven				6	0
						47						Flight Proven				6	0
						503488						Flight Proven				6	0
						7503						Flight Proven				6	0
						1998.1						Flight Proven				6	0
						1068.4						Flight Proven				6	0
						300.7						Flight Proven				6	0
						2						Flight Proven				6	0
						1.7						Flight Proven				6	0

Table F1. Database of Available Propulsion Systems

	A	O	P	O	R	S	Y	U	V	W	X	Y	Z	AA	AB	AC
66	IUS SRM-1 (ORBUS-21)					10374	0.94	9751.56				Flown				26 55303
69	LEASAT PKM					3656	0.91	3328.78				Flown				19 69431
70	Star 48A					2559	0.95	2431.05				Flown				10 20234
71	Star 48B(S)					2135	0.95	2028.25				Qualified				7 187136
72	Star 48B(L)					2141	0.95	2033.95				Qualified				7 341366
73	Star 62					2459						In Development				0
74	Star 75					8066	0.93	7501.38				In Development				24 75486
76	IUS SRM-2 (ORBUS-6)					2965	0.91	2725.45				Flown				11 32232
77	Star 30C					543	0.94	510.42				Flown				3 264694
78	Star 30E					626	0.95	594.7				Flown				3 775015
79	Star 37E					667	0.94	626.98				Flown				4 176282
80	Star 6					1149	0.94	1080.06				Flown				5 010673
81	Star 6A	0.1575				6 104403	0.795	4 853				15 F&T				0
82	Star 6B	0.1575				4 517289	0.723	3 266				285 F&T				0
83	Star 10	0.1854				10 29244	0.595	6 124				18 F&T				0
84	Star 12	0.254				17 64793	0.676	11 90				46 F&T				0
85	Star 12A	0.3048				27 69697	0.66	18 28				508 F&T				0
86	Star 13	0.3073				33 98507	0.67	22 77				9 F&T				0
87	Star 18C	0.3429				35 65017	0.869	30 98				248 F&T				0
88	Star 19D					37 93711	0.795	30 18				12 F&T				0
89	Star 19E					35 28395	0.81	28 58				105 F&T				0
90	Star 13F					30 57178	0.822	25 13				6 F&T				0
91	Star 15					40 16967	0.63	33 34				21 F&T				0
92	Star 17A					48 7385	0.928	45 13				17 F&T				0
93	Star 20 (Schemical)					128 1348	0.89	112 28				2 F&T				0
94	Star 20A					122 8694	0.934	114 76				2 F&T				0
95	Star 24					314 022	0.91	285 78				2 F&T				0
96	Star 24A					218 1769	0.918	199 85				248 F&T				0
97	Star 24B					197 8073	0.903	178 62				12 F&T				0
98	Star 24C					218 8197	0.915	200 22				105 F&T				0
99	Star 25					239 4111	0.917	218 54				6 F&T				0
100	Star 26					208 2466	0.917	218 64				21 F&T				0
101	Star 26B					268 1977	0.86	230 85				11 F&T				0
102	Star 26C					261 1868	0.91	237 68				27 F&T				0
103	Star 27					263 6023	0.88	231 97				248 F&T				0
104	Star 27A					361 1039	0.924	333 66				12 F&T				0
105	Star 27B					336 0283	0.919	308 81				105 F&T				0
106	Star 27C					344 4083	0.921	317 2				6 F&T				0
107	Star 27D					332 4401	0.918	305 18				21 F&T				0
108	Star 27E					331 7481	0.921	305 54				17 F&T				0
109	Star 27F					330 4669	0.921	304 38				2 F&T				0
110	Star 30BP					542 2964	0.931	504 85				12 F&T				0
111	Star 30E					626 3807	0.937	586 9				5 F&T				0
112	Star 31					667 0484	0.932	621 69				3 F&T				0
113	Star 37FM					1364 209	0.929	1285 63				11 F&T				0
114	Star 37XFP					1148 987	0.928	1068 26				4 F&T				0
115	Star 40					658 3745	0.924	603 69				2 F&T				0
116	Star 48A					978 2919	0.923	904 92				10 F&T				0
117	Star 48B					2556 628	0.948	2420 46				1 F&T				0
118	Star 48C					2135 399	0.941	2009 41				10 F&T				0
119	Star 62					2130 947	0.939	2009 41				1 F&T				0
120	Star 63D					2615 394	0.94	2458 47				1 F&T				0
121	Star 75					3499 107	0.929	3250 87				7 F&T				0
122	Star 75					8067 946	0.93	7503 19				1 F&T				0

Propulsion Appendix References

1. Hill, Philip G. and Carl R. Peterson, **Mechanics and Thermodynamics of Propulsion**, Addison-Wesley Publishing Co., Massachusetts, 1970, p. 322.
2. **Mechanics and Thermodynamics of Propulsion**, p. 323.
3. Wertz, James R. and Wiley J. Larson, **Space Mission Analysis and Design**, Kluwer Academic Publishers, Dordrecht, The Netherlands, 1991, pp. 273-276.
4. Gere, James M. and Stephen P. Timoshenko, **Mechanics of Materials**, 2nd Edition, PWS-KENT Publishing Co., Boston, 1984, p. 310.
5. **Spacecraft Subsystems**, UT Austin, January 1991, Propulsion Subsystem Database.
6. Monroe, Darrel, **Spacecraft Applications Lab Manual**, Spring 1991, pp. 217-223.
7. Wertz, James R. and Wiley J. Larson, **Space Mission Analysis and Design**, Kluwer Academic Publishers, Dordrecht, The Netherlands, 1991, pp. 585-597.

**ORIGINAL PAGE IS
OF POOR QUALITY**